UCSF
UC San Francisco Electronic Theses and Dissertations

Title
Elucidating the Role of Endocytosis in cAMP-dependent Transcription

Permalink
https://escholarship.org/uc/item/5h75n44w

Author
Peng, Grace Eulan

Publication Date
2019

Peer reviewed|Thesis/dissertation

Elucidating the Role of Endocytosis in cAMP-dependent Transcription

by
Grace Eulan Peng

DISSERTATION
Submitted in partial satisfaction of the requirements for degree of
DOCTOR OF PHILOSOPHY

in

Cell Biology

in the

GRADUATE DIVISION
of the
UNIVERSITY OF CALIFORNIA, SAN FRANCISCO

Approved:

DocuSigned by:
Mark von Zastrow
A4DF1018F0A2414...
                Mark von Zastrow
                Chair

DocuSigned by:
Orion Weiner
                Orion Weiner

DocuSigned by:
Noelle L'Etoile
54CC7336DCB447E...
                Noelle L'Etoile

                Committee Members

ACKNOWLEDGEMENTS

I need to scold everyone who encouraged me to go to graduate school and thank the many who helped me get through the end. This work could not have been done without the scientific and emotional support of many colleagues, friends and family - j'ai le cul bordé de nouilles.

First, this work absolutely could not have been done without the guidance, help, advice, brilliance and enthusiasm of my advisor, Mark von Zastrow. Before I joined the lab, I met with Mark to discuss potential projects and open areas for exploration in the lab. I received an email following my meeting with Mark presented below:

> I was scolded by lab members this afternoon for bad salesmanship skills regarding how many fabulous and sure fire projects are just waiting to be snatched up in the lab by a lucky graduate student such as you. Of course all of this is true but I really do want you to feel free to shape your project as it goes. More strongly than that, I think it an important part of your PhD training that you get in the habit if doing that, so you "own" your project. Nevertheless it is not realistic to think that you will have a detailed sense of a particular project this early and, in all seriousness, I may not have been sufficiently clear about some interesting starting points.

I joined the week after receiving this email, and one of the projects we discussed during that meeting ended up being the basis for my qualifying and fellowship proposals and is now found here in Chapter 3. This email describes well my interactions with Mark throughout my graduate career which were a balance between enthusiasm, criticism and realism. Mark as has always placed importance in ownership of one's project, and I have been grateful for the freedom to pursue interesting results and redirect when I hit a dead end. However, Mark has never been shy to interject with his theories and enthusiasm about my data or project. In reality, my graduate work was strongly shaped by Mark and his out of the box thinking. Though I was often quick to reject some of the crazy theories and analogies (semiconductors, comfy chairs), as they were out of my realm of comfort, these theories and Gedankenexperiments that we would discuss at length pushed me to think more about what could be possible.

career in research. I am forever grateful for her patience and dedication to teaching me and giving me a wonderful foundation that let me hit the ground running when I started in the Weiner lab.

The Weiner lab was my first introduction to UCSF. I remember feeling so intimidated by the brilliant minds in the lab and feeling massively overwhelmed as a non-graduate student at my first Granlibakken. Very quickly though, I found myself at home in the Weiner lab thanks to the warm and welcoming lab members Anna Reade, Anna Payne-Tobin Jost, and Delquin Gong. Many Weiner lab members served as great role models and examples of forging into the unknown with much passion and persistence. I'm fortunate to have continued friendships with everyone and thank them for their wise sage advice, even from the forever baby of the lab, Doug Tischer.

Thank you to Kelli Benedetti (NOOOODLES!!), Gloria Chu, Cynthia Nguyen, Steffi Wu, Tiffany Day, Stephanie Eto for all their support and love throughout graduate school. Adventuring outside of science has been crucial to happiness and success, whether it was searching for the best hand pulled noodles and dumplings, getting lost backpacking in super hot Utah, struggling to buy sandwich bags in Puerto Natales, or rage climbing when science got tough. To my friends outside of science, thank you for listening patiently as I bemoaned about my latest science problem with abstract food analogies and for distracting me with cute dogs, cherries, hikes and tasty food.

Lastly, I owe much to my family. My uncle Jeff and aunt Lucy have been great cheerleaders over the past 7 years. My brother Bruce asks me science questions whenever I visit, and keeping me humble, honest and curious. From my parents, Lucille and Philly, I inherited a great amount of stubbornness, and was always taught to satisfy my curiosities by going the source and looking things up, or through experimentation. I could not have done this without their love and support.

ABSTRACT

Elucidating the Role of Endocytosis in cAMP-dependent Transcription

Grace Eulan Peng

There is a growing body of evidence from the last decade that supports the ability of G protein-coupled receptors (GPCRs) to signal from the endosome. With examples of different subtypes (G_s, G_i, G_q) of GPCRs now recognized with this ability, we still have much to learn about the role of the endosomal signal. This work explores how endocytosis selectively promotes cAMP-dependent transcription by studying a G_s-coupled GPCR, the beta-2 adrenergic receptor (β2AR). To begin to investigate the mechanism of how the endosome signal is selective for transcription, I utilized recently developed tools including a cAMP fluorescence biosensor, and a knock-in cell line endogenously expressing fluorescently labeled protein kinase A catalytic subunit (PKAcat). I examined the effects of endocytic blockade on each step of the cAMP signaling cascade using primarily spinning disk confocal microscopy, genetic manipulations, biochemical and molecular biology methods. In this study we found that endocytosis greatly affected PKAcat nuclear accumulation, and that the accumulation in the nucleus was necessary for cAMP-dependent transcription of *PCK1*.

Because this is still a relatively new area of GPCR cell biology, many questions remain unanswered, including how does endocytosis affect the functional relationship between two receptors? β2ARs, known to signal from the endosome, have an antagonistic relationship with the M2 muscarinic acetylcholine receptor (M2R). These G_s- and G_i-coupled receptors, respectively, control the overall cAMP produced in the cell by stimulating or inhibiting the cAMP producing

enzyme. The functional relationship between these two receptors are a great example for studying the effects of endocytosis on integrative cellular signaling. This work explored the relationship between the β2AR and M2R both by examining the trafficking of each receptor and by registering the endosomal signal of the β2AR, cAMP-dependent transcription. I utilized already established imaging and molecular biology methods to probe the effect of M2R inhibition on β2AR-stimulated cAMP signaling. I additionally generated modified constructs complementary to existing nanobody biosensors to detect activated states of the M2R and $G\alpha_i$ protein. This work found that it was not necessary for M2R to undergo endocytosis in order to inhibit β2AR cAMP-dependent transcription.

TABLE OF CONTENTS

LIST OF FIGURES

Chapter 1

Chapter 2

Chapter 3

Chapter 4

Chapter 5

LIST OF TABLES

Chapter 2

Chapter 3

Appendix B

Chapter 1: Introduction

He who cannot draw on three thousand years is living from hand to mouth.
Johann Wolfgang von Goethe

1.1 Overview

One of first things I learned was that the G protein-coupled receptor (GPCR) field is extremely well studied and well established. It is possible that I did not appreciate that many of the components that I have been studying are so well described and their processes so well characterized. β2AR, aside from rhodopsin, was one of the early GPCRs studied and used as a model GPCR to understand GPCR trafficking and signaling. Protein Kinase A is the first protein kinase described, and CREB is one of the first transcription factors to be well characterized. Each of these have such a long history, that I will not be able to cover here in any sort of breadth.

This dissertation focuses on understanding endosomal signaling, the mechanism in which it occurs and the cellular consequences of signaling from the endosome. The following introduction attempts to provide some background and context on G protein-coupled receptors function, signaling and trafficking; the emergence of endosomal signaling for GPCRs; a key player in the cAMP signaling cascade, protein kinase A; and the model receptors studied, the beta-2 adrenergic receptor and the M2 muscarinic acetylcholine receptor.

1.2 The importance of being G protein-coupled receptors

Cellular signaling is an important process that allows cells to communicate with each other, as well as for a single cell to communicate what it senses in its extracellular environment. Cells sense their extracellular environment via external stimuli and transmit signals to mediate a proper response. Many of these responses are controlled by G protein-coupled receptors (GPCRs). G protein-coupled receptors (GPCRs) are an important class of receptors responsible for regulating many important processes, including cell migration, sight, taste, and smell (Pierce et al., 2002). These receptors are also known as serpentine receptors or seven transmembrane receptors (7TM) as they snake through the membrane seven times (Pierce et al., 2002). This large superfamily of protein receptors is one of the largest classes of pharmaceutical drug targets.

Classically, to initiate an intracellular signal, a ligand binds the GPCR on the extracellular surface, and induces a conformational change to activate the receptor (**Figure 1.1a**) (Weis & Kobilka, 2018). The activated GPCR acts as a guanine nucleotide exchange factor to activate the corresponding heterotrimeric G protein (Gαβγ) through exchange of GDP for GTP on Gα. Activated Gα protein dissociates from Gβγ, and each component can interact with effector proteins to propagate the signal response through downstream signaling cascades.
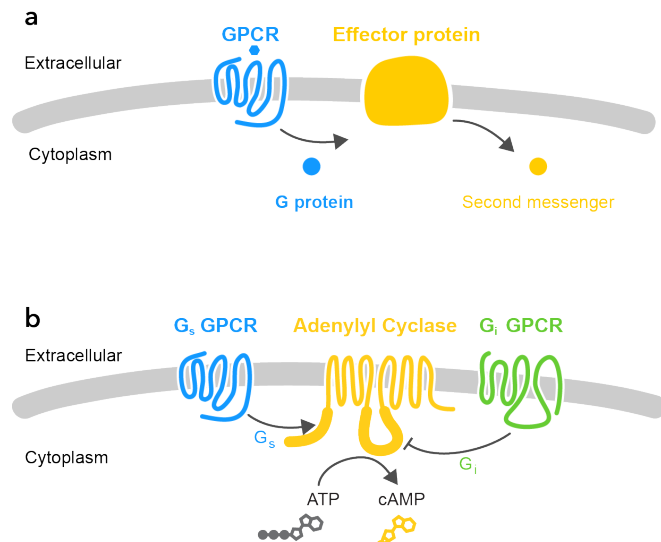
Figure 1.1 GPCR signaling cascade
a. Ligand (blue hexagon) binds to a GPCR on the extracellular face. The GPCR is activated and activates the G protein. The G protein interacts with the effector protein, which in turn stimulates the production or release of a second messenger.
b. G_s and G_i GPCR subtypes are activated by their corresponding ligands (blue hexagon and green star). The corresponding G proteins are activated and interact with the effector protein adenylyl cyclase to modulate the production of the second messenger, cAMP. G_s coupled receptors stimulate adenylyl cyclase while G_i coupled receptors inhibit adenylyl cyclase to increase or decrease cAMP production respectively.

There are multiple GPCR subtypes which couple to different G proteins (e.g. $G\alpha_s$, $G\alpha_{i/o}$, $G\alpha_{q/11}$, $G\alpha_{12/13}$) all of which can mediate distinct responses by interacting with different effector proteins such as adenylyl cyclases (ACs), phospholipases, phosphodiesterases (PDEs) and ion channels (Pierce et al., 2002). Two subtypes, $G\alpha_s$ and $G\alpha_i$, can interact with adenylyl cyclases to control cAMP production (**Figure 1.1b**) (Alberts et al., 2002). $G\alpha_s$ stimulates while $G\alpha_i$ inhibits adenylyl cyclase to increase and decrease cyclic adenosine monophosphate (cAMP) production.

cAMP acts as a second messenger in the $G\alpha_s$ coupled receptor signaling pathway to promote intracellular signaling and is regulated by adenylyl cyclases and phosphodiesterases for its synthesis and degradation, respectively (Pierce et al., 2002). One important function of cAMP is to activate a downstream enzyme in the signaling cascade, protein kinase A (PKA). Activated PKA phosphorylates many substrates including the transcription factor cAMP response element-binding protein (CREB) to promote the transcription of genes with cAMP responsive element (CRE) sites.

1.3 GPCR trafficking and signaling and the emergence of endosomal signaling

Agonist binding to a GPCR activates the receptor and initiates intracellular signaling. To turn off or attenuate the G protein signaling response, GPCRs undergo a process known as desensitization (**Figure 1.2**). First, receptors are phosphorylated by G protein-coupled receptor kinases (Chuang et al., 1996; Pitcher et al.,

Figure 1.2 Desensitization and sequestration of GPCRs
GRKs phosphorylate GPCRs which recruit arrestin (green). After arrestin binding, GPCRs enter clathrin coated pits (yellow). As clathrin coated pits grow, Dynamin (teal) forms a ring around the neck to prepare for scission and vesicles pinch off. The chemical inhibitors PitStop, Dynasore and Dyngo-4A inhibit clathrin and dynamin. Genetic manipulations block endocytosis through clathrin depletion by siRNA for CHC17 and through a dominant negative mutant of dynamin.

1998). Phosphorylation of the receptor by GRKs increases the affinity for the protein arrestin, binding arrestin "arrests" GPCR signaling (Chuang et al., 1996; Gurevich & Gurevich, 2006). These steps are essential for GPCR signaling shut off at the plasma membrane. Some GPCRs, can then undergo agonist-induced internalization by associating with the clathrin adaptor protein AP2 and clathrin in clathrin coated pits (Mellman, 1996). Dynamin assembles a ring at the neck of the clathrin coated pit, and through scission, endosomes are pinched off the plasma membrane and trafficked intracellularly (Kaksonen & Roux, 2018).

Internalization removes receptors from the plasma membrane, temporarily reducing the number of receptors able to bind agonist and signal. In endosomes, receptors may remain phosphorylated, therefore unable to couple to and activate G proteins (Tran et al., 2007). Additionally, as endosomes intracellularly traffic, the lumen acidifies and destabilizes the agonist bound to the receptor (Murphy et al., 2009). Through the processes of desensitization and internalization, all of these effects reduce the ability of receptors to signal. Because the desensitization process

precedes receptor internalization, GPCRs have classically though to be inactive in endosomes. Until recently, endosomal signaling by GPCRs had not been thought to occur because of the classical paradigm of internalization as a consequence of a signaling shut off mechanism.

Support for GPCR signaling from the endosome began about a decade ago. Evidence that signaling was not limited at the plasma membrane, but also extended to the endosome was first found in yeast (Slessareva et al., 2006). This study used a knock out yeast strain screen aimed at finding candidate Gpa1 (Gα) effectors by studying mating responses. The screen identified proteins that interact with Gpa1 to function at the endosome instead of at the plasma membrane.

Initial evidence supporting GPCR endosomal signaling in mammalian cells began with the sphingosine-1 phosphate receptor (Mullershausen et al., 2009), and the polypeptide hormone receptors, thyroid stimulating hormone receptor (TSHR, Calebiro et al., 2009) and parathyroid hormone receptor (PTHR, Ferrandon et al., 2009). These initial reports showed a persistent signaling dependent on G proteins. This persistent signal continuing long after what the acute plasma membrane response. Additionally, this persistent or sustained signal was difficult to reverse after washout or ligand removal. These results supported the hypothesis of G protein activated signaling from the endosomes. Most of the evidence supporting GPCR endosomal signaling has been found with $G\alpha_s$ coupled receptors (Calebiro et al., 2009; Feinstein et al., 2013; Ferrandon et al., 2009; Irannejad et al., 2013; Kotowski et al., 2011; Lyga et al., 2016; Merriam et al., 2013; Yarwood et al., 2017), but there is growing support of endosomal signaling for multiple subtypes including $G\alpha_i$ and $G\alpha_q$ (English et al., 2018; Gilliland et al., 2013; Jensen et al., 2017; Mullershausen et al., 2009; Stoeber et al., 2018).

Several types of experimental methods and assays have been used to probe endosomal signaling in different GPCRs. One method blocks endocytosis by inhibiting clathrin and dynamin using either chemical inhibitors such as PitStop, Dynasore, Dyngo-4A, or genetic manipulations by siRNA depletion of clathrin or dominant negative dynamin (K44A or K44E, **Figure 1.2**) (Hinshaw, 2000; Mccluskey et al., 2013; Vassilopoulos et al., 2009; von Kleist et al., 2011). Another method, when possible, has been to use a combination of agonist and antagonist with different membrane permeabilities to determine from where the signal originates (i.e. agonist followed by membrane impermeable antagonist to eliminate the plasma membrane signal) (Ferrandon et al., 2009; Stoeber et al., 2018). Additionally, an agonist washout method has also been used to identify persistent or sustained signaling in GPCRs through the observation of slow or a lack of signaling reversal (Calebiro et al., 2009; Ferrandon et al., 2009). Lastly, newer methods have been developed to probe endosomal signaling. These methods have adapted single chain and single domain camelid antibodies known as nanobodies. Nanobodies are conformationally sensitive antibodies that have been used to detect activated GPCRs and G proteins (Rasmussen, Choi, et al., 2011; Rasmussen, DeVree, et al., 2011). These nanobodies have been adapted to be conformational biosensors for microscopy by the addition of a fluorescent protein. These nanobody biosensors have proven particularly useful in detecting where activated GPCR and G proteins exist in the cell after agonist addition, as nanobody biosensors have detected activated GPCRs and G proteins at the plasma membrane, the endosome and also the Golgi (Irannejad et al., 2017, 2013; Stoeber et al., 2018).

In the past decade GPCR endosomal signaling through G protein activation has become readily recognized. Much of the work that has been done to characterize and describe endosomal signaling comes from studies on three receptors, TSHR, PTHR and β2AR (Calebiro et al., 2009; Feinstein et al., 2011; Ferrandon et al., 2009; Godbole et al., 2017; Irannejad et al., 2013; Jean-

7

Alphonse et al., 2016; Tsvetanova et al., 2017; Tsvetanova & von Zastrow, 2014). Work on these three receptors have shown multiple mechanisms of propagating the signal initiated from the endosome. Much remains unknown as we continue to uncover the mechanisms and importance of signaling from the endosome.

1.4 Beta-2 Adrenergic Receptors

The beta adrenergic receptors (βARs) are a family of receptors that respond to catecholamines and are important in mediating a wide range of physiological responses in the cardiovascular, pulmonary, metabolic and central nervous systems. Within the family are three subtypes of receptors, the β1ARs, β2ARs, and β3ARs (Wallukat, 2002). In general, the βARs have been well studied, and the β2AR is a prototypical GPCR whose trafficking and signaling has been extensively studied and well characterized.

β2ARs are known to undergo desensitization followed by receptor internalization (Wallukat, 2002). After internalization, receptors can recycle back to the plasma membrane or traffic to the lysosome for degradation after prolonged exposure to agonist. β2ARs primarily couple to $G\alpha_s$ protein to initiate the cAMP signaling cascade as previously described (**Figure 1.1b**) (Wallukat, 2002). This signaling, classically thought to occur at the plasma membrane, was recently found to exist at the endosomal as well. The work done to investigate and describe β2AR endosomal signaling benefitted from the development of new tools.

The first evidence for β2AR endosomal signaling used a combination of signaling and microscopy assays with newly developed conformational biosensors. These conformation biosensors comprised of a conformationally sensitive camelid antibodies, termed nanobodies, fused to a fluorescent protein. Previously, the nanobodies had been used to stabilize activated receptor and G protein states for x-ray crystallography (Rasmussen, Choi, et al., 2011; Rasmussen, DeVree, et al., 2011). These conformational biosensors were now useful in detecting where activated GPCRs and G proteins exist in the cell. Nb80 and Nb37, the nanobodies that detect activated β2AR and $G\alpha_s$ protein were present at both the plasma membrane, and subsequently at the endosome after

agonist addition (Irannejad et al., 2013). These results suggested that the β2AR is capable of signaling from the endosome as it was in an activated state at the endosome and the G protein which it couples to was activated as well. These results coupled to a moderate reduction in cAMP production when the β2AR was stimulated and endocytosis was blocked, suggested that the endosome contributed to the cellular cAMP levels.

This study provided evidence for β2AR endosomal signaling, but the consequences of β2AR remained unknown. Another study investigated downstream signaling of β2AR by comparing the transcriptional profiles using microarrays between samples when β2AR was stimulated and endocytosis was allowed vs blocked (Tsvetanova & von Zastrow, 2014). As a result, a suite of genes was discovered to be induced when endocytosis was allowed. These results suggested that β2AR signaling has an endocytic-dependent transcriptional component. To confirm these results, an orthogonal approach of generating cAMP through bacterial-derived photoactivated adenylyl cyclase (bPAC) was used to interrogate the spatial component of cAMP signaling. bPAC was directed to different locations in the cell (plasma membrane, endosome, cytoplasm) and was light activated to produce cAMP. The endosomal and cytoplasmic bPAC but not the plasma membrane bPAC significantly induced the endocytosis-sensitive transcriptional targets previously found by microarray. This result corroborated the idea that β2AR endosomal signaling can confer a specific selective effect on the downstream signaling response.

Taken together, these results suggest that β2AR signals from the endosome with a moderate amount of cAMP that results in a significant transcriptional response. Exploration in understanding how such signaling selectivity is conferred will be important in understanding β2AR endosomal signaling and the importance in overall cellular signaling.

1.5 Protein Kinase A

One of the important players in the cAMP signaling cascade is cAMP-dependent protein kinase A (PKA). PKA is activated after binding to cAMP, after activation PKA can then go on to phosphorylate many substrates to propagate the signaling response which is responsible for the regulation of metabolism, transcription, cell growth and differentiation (Skålhegg & Tasken, 2000). The PKA holoenzyme is tetrameric enzyme composed of two regulatory (PKAreg or R) and two catalytic (PKAcat or C) subunits (Taylor, Kristoffer). PKAreg contains two cAMP binding sites and associates with A kinase anchoring proteins (AKAPs) to localize PKA holoenzyme to different subcellular locations in the cell (Søberg & Skålhegg, 2018; Taylor et al., 2012). After cAMP binds PKAreg, this induces a conformational change in PKAreg, as a result, PKAcat is then released and activated (Zhang et al., 2012).

There are two primary types of PKA holoenzyme, PKA type I (PKAI) and PKA type II (PKAII), each are designated by which PKAreg (RI or RII respectively) exists in the holoenzyme (Søberg & Skålhegg, 2018). Of these PKA regulatory subunit types, each have two isoforms – RIα and RIβ, RIIα and RIIβ (Carnegie et al., 2009; Scott et al., 1990; Wu et al., 2007). PKAI and PKAII are known to associate with different proteins, localizing PKA to different subcellular locations (Autenrieth et al., 2016; Beene & Scott, 2007; Calejo & Taskén, 2015). One way this differential localization is thought to occur is through AKAPs as AKAPs bind to RII with higher affinity compared to RI (Carr et al., 1991). RI is primarily found to be diffuse in the cytoplasm of the cell, but RI and dual-specific AKAPs may exist (Day et al., 2011; Dema et al., 2015; Jarnaess & Taskén, 2007). There are also two primary PKAcat isoforms, Cα and Cβ. PKAcatα is the primary form of catalytic subunit in the cell and ubiquitously expressed in many tissues (Uhler et al., 1986). Recent work estimated concentrations of PKA subunits in HEK293T cells and found approximately 2 μM PKAreg (RI and

RII) and 0.2 µM PKAcat (Walker-Gray et al., 2017). Additionally, PKAreg binds PKAcat with sub-nanomolar K_d (Kim et al., 2005; Wu et al., 2007).

In understanding how PKAcat is spatially restricted, contradictory reports arose in whether or not PKAcat is released from PKAreg after cAMP elevation. These studies propose different possibilities in how PKAcat signaling is spatially restricted (Smith et al., 2017; Tillo et al., 2017; Walker-Gray et al., 2017). Two of the studies agree that PKAcat is released from PKAreg after cAMP elevation, but myristoylation of PKAcat allows it to associate with the membrane to preferentially phosphorylate substrates there (Tillo et al., 2017; Walker-Gray et al., 2017). Additionally, the spatial restriction of PKAcat could be explained by the increase in recapture by PKAreg because of the stoichiometric ratio between PKAreg and PKAcat (~10:1) (Walker-Gray et al., 2017). Lastly, an alternative mechanism was proposed where PKAcat remains tethered to PKAreg, thereby heavily restricting the substrates PKAcat can phosphorylate (Smith et al., 2017). It is possible that these mechanisms may not be mutually exclusive and could exist in the same cell. Which mechanisms occur may be dependent on the subcellular locations of PKAcat.

In addition to the PKAcat activity in the cytoplasm, PKAcat has also been found in the nucleus. PKAcat activity in the nucleus has been shown to be important for cAMP-dependent transcription through the phosphorylation of cAMP regulatory element binding protein (CREB) at Ser133. PKAcat has been found to diffuse into the nucleus (Harootunian et al., 1993). Additionally, AKAP95 microdomains in the nucleus contains both PKAcat and PDE4 (Clister et al., 2019). In this case nuclear PKAcat to mediate a response, high levels of cAMP are needed to overcome degradation by PDEs.

Although much work has been done to understand how PKAcat enters the nucleus, no nuclear localization sequence has been found. Other than simple diffusion, two other components for nuclear localization have been suggested. First, PKAcat has been shown to bind A kinase interacting protein (AKIP1) which has been shown to target PKAcat into the nucleus (Sastri et al., 2005). Additionally, a posttranslational modification has been shown to reduce nuclear levels of PKAcat. PKAcat Asn2 has been found to undergo deamidation through a non-enzymatic beta aspartyl shift mechanism (Gesellchen et al., 2006; Wright, 1991). Higher levels of PKAcat have been found in the nucleus when the second residue of PKAcat remains as Asn and not Asp (Pepperkok et al., 2000).

Although the mechanism for PKAcat remains unclear, nuclear PKAcat export is well described. In the nucleus, PKAcat activity is regulated by protein kinase inhibitor (PKI). Three isoforms of PKI exist, PKIα, PKIβ, PKIγ, and inhibit PKAcat by acting as a pseudosubstrate (Gamm & Uhler, 1995; Herberg et al., 1999). PKI has a well described nuclear export sequence, and after binding PKAcat, PKI transports PKAcat out of the nucleus into the cytoplasm (Wen et al., 1995).

PKAcat has been implicated as an important key player in intracellular signaling. In addition to the plasma membrane, PKAcat exists in many subcellular locations, such as the Golgi which may poise important signaling components in the right location to promote endosomal signaling (Godbole et al., 2017). How such a diffusible protein is able to help propagate a specific response remains unexplored.

1.6 M2 Muscarinic Acetylcholine Receptors

The muscarinic acetylcholine receptor family of GPCRs regulate important basic physiological functions including many processes in the central nervous system and autonomic effector organs (Bubser et al., 2012; Caulfield, 1993). There are five subtypes of the muscarinic acetylcholine receptor family, M1-5, all of which signal through heterotrimeric G proteins and initiate downstream signaling cascades through second messengers (Bubser et al., 2012; Caulfield, 1993; Wess et al., 2007).

After activation with acetylcholine, M2R activates $G\alpha_i$ which inhibits the production of cAMP through adenylyl cyclase and $G\beta\gamma$ activates G protein inward rectifying potassium channels (GIRKs) (Bubser et al., 2012; Felder, 1995). Like many GPCRs, M2Rs are internalized following agonist-induced activation (Robin Pals-Rylaarsdam et al., 1997; Reiner & Nathanson, 2008). This process has been traditionally preceded with functional desensitization of cellular signaling responses. The phosphorylation sites responsible for M2R desensitization and internalization reside in the third intracellular loop, removal or mutation of specific Ser/Thr residues blocks desensitization and internalization (R. Pals-Rylaarsdam & Hosey, 1997).

Previously, M2Rs have been found to exist in early endosome antigen 1 (EEA1) positive endosomes after agonist-induced internalization (Delaney et al., 2002). However, the mechanism of how M2R internalizes remains unclear as M2Rs have not been found to internalize through well recognized mechanisms. Previous studies have conflicting evidence in determining which components are involved in M2R endocytosis. There is some evidence for a caveolin-independent, clathrin-independent and dynamin-independent pathway, and therefore a very non-traditional pathway (Delaney et al., 2002; Roseberry & Hosey, 2001). A recent study challenges these earlier

reports as they find a dependence on clathrin and dynamin for endocytosis (Jones et al., 2006).

Another clue comes from a study that claims that the clathrin-dependent endocytosis sequence

can be obscured by a clathrin-independent endocytosis sequence, thereby promoting clathrin-

independent endocytosis of M2R (Wan et al., 2015). Given the conflicting evidence, it is clear that

there are be several methods of endocytosis for the M2R, and which mechanism for endocytosis

could be dependent on the cell type.

The M2 muscarinic acetylcholine receptors (M2Rs) have important roles in the brain including in depression, cognition, learning and memory, and is additionally known to be important in heart function (Bainbridge et al., 2008; Brodde
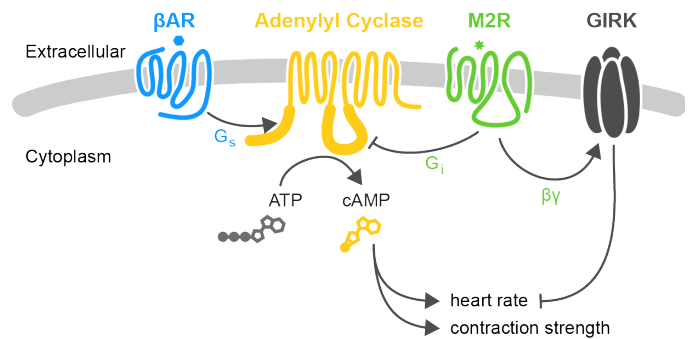
Figure 1.3 M2R and βAR function in the heart
M2Rs are important in setting the basal heart rate and reducing heart rate after βAR induced heart rate increase.

& Michel, 1999; Bubser et al., 2012; Dhein et al., 2001; Mysliveček & Trojan, 2003; Wess et al.,

2007). In the heart, M2R is important for regulating contraction strength and heart rate under basal

conditions and under adrenaline (also known as epinephrine) induced conditions. Upon an

adrenaline rush, the $G\alpha_s$ coupled receptors, β1 and β2 adrenergic receptors (β1AR and β2AR)

stimulate stronger contractions (positive inotropy) and faster heart rate (positive chronotropy)

through AC mediated effects (**Figure 1.3**) (Brodde & Michel, 1999; Dzimiri, 1999). This process is

modulated by M2R to return the contraction strength (negative inotropy) and heart rate (negative

chronotropy) back to the basal level through the inhibition of AC and the activation of GIRK

channels (Brodde & Michel, 1999; Harvey, 2012).

The evidence for GPCR endosomal signaling initially began mostly with $G\alpha_s$ coupled receptors but has expanded to different GPCR subtypes including $G\alpha_i$ and $G\alpha_q$. However, whether M2R signals from the endosome remains uncertain. Given the important roles M2R plays in many physiological processes, it is critical to determine whether M2R signals from the endosome, what its specific signaling effects are and how it could contribute to overall cellular signaling. Work with the M2R has already provided a nanobody used for the structural determination of the M2R by x-ray crystallography (Kruse et al., 2013). Adapting these nanobodies for use as conformational biosensors could prove useful in answering these questions.

1.7 References

Alberts, B., Johnson, A., Lewis, J., Raff, M., Roberts, K., & Peter Walter. (2002). *Signaling through
G-Protein-Linked Cell-Surface Receptors* (4gh ed.). Retrieved from
http://www.ncbi.nlm.nih.gov/books/NBK26912/

Autenrieth, K., Bendzunas, N. G., Bertinetti, D., Herberg, F. W., & Kennedy, E. J. (2016). Defining
A-Kinase Anchoring Protein (AKAP) Specificity for the Protein Kinase A Subunit RI (PKA-RI).
ChemBioChem, *17*(8), 693–697. https://doi.org/10.1002/cbic.201500632

Bainbridge, N. K., Koselke, L. R., Jeon, J., Bailey, K. R., Wess, J., Crawley, J. N., & Wrenn, C. C.
(2008). Learning and memory impairments in a congenic C57BL/6 strain of mice that lacks
the M2 muscarinic acetylcholine receptor subtype. *Behavioural Brain Research*, *190*(1), 50–
58. https://doi.org/10.1016/j.bbr.2008.02.001

Beene, D. L., & Scott, J. D. (2007). A-kinase anchoring proteins take shape. *Current Opinion in Cell
Biology*, *19*(2), 192–198. https://doi.org/10.1016/J.CEB.2007.02.011

Brodde, O. E., & Michel, M. C. (1999). Adrenergic and muscarinic receptors in the human heart.
Pharmacological Reviews, *51*(4), 651–690. Retrieved from
http://www.ncbi.nlm.nih.gov/pubmed/10581327

Bubser, M., Byun, N., Wood, M. R., & Jones, C. K. (2012). Muscarinic receptor pharmacology and
circuitry for the modulation of cognition. In *Handbook of Experimental Pharmacology* (Vol.
208). https://doi.org/10.1007/978-3-642-23274-9_7

Calebiro, D., Nikolaev, V. O., Gagliani, M. C., De Filippis, T., Dees, C., Tacchetti, C., … Lohse, M.
J. (2009). Persistent cAMP-signals triggered by internalized G-protein-coupled receptors.
PLoS Biology, *7*(8). https://doi.org/10.1371/journal.pbio.1000172

Calejo, A. I., & Taskén, K. (2015). Targeting protein-protein interactions in complexes organized by
A kinase anchoring proteins. *Frontiers in Pharmacology*, *6*(SEP), 1–13.

https://doi.org/10.3389/fphar.2015.00192

Carnegie, G. K., Means, C. K., & Scott, J. D. (2009). A-kinase anchoring proteins: From protein complexes to physiology and disease. *IUBMB Life*, *61*(4), 394–406. https://doi.org/10.1002/iub.168

Carr, D. W., Stofko-Hahn, R. E., Fraser, I. D., Bishop, S. M., Acott, T. S., Brennan, R. G., & Scott, J. D. (1991). Interaction of the regulatory subunit (RII) of cAMP-dependent protein kinase with RII-anchoring proteins occurs through an amphipathic helix binding motif. *The Journal of Biological Chemistry*, *266*(22), 14188–14192. Retrieved from http://www.ncbi.nlm.nih.gov/pubmed/1860836

Caulfield, M. P. (1993). Muscarinic Receptors-Characterization, coupling and function. *Pharmacology and Therapeutics*, *58*(3), 319–379. https://doi.org/10.1016/0163-7258(93)90027-B

Chuang, T. T., Iacovelli, L., Sallese, M., & De Blasi, A. (1996). G protein-coupled receptors: heterologous regulation of homologous desensitization and its implications. *Trends in Pharmacological Sciences*, *17*(11), 416–421. https://doi.org/10.1016/S0165-6147(96)10048-1

Clister, T., Greenwald, E. C., Baillie, G. S., Zhang, J., & Zhang Correspondence, J. AKAP95 Organizes a Nuclear Microdomain to Control Local cAMP for Regulating Nuclear PKA _ Elsevier Enhanced Reader.pdf. , 26 Cell Chemical Biology § (2019).

Day, M. E., Gaietta, G. M., Sastri, M., Koller, A., Mackey, M. R., Scott, J. D., … Taylor, S. S. (2011). Isoform-specific targeting of PKA to multivesicular bodies. *Journal of Cell Biology*, *193*(2), 347–363. https://doi.org/10.1083/jcb.201010034

Delaney, K. A., Murph, M. M., Brown, L. M., & Radhakrishna, H. (2002). Transfer of M2 muscarinic acetylcholine receptors to clathrin-derived early endosomes following clathrin-independent

endocytosis. *Journal of Biological Chemistry*, *277*(36), 33439–33446. https://doi.org/10.1074/jbc.M205293200

Dema, A., Perets, E., Schulz, M. S., Deák, V. A., & Klussmann, E. (2015). Pharmacological targeting of AKAP-directed compartmentalized cAMP signalling. *Cellular Signalling*, *27*(12), 2474–2487. https://doi.org/10.1016/J.CELLSIG.2015.09.008

Dhein, S., van Koppen, C. J., & Brodde, O. E. (2001). Muscarinic receptors in the mammalian heart. *Pharmacological Research : The Official Journal of the Italian Pharmacological Society*, *44*(1951), 161–182. https://doi.org/10.1006/phrs.2001.0835

Dzimiri, N. (1999). Regulation of beta-adrenoceptor signaling in cardiac function and disease. *Pharmacological Reviews*, *51*(3), 465–501. Retrieved from http://www.ncbi.nlm.nih.gov/pubmed/10471415

English, E. J., Mahn, S. A., & Marchese, A. (2018). Endocytosis is required for CXC chemokine receptor type 4 (CXCR4)-mediated Akt activation and antiapoptotic signaling. *The Journal of Biological Chemistry*, *293*(29), 11470–11480. https://doi.org/10.1074/jbc.RA118.001872

Feinstein, T. N., Wehbi, V. L., Ardura, J. a, Wheeler, D. S., Ferrandon, S., Gardella, T. J., & Vilardaga, J.-P. (2011). Retromer terminates the generation of cAMP by internalized PTH receptors. *Nature Chemical Biology*, *7*(5), 278–284. https://doi.org/10.1038/nchembio.545

Feinstein, T. N., Yui, N., Webber, M. J., Wehbi, V. L., Stevenson, H. P., King, J. D., … Vilardaga, J.-P. (2013). Noncanonical control of vasopressin receptor type 2 signaling by retromer and arrestin. *The Journal of Biological Chemistry*, *288*(39), 27849–27860. https://doi.org/10.1074/jbc.M112.445098

Felder, C. C. (1995). Muscarinic acetylcholine receptors: signal transduction through multiple effectors. *The FASEB Journal : Official Publication of the Federation of American Societies for Experimental Biology*, *9*(8), 619–625. https://doi.org/10.1016/j.autneu.2006.10.006

Ferrandon, S., Feinstein, T. N., Castro, M., Wang, B., Bouley, R., Potts, J. T., … Vilardaga, J.-P. (2009). *Sustained cyclic AMP production by parathyroid hormone receptor endocytosis*. *5*(10), 734–742. https://doi.org/10.1038/nchembio.206

Gamm, D. M., & Uhler, M. D. (1995). Isoform-specific differences in the potencies of murine protein kinase inhibitors are due to nonconserved amino-terminal residues. *The Journal of Biological Chemistry*, *270*(13), 7227–7232. https://doi.org/10.1074/jbc.270.13.7227

Gesellchen, F., Bertinetti, O., & Herberg, F. W. (2006). Analysis of posttranslational modifications exemplified using protein kinase A. *Biochimica et Biophysica Acta (BBA) - Proteins and Proteomics*, *1764*(12), 1788–1800. https://doi.org/10.1016/J.BBAPAP.2006.10.001

Gilliland, C. T., Salanga, C. L., Kawamura, T., Trejo, J., & Handel, T. M. (2013). The chemokine receptor CCR1 is constitutively active, which leads to G protein-independent, β-arrestin-mediated internalization. *The Journal of Biological Chemistry*, *288*(45), 32194–32210. https://doi.org/10.1074/jbc.M113.503797

Godbole, A., Lyga, S., Lohse, M. J., & Calebiro, D. (2017). Internalized TSH receptors en route to the TGN induce local Gs-protein signaling and gene transcription. *Nature Communications*, *8*(1), 23–42. https://doi.org/10.1038/s41467-017-00357-2

Gurevich, V. V., & Gurevich, E. V. (2006). The structural basis of arrestin-mediated regulation of G-protein-coupled receptors. *Pharmacology & Therapeutics*, *110*(3), 465–502. https://doi.org/10.1016/J.PHARMTHERA.2005.09.008

Harootunian, A. T., Adams, S. R., Wen, W., Meinkoth, J. L., Taylor, S. S., & Tsien, R. Y. (1993). Movement of the free catalytic subunit of cAMP-dependent protein kinase into and out of the nucleus can be explained by diffusion. *Molecular Biology of the Cell*, *4*(10), 993–1002. https://doi.org/10.1091/mbc.4.10.993

Harvey, R. D. (2012). *Muscarinic Receptor Agonists and Antagonists: Effects on Cardiovascular*

Function. https://doi.org/10.1007/978-3-642-23274-9_13

Herberg, F. W., Doyle, M. L., Cox, S., & Taylor, S. S. (1999). *Dissection of the Nucleotide and*

Metal–Phosphate Binding Sites in cAMP-Dependent Protein Kinase†.

https://doi.org/10.1021/BI982672W

Hinshaw, J. E. (2000). Dynamin and Its Role in Membrane Fission. *Annual Review of Cell and*

Developmental Biology, *16*(1), 483–519. https://doi.org/10.1146/annurev.cellbio.16.1.483

Irannejad, R., Pessino, V., Mika, D., Huang, B., Wedegaertner, P. B., Conti, M., & von Zastrow, M.

(2017). Functional selectivity of GPCR-directed drug action through location bias. *Nature*

Chemical Biology, *13*(7), 799–806. https://doi.org/10.1038/nchembio.2389

Irannejad, R., Tomshine, J. C., Tomshine, J. R., Chevalier, M., Mahoney, J. P., Steyaert, J., … von

Zastrow, M. (2013). Conformational biosensors reveal GPCR signalling from endosomes.

Nature, *495*(7442), 534–538. https://doi.org/10.1038/nature12000

Jarnaess, E., & Taskén, K. (2007). Spatiotemporal control of cAMP signalling processes by

anchored signalling complexes. *Biochemical Society Transactions*, *35*(Pt 5), 931–937.

https://doi.org/10.1042/BST0350931

Jean-Alphonse, F. G., Wehbi, V. L., Chen, J., Noda, M., Taboas, J. M., Xiao, K., & Vilardaga, J.-P.

(2016). β2-adrenergic receptor control of endosomal PTH receptor signaling via Gβγ. *Nature*

Chemical Biology, *13*(3), 259–261. https://doi.org/10.1038/nchembio.2267

Jensen, D. D., Lieu, T. M., Halls, M. L., Veldhuis, N. A., Imlach, W. L., Mai, Q. N., … Bunnett, N.

W. (2017). Neurokinin 1 receptor signaling in endosomes mediates sustained nociception and

is a viable therapeutic target for prolonged pain relief. *Science Translational Medicine*, *9*(392),

1–16. https://doi.org/10.1126/scitranslmed.aal3447

Jones, K., Echeverry, M., Mosser, V., Gates, A., & Jackson, D. (2006). Agonist mediated

internalization of M2 mAChR is beta-arrestin-dependent. *Journal of Molecular Signaling*, *1*, 7.

https://doi.org/10.1186/1750-2187-1-7

Kaksonen, M., & Roux, A. (2018). *Mechanisms of clathrin-mediated endocytosis*. *19*(5), 313–326.

https://doi.org/10.1038/nrm.2017.132

Kim, C., Xuong, N.-H., & Taylor, S. S. (2005). Crystal structure of a complex between the catalytic

and regulatory (RIalpha) subunits of PKA. *Science (New York, N.Y.)*, *307*(5710), 690–696.

https://doi.org/10.1126/science.1104607

Kotowski, S. J., Hopf, F. W., Seif, T., Bonci, A., & von Zastrow, M. (2011). Endocytosis Promotes

Rapid Dopaminergic Signaling. *Neuron*, *71*(2), 278–290.

https://doi.org/10.1016/j.neuron.2011.05.036

Kruse, A. C., Ring, A. M., Manglik, A., Hu, J., Hu, K., Eitel, K., … Kobilka, B. K. (2013). Activation

and allosteric modulation of a muscarinic acetylcholine receptor. *Nature*, *504*(7478), 101–106.

https://doi.org/10.1038/nature12735

Lyga, S., Volpe, S., Werthmann, R. C., Gotz, K., Sungkaworn, T., Lohse, M. J., … Calebiro, D.

(2016). Persistent cAMP Signaling by Internalized LH. *Endocrinology*, *157*(April), 1613–1621.

https://doi.org/10.1210/en.2015-1945

Mccluskey, A., Daniel, J. A., Hadzic, G., Chau, N., Clayton, E. L., Mariana, A., … Robinson, P. J.

(2013). Building a better dynasore: The dyngo compounds potently inhibit dynamin and

endocytosis. *Traffic*, *14*(12), 1272–1289. https://doi.org/10.1111/tra.12119

Mellman, I. (1996). ENDOCYTOSIS AND MOLECULAR SORTING. In *Annu. Rev. Cell Dev. Biol* (Vol.

12). Retrieved from www.annualreviews.org

Merriam, L. A., Baran, C. N., Girard, B. M., Hardwick, J. C., May, V., & Parsons, R. L. (2013).

Cellular/Molecular Pituitary Adenylate Cyclase 1 Receptor Internalization and Endosomal

Signaling Mediate the Pituitary Adenylate Cyclase Activating Polypeptide-Induced Increase in

Guinea Pig Cardiac Neuron Excitability. https://doi.org/10.1523/JNEUROSCI.4999-12.2013

Mullershausen, F., Zecri, F., Cetin, C., Billich, A., Guerini, D., & Seuwen, K. (2009). Persistent

  signaling induced by FTY720-phosphate is mediated by internalized S1P1 receptors. *Nature*

  Chemical Biology, *5*(6), 428–434. https://doi.org/10.1038/nchembio1209-954a

Murphy, J. E., Padilla, B. E., Hasdemir, B., Cottrell, G. S., & Bunnett, N. W. (2009). Endosomes: a

  legitimate platform for the signaling train. *Proceedings of the National Academy of Sciences of*

  the United States of America, *106*(42), 17615–17622.

  https://doi.org/10.1073/pnas.0906541106

Mysliveček, J., & Trojan, S. (2003). Regulation of adrenoceptors and muscarinic receptors in the

  heart. *General Physiology and Biophysics*, *22*(1), 3–14.

Pals-Rylaarsdam, R., & Hosey, M. M. (1997). Two Homologous Phosphorylation Domains

  Differentially Contribute to Desensitization and Internalization of the m2 Muscarinic

  Acetylcholine Receptor. *Biochemistry*, *272*(22), 14152–14158.

  https://doi.org/10.1074/jbc.272.22.14152

Pals-Rylaarsdam, Robin, Gurevich, V. V., Lee, K. B., Ptasienski, J. A., Benovic, J. L., & Hosey, M.

  M. (1997). Internalization of the m2 muscarinic acetylcholine receptor. Arrestin- independent

  and -dependent pathways. *Journal of Biological Chemistry*, *272*(38), 23682–23689.

  https://doi.org/10.1074/jbc.272.38.23682

Pepperkok, R., Hotz-Wagenblatt, A., König, N., Girod, A., Bossemeyer, D., & Kinzel, V. (2000).

  Intracellular distribution of mammalian protein kinase A catalytic subunit altered by conserved

  Asn2 deamidation. *Journal of Cell Biology*, *148*(4), 715–726.

  https://doi.org/10.1083/jcb.148.4.715

Pierce, K. L., Premont, R. T., & Lefkowitz, R. J. (2002). Seven-transmembrane receptors. *Nature*

  Reviews Molecular Cell Biology, *3*(9), 639–650. https://doi.org/10.1038/nrm908

Pitcher, J. A., Freedman, N. J., & Lefkowitz, R. J. (1998). *G PROTEIN-COUPLED RECEPTOR*

KINASES. Retrieved from www.annualreviews.org

Rasmussen, S. G. F., Choi, H.-J., Fung, J. J., Pardon, E., Casarosa, P., Chae, P. S., … Kobilka, B. K. (2011). Structure of a nanobody-stabilized active state of the β(2) adrenoceptor. *Nature, 469*(7329), 175–180. https://doi.org/10.1038/nature09648

Rasmussen, S. G. F., DeVree, B. T., Zou, Y., Kruse, A. C., Chung, K. Y., Kobilka, T. S., … Kobilka, B. K. (2011). Crystal structure of the β2 adrenergic receptor-Gs protein complex. *Nature*, *477*(7366), 549–555. https://doi.org/10.1038/nature10361

Reiner, C., & Nathanson, N. M. (2008). The internalization of the M2 and M4 muscarinic acetylcholine receptors involves distinct subsets of small G-proteins. *Life Sciences*, *82*(13–14), 718–727. https://doi.org/10.1016/j.lfs.2008.01.013

Roseberry, A. G., & Hosey, M. M. (2001). Internalization of the M2 muscarinic acetylcholine receptor proceeds through an atypical pathway in HEK293 cells that is independent of clathrin and caveolae. *Journal of Cell Science*, *114*(Pt 4), 739–746. https://doi.org/10.1074/jbc.272.38.23682

Sastri, M., Barraclough, D. M., Carmichael, P. T., & Taylor, S. S. (2005). A-kinase-interacting protein localizes protein kinase A in the nucleus. *Proceedings of the National Academy of Sciences*, *102*(2), 349–354. https://doi.org/10.1073/pnas.0408608102

Scott, J. D., Stofko, R. E., McDonald, J. R., Comer, J. D., Vitalis, E. A., & Mangili, J. A. (1990). Type II regulatory subunit dimerization determines the subcellular localization of the cAMP-dependent protein kinase. *The Journal of Biological Chemistry*, *265*(35), 21561–21566. Retrieved from http://www.ncbi.nlm.nih.gov/pubmed/2147685

Skålhegg, B. S., & Tasken, K. (2000). [Frontiers in Bioscience 5, d678-693, August 1, 2000]. Retrieved August 13, 2019, from Front Biosci. website: https://www.bioscience.org/2000/v5/af/A543/fulltext.htm

Slessareva, J. E., Routt, S. M., Temple, B., Bankaitis, V. A., & Dohlman, H. G. (2006). Activation of the Phosphatidylinositol 3-Kinase Vps34 by a G Protein α Subunit at the Endosome. *Cell*, *126*(1), 191–203. https://doi.org/10.1016/J.CELL.2006.04.045

Smith, F. D., Esseltine, J. L., Nygren, P. J., Veesler, D., Byrne, D. P., Vonderach, M., … Scott, J. D. (2017). Local protein kinase A action proceeds through intact holoenzymes. *Science*, *356*(6344), 1288–1293. https://doi.org/10.1126/science.aaj1669

Søberg, K., & Skålhegg, B. S. (2018). The Molecular Basis for Specificity at the Level of the Protein Kinase a Catalytic Subunit. *Frontiers in Endocrinology*, *9*, 538. https://doi.org/10.3389/fendo.2018.00538

Stoeber, M., Jullié, D., Lobingier, B. T., Laeremans, T., Steyaert, J., Schiller, P. W., … von Zastrow, M. (2018). A Genetically Encoded Biosensor Reveals Location Bias of Opioid Drug Action. *Neuron*, *98*(5), 963-976.e5. https://doi.org/10.1016/J.NEURON.2018.04.021

Taylor, S. S., Ilouz, R., Zhang, P., & Kornev, A. P. (2012). Assembly of allosteric macromolecular switches: lessons from PKA. *Nature Reviews Molecular Cell Biology*, *13*. https://doi.org/10.1038/nrm3432

Tillo, S. E., Xiong, W.-H. H., Takahashi, M., Smoody, B. F., Stork, P. J. S. S., Zhong Correspondence, H., … Zhong, H. (2017). Liberated PKA Catalytic Subunits Associate with the Membrane via Myristoylation to Preferentially Phosphorylate Membrane Substrates. *Cell Reports*, *19*(3), 617–629. https://doi.org/10.1016/j.celrep.2017.03.070

Tran, T. M., Friedman, J., Baameur, F., Knoll, B. J., Moore, R. H., & Clark, R. B. (2007). Characterization of β2-Adrenergic Receptor Dephosphorylation: Comparison with the Rate of Resensitization. *Molecular Pharmacology*, *71*(1), 47–60. https://doi.org/10.1124/MOL.106.028456

Tsvetanova, N. G., Trester-Zedlitz, M., Newton, B. W., Riordan, D. P., Sundaram, A. B., Johnson,

J. R., … von Zastrow, M. (2017). G Protein–Coupled Receptor Endocytosis Confers

Uniformity in Responses to Chemically Distinct Ligands. *Molecular Pharmacology*, *91*(2), 145–

156. https://doi.org/10.1124/mol.116.106369

Tsvetanova, N. G., & von Zastrow, M. (2014). Spatial encoding of cyclic AMP signaling specificity

by GPCR endocytosis. *Nature Chemical Biology*, *10*(12), 1061–1065.

https://doi.org/10.1038/nchembio.1665

Uhler, M. D., Chrivia, J. C., & McKnight, G. S. (1986). Evidence for a second isoform of the

catalytic subunit of cAMP-dependent protein kinase. *The Journal of Biological Chemistry*,

261(33), 15360–15363. Retrieved from http://www.ncbi.nlm.nih.gov/pubmed/3023318

Vassilopoulos, S., Esk, C., Hoshino, S., Funke, B. H., Chen, C.-Y., Plocik, A. M., … Brodsky, F. M.

(2009). A Role for the CHC22 Clathrin Heavy-Chain Isoform in Human Glucose Metabolism.

Science, *324*(5931), 1192–1196. https://doi.org/10.1126/science.1171529

von Kleist, L., Stahlschmidt, W., Bulut, H., Gromova, K., Puchkov, D., Robertson, M. J., …

Haucke, V. (2011). Role of the Clathrin Terminal Domain in Regulating Coated Pit Dynamics

Revealed by Small Molecule Inhibition. *Cell*, *146*(3), 471–484.

https://doi.org/10.1016/J.CELL.2011.06.025

Walker-Gray, R., Stengel, F., & Gold, M. G. (2017). Mechanisms for restraining cAMP-dependent

protein kinase revealed by subunit quantitation and cross-linking approaches. *Proceedings of

the National Academy of Sciences of the United States of America*, *114*(39), 10414–10419.

https://doi.org/10.1073/pnas.1701782114

Wallukat, G. (2002). The β-Adrenergic Receptors. *Herz*, *27*(7), 683–690.

https://doi.org/10.1007/s00059-002-2434-z

Wan, M., Zhang, W., Tian, Y., Xu, C., Xu, T., Liu, J., & Zhang, R. (2015). Unraveling a molecular

determinant for clathrin-independent internalization of the M2 muscarinic acetylcholine

receptor. *Scientific Reports*, *5*(May), 11408. https://doi.org/10.1038/srep11408

Weis, W. I., & Kobilka, B. K. (2018). The Molecular Basis of G Protein–Coupled Receptor Activation. *Annual Review of Biochemistry*, *87*(1), 897–919. https://doi.org/10.1146/annurev-biochem-060614-033910

Wen, W., Meinkotht, J. L., Tsien, R. Y., & Taylor, S. S. (1995). Identification of a signal for rapid export of proteins from the nucleus. *Cell*, *82*(3), 463–473. https://doi.org/10.1016/0092-8674(95)90435-2

Wess, J., Eglen, R. M., & Gautam, D. (2007). Muscarinic acetylcholine receptors: mutant mice provide new insights for drug development. *Nat. Rev Drug Discov*, *6*(9), 721–733. https://doi.org/nrd2379 [pii]\r10.1038/nrd2379

Wright, H. T. (1991). Sequence and structure determinants of the nonenzymatic deamidation of asparagine and glutamine residues in proteins. *"Protein Engineering, Design and Selection,"* *4*(3), 283–294. https://doi.org/10.1093/protein/4.3.283

Wu, J., Brown, S. H. J., von Daake, S., & Taylor, S. S. (2007). PKA type IIalpha holoenzyme reveals a combinatorial strategy for isoform diversity. *Science (New York, N.Y.)*, *318*(5848), 274–279. https://doi.org/10.1126/science.1146447

Yarwood, R. E., Imlach, W. L., Lieu, T., Veldhuis, N. A., Jensen, D. D., Klein Herenbrink, C., … Bunnett, N. W. (2017). Endosomal signaling of the receptor for calcitonin gene-related peptide mediates pain transmission. *Proceedings of the National Academy of Sciences of the United States of America*, *114*(46), 12309–12314. https://doi.org/10.1073/pnas.1706656114

Zhang, P., Smith-Nguyen, E. V., Keshwani, M. M., Deal, M. S., Kornev, A. P., & Taylor, S. S. (2012). Structure and Allostery of the PKA RII Tetrameric Holoenzyme. *Science*, *335*(6069), 712–716. https://doi.org/10.1126/science.1213979

Chapter 2: A cellular basis for location-aware cAMP signaling from endosomes

Grace Peng conceived of the project, generated constructs and performed most experiments and data analysis, and wrote the manuscript presented in this chapter. Veronica Pessino generated the HEK293T mNG2-PKAcat cell line. Aaron Marley generated and developed the cAMP fluorescence biosensor. Bo Huang provided advice and contributed to the development of the HEK293T mNG2-PKAcat cell line. Mark von Zastrow contributed to project development, data analysis, and the writing of the manuscript.

2.1 Abstract

G protein-coupled receptors are capable of sustaining their signaling response well after internalization, where the endosomal signal has been strongly linked to promote gene transcription. Inhibition of endocytosis leads to an altered signaling state. How these signals contribute to the overall cellular response and how cells distinguish between these signals to provide differential and consequential cellular signals remain unanswered. Here, using endogenously expressed beta-2 adrenergic receptor in HEK293s, we break down the overall cellular cAMP response and find that endocytosis promotes nuclear accumulation of protein kinase A catalytic subunit. Without endocytosis, this key step and the subsequent signaling events fail to generate the profound transcriptional response.

2.2 Introduction

GPCRs comprise nature's largest family of signaling receptors, which regulate essentially every physiological process and consequently are important drug targets (Allen & Roth, 2011; Hauser et al., 2017). A considerable amount is known about biochemical and biophysical aspects of GPCR function and regulation, but how GPCR-mediated signaling is organized and integrated at the level of intact cellular physiology remains relatively poorly understood. An interesting recent advance is that ligand-induced activation of GPCRs and cognate G proteins, although long believed to be restricted to the plasma membrane, can also occur from endosomes (Lobingier & von Zastrow, 2019; Tsvetanova et al., 2015). A fundamental question raised by this advance is what significance the additional spatial dimension of signaling afforded by endosomal activation has on integrated cellular function.

G protein activation by GPCRs in endosomes was initially recognized through studies of signaling initiated by a polypeptide hormone-activated GPCR, Ste2p, in yeast (Slessareva et al., 2006). Ste2p initiates G protein (Gpa1)-dependent activation of protein kinase cascades from the plasma membrane and then is internalized, engaging in endosomes a variant Gpa1-containing heterotrimer that stimulates local generation of the membrane-delimited lipid mediator, PtdIns(3)P. Endosomal activation of GPCR-G protein signaling has been described most extensively in mammalian cells through the study of receptors that couple via heterotrimeric G_s to the generation of cAMP, which is soluble and diffusible rather than membrane-delimited (Calebiro et al., 2009; Ferrandon et al., 2009; Irannejad et al., 2013; Kotowski et al., 2011; Lyga et al., 2016). Nevertheless, initiating cAMP synthesis from endosomes relative to the plasma membrane can produce different cellular effects.

One strategy for producing a different effect through endosomal generation of a diffusible mediator is to use the location of synthesis secondarily, by changing the amount or timing of overall mediator production. Mammalian polypeptide hormone receptors provide a clear example because they produce a transient cAMP elevation when activated at the cell surface and a sustained elevation after endocytosis (Calebiro et al., 2009; Ferrandon et al., 2009). An alternative strategy is to use the altered location of mediator production as a primary determinant of signaling specificity from endosomes, separately from changes in the overall amount or timing of mediator produced. However, in contrast to membrane-delimited responses for which location is inherently critical, the cAMP cascade involves diffusible mediators so it is not known how location could possibly be a salient variable.

cAMP-dependent transcriptional signaling by the human beta-2 adrenergic receptor (β2AR) provides an interesting example. β2ARs activate G_s-dependent production of cAMP from the plasma membrane and additionally from endosomes after ligand-induced internalization mediated by receptor clustering in clathrin-coated pits followed by dynamin-dependent vesicle formation (von Zastrow & Kobilka, 1992; Zhang et al., 1996). However, unlike polypeptide hormone receptors that linger in the endocytic network and produce a sustained cAMP response after endocytosis, β2ARs recycle rapidly and produce a transient cAMP response both from the plasma membrane and from endosomes (Calebiro et al., 2009; Ferrandon et al., 2009; Irannejad et al., 2013). Further, inhibiting endocytosis by manipulating clathrin abundance or dynamin activity produces only a small inhibition of signaling measured the level of global cAMP elevation (Irannejad et al., 2013). Nevertheless, when signaling is measured at the level of cAMP-responsive gene expression, endocytic blockade produces a strong inhibition (Tsvetanova & von Zastrow, 2014). Moreover, the subcellular location of cAMP production has been shown to be a primary determinant of the

cAMP-dependent transcriptional response, separately from additional effects on the overall amount of cytoplasmic cAMP produced (Tsvetanova & von Zastrow, 2014).

How such 'location-aware' downstream transduction is conveyed through the β2AR-initiated cAMP cascade remains unclear. Additionally, transcriptional signaling initiated by endosomal activation of the cAMP cascade is a particularly interesting example of location-dependent signaling because cAMP is not the only potentially diffusible mediator in this cascade. The other is the catalytic subunit of protein kinase A (PKAcat), which can be unleashed upon binding of cAMP to regulatory subunits in PKA holoenzyme to operate as a diffusible and autonomously active kinase (Søberg & Skålhegg, 2018). Thus transcriptional control via the cAMP cascade conveys location-aware information through two potentially diffusible mediators.

Yet another interesting property of cAMP-dependent transcriptional signaling is its distance scale. Localized operation of the cAMP cascade is well described in the cytoplasm and plasma membrane, where specificity of downstream coupling can be achieved by enforced proximity through protein scaffolding or membrane tethering that positions effectors adjacent to sites of diffusible mediator production (Agarwal et al., 2016; Esseltine & Scott, 2013; Lohse et al., 2017). However, this strategy is typically limited to a near-molecular distance scale because, beyond this distance, concentration elevations that result from local mediator production are largely dissipated as a consequence of rapid diffusion. cAMP-dependent transcription presents a unique challenge because a key effector in this pathway, the cAMP response element binding protein (CREB), is restricted to the nucleus by constitutive association with chromatin and cAMP response element (CRE) motifs present in cognate gene promoters (Montminy & Bilezikjian, 1986). Accordingly, location-aware information conveyed by the cAMP cascade must span a considerable distance

and cross two subcellular compartments that are separated by a double-layered nuclear membrane.

Here we investigate how endocytosis achieves location-aware transcriptional control in a well-established cellular model system, with all signaling components expressed at endogenous levels and using activation by endogenous receptors. We delineate a cellular strategy in which cAMP acts largely as a global mediator and nuclear entry of PKAcat conveys information about location, with these discrete biochemical information streams operating in concert to specify the location-aware downstream transcriptional response.

2.3 Results

Limited effect of endocytosis on global cytoplasmic cAMP

We focused on human embryonic kidney (HEK293) cells as a model system because these cells endogenously express β2ARs that are coupled via G_s to stimulation of the cAMP/PKA cascade, mediate sequential phases of β2AR-Gs activation in the plasma membrane followed by endosomes, and require endogenous β2AR-Gs activation in endosomes to produce a full transcriptional response (Irannejad et al., 2013; Tsvetanova & von Zastrow, 2014; Violin et al., 2008). In principle, endocytosis could promote transcription through effects on the overall amount of cellular cAMP production, its timing or location. Transcriptional control in HEK293 cells was shown previously to depend on the subcellular location of cAMP production, independently of changes in overall amount, but it remains unknown if endosomal β2AR-Gs activation has additional effects on amount or timing that contribute to downstream pathway selectivity (Tsvetanova & von Zastrow, 2014). Further, recent studies differ in whether endocytosis has any effect on the amount or timing of global cAMP elevation. Thus we began by investigating this question.

We previously used a luminescence-based cAMP biosensor to examine cytoplasmic cAMP elevation elicited by endogenous B2AR activation in living cells, at 37℃ and in the absence of phosphodiesterase inhibitors (Goulding et al., 2018; Irannejad et al., 2013). We improved this assay by adding an IRES-linked renilla luciferase cassette to enable normalization for possible well-to-well differences in cell number or transfection efficiency (see Methods). Application of the B2AR agonist isoproterenol (Iso) at 100 nM (a near-saturating concentration) produced a robust increase in the normalized luminescence response reporting cytoplasmic cAMP elevation (**Figures 2.1a & S2.1a**). Endocytic blockade imposed by over-expression of a dominant negative mutant version of dynamin (Dyn1-K44E, van der Bliek et al., 1993), whose effectiveness we verified in our system

(**Figures S2.1b&c**), caused a small but consistent reduction of the global cAMP response (**Figures 2.1a & S2.1a**). We observed similar results using two independent strategies to impose endocytic blockade, RNAi-mediated depletion of clathrin heavy chain and chemical inhibition of dynamin using Dyngo-4A (**Figures S2.1b-d**) (Mccluskey et al., 2013; Vassilopoulos et al., 2009). In contrast to the modest effect of endocytic blockade on overall cAMP elevation, the downstream transcriptional response assessed using endogenous *PCK1* as a validated cAMP/PKA-responsive target gene was profoundly inhibited (**Figures 2.1b & S2.1e**).

We considered that even a small inhibition of upstream cytoplasmic cAMP elevation could explain a much larger effect on the downstream transcriptional response if there is sufficient non-linearity in the transduction cascade. To test this, we reduced cytoplasmic cAMP elevation independently of endocytic manipulations by decreasing the concentration of isoproterenol applied to activate endogenous B2ARs. Remarkably, even when applied at very low concentrations that produce an amount of overall cytoplasmic cAMP elevation substantially lower than that produced by 100 nM isoproterenol with endocytic blockade (**Figures 2.1c & S2.1f**), the downstream transcriptional response was still higher than observed in the presence of 100 nM isoproterenol with endocytic blockade (**Figure 2.1d**).

We compared different isoproterenol doses and the different methods of endocytic blockade by looking at how the overall cAMP and *PCK1* transcriptional responses were affected by these conditions (**Figure 2.1e**). We found that in the presence of endocytosis (100 nM, 10 nM, 1 nM Iso) the *PCK1* response was stronger than the cAMP response. In contrast, we saw the opposite with the endocytic blockade methods (mutant dynamin, clathrin RNAi depletion, dynamin chemical inhibitor), where the cAMP response was stronger than the *PCK1* response. These results suggest

that the overall cAMP elevation was not primarily responsible for the endocytic-dependence of B2AR-stimulated *PCK1* transcription.

We used the luminescence biosensor to determine the maximal response from each condition as it has been widely used before. To detect the kinetics of the cAMP response, we applied a fluorescence-based cAMP biosensor that achieves similarly high sensitivity as the luminescence biosensor but reports directly through an intramolecular conformational change independent of other cellular reactions. This probe, generated by fusing a circularly permuted green fluorescent protein variant to a high-affinity cAMP-binding domain (see Methods), resolved the endogenous cAMP response into two kinetic phases. An initial, transient peak of high cAMP concentration was observed immediately after isoproterenol application and decayed over 10-15 min. The cytoplasmic cAMP elevation observed during this 'peak phase' was sufficient to saturate the biosensor response (defined using forskolin and the PDE inhibitor IBMX to drive supra-physiologic cAMP elevation). Based on in vitro characterization of the sensor, we estimated this peak cytoplasmic cAMP concentration to briefly exceed ~5 µM (**Figure S2.1g**). After the transient peak decayed, a second phase of the response was observed in which cytoplasmic cAMP remained moderately elevated and still dependent on agonist because it returned to baseline after antagonist (Alp) application (**Figure 2.1f**, teal curve). The cAMP concentration achieved during this 'plateau phase' was substantially lower than in the peak phase and, based on in vitro characterization of the sensor, we estimated to be in the range of 100-500 nM (**Figure S2.1g**). Endocytic blockade caused a reliable but partial reduction in the magnitude of cytoplasmic cAMP elevation observed in the peak phase of the endogenous B2AR-Gs response but it had little effect on the plateau phase (**Figure 2.1f**, magenta curve) or on the overall timing of the cAMP response (**Figure S2.1h**).

These results, taken together, indicate that endocytosis indeed increases the global cytoplasmic

cAMP response elicited by endogenous B2AR-Gs activation. However this effect is modest when

compared to the much larger effect of endocytosis on downstream transcription, and is limited

primarily to the early peak of cytoplasmic cAMP elevation that dissipates before the transcriptional

response. Thus our results add further support to the previous conclusion that endosomal

activation of endogenous B2AR-Gs promotes transcriptional signaling primarily by moving the

location of upstream cascade activation, rather than by increasing the amount of timing of overall

cytoplasmic cAMP elevation. They also indicate that the 'location-aware' nature of the

transcriptional response elicited by B2AR-Gs activation must originate at a stage in the signaling

pathway downstream of cAMP production itself, motivating us to extend our search.

Endocytosis is not required for cytoplasmic PKAcat mobilization

We next investigated PKA because this signaling node is immediately downstream of cAMP

production, and PKA is directly activated by cAMP. We focused on the catalytic subunit of PKA

(PKAcat) because it possesses the kinase activity required to drive downstream transcription.

PKAcat can be physically unleashed as a diffusible and autonomously active kinase after cAMP

binds to PKA regulatory subunits (PKAreg) (Hagiwara et al., 1993; Søberg & Skålhegg, 2018).

To visualize PKAcat in living cells and at endogenous levels, we applied a previously described

strategy using CRISPR-based genome editing and split fluorescent protein tagging to label the

native PRKACA gene with mNeonGreen2 (mNG2, **Figures 2.2a & S2.2a**) (Feng et al., 2017;

Kamiyama et al., 2016). Consistent with previous studies describing fully native PKAcat localization

in fixed cells, endogenously labeled PKAcat protein (mNG2-PKAcat) was non-uniformly distributed

in the cytoplasm of unstimulated cells, with a major fraction of protein concentrated adjacent to the nucleus (**Figure 2.2b**) (Leonetti et al., 2016; Nigg et al., 2000).

In unstimulated cells, mNG2-PKAcat remained non-uniformly distributed in the cytoplasm without detectable movement over time (**Figure 2.2b**, top row of images). In contrast, after adding isoproterenol to drive B2AR-Gs activation, endogenously labeled PKAcat dispersed rapidly in the cytoplasm and then returned to a perinuclear distribution pattern similar to that observed in unstimulated cells (**Figure 2.2b**) (Irannejad et al., 2017; Nigg et al., 2000).

Similar results were obtained under conditions of endocytic blockade. PKAcat remained non-uniformly localized in the cytoplasm in unstimulated cells (**Figure 2.2c**, top row), and dispersed rapidly and then relocalized after application of isoproterenol (**Figure 2.2c**, bottom row). We quantified these results over multiple experiments by determining PKAcat fluorescence intensity as a function of time after agonist addition in a region of interest corresponding to the perinuclear pool (**Figure 2.2d**, green oval). The initial phase of PKAcat dispersal throughout the cytoplasm decreased labeled PKAcat fluorescence in the perinuclear region, and relocalization was indicated by a subsequent increase. This analysis verified pronounced dispersal of the perinuclear pool of labeled PKAcat within less than a minute after application of isoproterenol and an apparently complete recovery to the pre-stimulation baseline within ~30 minutes, despite agonist still being present. Endocytic blockade produced no detectable effect on PKAcat dispersal elicited by isoproterenol, and little or no effect on the subsequent relocalization of PKAcat to the perinuclear region of the cell after continued agonist exposure (**Figures 2.2d & S2.2b**).

The timing of these events generally mirrored the global cAMP response, with PKAcat dispersing throughout the cytoplasm occurring during the peak phase of the cytoplasmic cAMP response and relocalizating to the perinuclear pool during the plateau phase. Together, these results indicate that PKAcat relocalization in the cytoplasm effectively mirrors the biphasic global cytoplasmic cAMP elevation elicited by B2AR-Gs activation and does not require endocytosis.

Endocytosis promotes CREB phosphorylation

After failing to discern a large effect of endocytosis on PKAcat localization or redistribution in the cytoplasm, we asked if endocytosis affects functional kinase activity in the nucleus. To do so we focused on the phosphorylation CREB at Ser133, a consensus site that is essential for the transcriptional response (Brindle & Montminy, 1992; Gonzalez & Montminy, 1989; Mayr & Montminy, 2001). Phosphorylated CREB (pCREB) was determined as a function of time after isoproterenol addition and normalized to total CREB as a loading control. Isoproterenol produced a robust increase in this response that peaked within 30 minutes and remained significantly elevated for over an hour. Endocytic blockade imposed by K44E mutant dynamin produced a pronounced inhibition of this response, suppressing the sustained elevation observed in the response beginning at ~30 min and continuing thereafter (**Figures 2.3a&b**).

Similar results were obtained using clathrin knockdown as an independent genetic method to impose endocytic blockade (**Figures 2.3c&d**). Again, the main effect of endocytic blockade was inhibition of CREB phosphorylation detected in the prolonged presence of isoproterenol. Together, these results indicate that endocytosis, while having only a modest effect on upstream cAMP elevation and no obvious effect on PKAcat localization or redistribution in the cytoplasm, is essential for the downstream step of CREB phosphorylation in the nucleus.

Endocytosis promotes accumulation of PKAcat in the nucleus

Having identified phosphorylation in the nucleus as an endocytosis-dependent step in the pathway, we next investigated the basis for this effect. Two potential routes for cAMP-dependent phosphorylation of nuclear CREB have been described. One route occurs through cAMP-mediated dissociation of PKAcat from PKA holoenzyme in the cytoplasm followed by diffusion of unleashed PKAcat through the nuclear pore complex (Hagiwara et al., 1993; Harootunian et al., 1993). A second route occurs through activation of a discrete pool of PKA holoenzyme that is restricted to the nucleus by cAMP that diffuses into the nucleus through nuclear pores (Clister et al., 2019). The second route is known to require sustained high levels of cytoplasmic cAMP elevation, which our results indicate are not produced by endogenous B2AR-Gs activation. For this reason, and because our imaging data detected PKAcat predominantly in the cytoplasm, we focused on the first route. Specifically, we asked if PKAcat undergoes nuclear accumulation in response to endogenous B2AR activation and, if so, whether this cross-compartment accumulation process is dependent on endocytosis.

We began by examining native (unlabeled) PKAcat in HEK293 cells, using subcellular fractionation to separate nuclei from cytoplasm (**Figure 2.4a**) followed by immunoblot analysis. Endogenous B2AR activation produced a clearly detectable increase in PKAcat recovered in nuclei, verified using endogenous HDAC2 as a nuclear loading control, and this effect occurred with a time course paralleling the nuclear pCREB response (**Figures 2.4b&c**). Significantly, and fully consistent with the CREB phosphorylation data, nuclear accumulation of native PKAcat was significantly inhibited in the presence of endocytic blockade (**Figures 2.4d&e**).

Despite a clear increase in PKAcat present in the nuclear fraction, we were unable to detect a corresponding loss in the cytoplasmic fraction in response to endogenous B2AR activation (**Figures 2.4c&e**, gray lines). This suggests that nuclei contain only a very small fraction of total cellular PKAcat, enabling nuclear accumulation to occur without detectable depletion of the much larger cytoplasmic pool. We verified this by comparing amounts of PKAcat recovered in isolated nuclei to those in the starting whole cell lysate, normalizing each amount to HDAC2 to assure equal nuclear representation in each fraction. This analysis verified that, indeed, the amount of native PKAcat present in nuclei is small relative to the amount present in the whole cell lysate under all conditions (**Figures 2.4f&g**). Overall, we estimated the nuclear fraction of PKAcat to be on the order of 1-2% of the total amount present in the cell.

Similar results were obtained in gene-edited cells (HEK293T mNG2-PKAcat), in which it was possible to estimate relative protein concentrations by mNG2 fluorescence intensity imaged by confocal microscopy through a mid-section of the cell. mNG2-PKAcat fluorescence was much lower in the nucleus than in the cytoplasm, and a particularly large difference in apparent concentration was evident between the nucleus and perinuclear pool (**Figure 2.5a**).

We next asked if it is possible to detect regulated nuclear accumulation of endogenously labeled PKAcat by live imaging. Nuclear accumulation of labeled PKAcat was easily observed in gene-edited cells after application of forskolin combined with IBMX (**Figure S2.3a**), consistent with previous results showing native PKAcat accumulation in nuclei after supra-physiologic cAMP cascade activation (Nigg et al., 2000). However, we were initially unable to detect nuclear accumulation in response to activation of endogenous B2AR-Gs using isoproterenol (**Figure 2.5b**, top row). Based on the biochemical results indicating that only a very small amount of PKAcat

accumulates in the nucleus in response to endogenous B2AR-Gs activation, we reasoned that it might be difficult to detect such accumulation to be visible by microscopy due to the inherent signal-to-noise limitations of live cell imaging. We also considered the possibility that the added molecular mass contributed by mNG2 (~25 kDa) in the cytoplasm might reduce the ability of labeled PKAcat to enter the nucleus.

To address these potential limitations, we sought to increase the sensitivity of our live imaging assay and decrease the mass of the endogenously labeled PKAcat during nuclear entry. We addressed both by taking advantage of the fact that the genome-edited version of PKAcat possesses only the last beta-strand of mNG2 ($PKAcat_{11}$), encoding a non-fluorescent polypeptide adding only a small amount (~2 kDa) of molecular mass to PKAcat relative to the native protein, and then the fluorescent species is formed in a second step by assembly with $mNG2_{1-10}$ in the cytoplasm. As split mNG2 protein complementation is a time-dependent process, we reasoned that some fraction of non-complexed $PKAcat_{11}$ likely exists in the cytoplasm at steady state, and that this might be 'trapped' after nuclear entry by complex formation with a nucleus-localized version of $mNG2_{1-10}$ (NLS-$mNG2_{1-10}$; **Figure 2.5c**). This strategy appeared to be successful because isoproterenol application produced a visible increase in nuclear mNG2 fluorescence in cells co-expressing NLS-$mNG2_{1-10}$ (**Figure 2.5b**, bottom row).

We verified this effect by blinded quantification of fixed specimens using an IRES-linked blue fluorescent protein marker to identify those cells transiently co-expressing NLS-$mNG2_{1-10}$ (**Figure 2.5d**). When nuclear fluorescence was measured in live image series, isoproterenol produced an increase in nuclear mNG2-PKAcat fluorescence that was clearly detectable above experimental background and exhibited a time-dependence similar to the nuclear accumulation of native PKAcat

detected biochemically (**Figures 2.5e&f**). Moreover, endocytic blockade inhibited the isoproterenol-induced nuclear accumulation of endogenously labeled PKAcat (**Figures 2.5g&h**). Taken together, these observations independently verify that endogenous B2AR-Gs activation indeed drives PKAcat accumulation in the nucleus, and that this process requires endocytosis.

A diffusible pool of PKAcat during the plateau phase of the cAMP response

After identifying PKAcat nuclear accumulation as a key endocytosis-dependent step in the integrated signaling pathway, we next asked how this is possible. Unleashed PKAcat enters the nucleus by diffusion through nuclear pores (Harootunian et al., 1993), inherently requiring the presence of a diffusible pool of PKAcat outside of the pore to drive net entry of PKAcat by mass action. However, our imaging data indicate that PKAcat is non-uniformly localized in the cytoplasm during the plateau signaling phase and exhibits a pronounced perinuclear accumulation similar to that in unstimulated cells. In unstimulated cells, such localization reflects PKAcat being stably bound in inactive holoenzyme complexes that cannot enter the nucleus due to their large size and anchoring to cytoplasmic structures through binding to AKAPs. Accordingly, it was not clear from our imaging data if there even exists a diffusible pool of PKAcat in the cytoplasm that could possibly support nuclear entry of PKAcat during the time that such entry is detected.

This apparent paradox forced us to reconsider our interpretation of cytoplasmic PKAcat localization at steady state. While a non-uniform protein distribution inherently implies some degree of protein immobilization, it does not necessarily rule out the existence of a diffusible pool. To test this possibility in a more sensitive way, we carried out fluorescent recovery after photobleaching (FRAP) analysis and used recovery of fluorescent protein in the photobleached volume to detect the presence of a diffusible pool. In unstimulated cells, little recovery of PKAcat fluorescence

occurred over a 5 minute imaging period after photobleaching (**Figure 2.6a**, top row; boxes indicate the photobleached area), verifying that the vast majority of PKAcat is indeed immobilized under this condition (**Figures 2.6a & S2.4a**). However, after prolonged isoproterenol exposure driving cells into the plateau phase of cAMP signaling, fluorescence recovery in the localized perinuclear pool was substantially increased (**Figure 2.6a**, bottom row). Quantification across multiple experiments verified this result, indicating that ~50% of endogenously labeled PKAcat is exchangeable during the plateau phase of the integrated response (**Figures 2.6a & S2.4a**). Thus there does indeed exist a substantial diffusible pool of PKAcat in the cytoplasm during the plateau phase of the endogenous cAMP response during which PKA accumulation occurs. Interestingly, endocytic blockade did not detectably affect the FRAP recovery curve (**Figure 2.6b**). These results suggest that the presence of diffusible PKAcat represents a changed global property of the cytoplasm that is characteristic of the plateau signaling phase, likely due to the moderate elevation of global cAMP concentration, which is not itself endocytosis-dependent.

Nuclear entry of PKAcat is sufficient to explain the transcriptional response

We next compared the time course of endocytosis-dependent nuclear PKAcat entry to downstream events in the integrated transduction pathway. The ultimate transcriptional response clearly lagged nuclear PKAcat accumulation, first becoming detectable after agonist exposure for 30-45 minutes (**Figure 2.7a&b**) despite the endocytosis-dependent component of native PKAcat accumulation reaching a plateau within 20-30 minutes (**Figure 2.7c**). Further, when intermediate events were plotted on the same time scale, a clear temporal order was evident (**Figures 2.7c-e**). Accordingly, downstream steps in the pathway follow nuclear accumulation of PKAcat, both in their kinetics and dependence on endocytosis. These results indicate that nuclear entry of PKAcat is the critical step in the integrated transduction cascade at which the dependence on endogenous

B2AR-Gs activation in endosomes is introduced, and suggest that this step is sufficient to explain

the location-aware nature of downstream transcriptional control.

2.4 Discussion

The present study addressed the question of how GPCR-Gs activation in endosomes is coupled downstream to a cAMP-dependent transcriptional response. We focused on the B2AR as an interesting example because the transcriptional response elicited by this GPCR, when studied at its endogenous expression level, is endocytosis-dependent even though B2AR-Gs activation from endosomes does not produce a large increase in the overall amount or duration of cytoplasmic cAMP elevation. This provides additional support for the conclusion that transcriptional signaling elicited by endogenous B2AR-Gs activation is determined primarily by the subcellular location of upstream cascade activation, rather than by its overall amount or timing. We investigated the cellular basis of such 'location-aware' downstream signaling, and resolved the overall cAMP response elicited by endogenous B2AR-Gs activation into two phases. A peak phase is characterized by a large but transient increase in the overall concentration of cAMP, and this is followed by a plateau phase of more moderate cAMP elevation which persists in the continued presence of agonist but is still agonist-dependent (**Figures 2.8a&b**). PKAcat rapidly disperses throughout the cytoplasm during the peak phase of the overall cAMP response and re-accumulates in the perinuclear pool during the plateau phase, effectively mirroring the overall cAMP response (**Figure 2.8c**). Interestingly, neither of these behaviors requires endocytosis, and the endocytosis-dependent nature of the downstream transductional response is introduced instead one step downstream – at the stage of nuclear accumulation of PKAcat – with subsequent steps in the pathway following both in their kinetics and sensitivity to endocytic inhibition. Taken together, these results support a model of endosomal signaling via the cAMP cascade that uses the subcellular location of activation as a primary cue, and conveys location-aware information downstream by nuclear accumulation of PKAcat.

Previous studies indicate that polypeptide hormone receptors use endocytosis to produce a high level of cAMP accumulation in the cytoplasm which is sustained after agonist removal. We show here that the B2AR produces high-level cAMP accumulation transiently, defining the peak phase of the response, and that this phase is only moderately prolonged by endocytosis. The transient peak is followed by a markedly reduced (~10-fold) degree of cAMP elevation, defining the plateau phase, which is only slightly enhanced by endocytosis and remains ligand-dependent because it is rapidly reversed by antagonist. Previous studies have identified a cellular mechanism for transducing the nuclear effects of sustained and high-level cAMP elevation, based on the activation of a discrete pool of PKA holoenzyme that is restricted to the nucleus and is relatively insensitive to cAMP based on scaffolding with PDE4 (Clister et al., 2019). This mechanism is unlikely to transduce the transcriptional response elicited by endosomal B2AR-Gs activation because cytoplasmic cAMP reaches a high concentration only transiently. Thus we believe that the downstream transduction of endosomal B2AR-Gs activation relies on a different cellular mechanism, based instead on nuclear accumulation of PKAcat from the cytoplasm.

We anticipate that these different cellular mechanisms for achieving downstream signaling selectivity to the nucleus can operate together in the same cells, and are deployed to different degrees depending on the particular receptor activated. Considering that polypeptide hormone receptors and B2ARs have been shown to be able to transit the same endosomes after ligand-induced internalization, it is also possible that these mechanisms operate together in the same compartment and contribute to synergistic effects across GPCRs. We also note that endocytosis inherently changes the location of upstream cascade activation irrespective of the particular GPCR internalized, and that unleashing of PKAcat from the perinuclear cytoplasmic pool was shown previously to contribute to cAMP-dependent signal transduction to the nucleus elicited by

47

polypeptide hormone receptors. Conversely, the present results indicate that endocytosis produces a moderate increase in the duration of the peak phase of high-level cAMP accumulation elicited by the B2AR, albeit not to the extent of producing a sustained and high-level cAMP accumulation response as is the case for polypeptide hormone receptors. Accordingly, these fundamentally different cellular mechanisms of endosomal signal specification may operate together even for an individual GPCR. If so, this could enable cells to further enhance the specificity of signaling downstream of endosomal GPCR-Gs activation.

These results provide significant insight into the cellular basis of location-aware cAMP signaling from endosomes, but they also raise additional questions about its underlying biochemical basis that remain to be investigated. For example, it is presently unknown which adenylyl cyclase isoform(s) mediate location-aware signaling from endosomes. Mammals express nine transmembrane adenylyl cyclase (AC) isoforms that are directly activated by G_s, with two presently implicated in sustained cAMP signaling from endosomes elicited by polypeptide hormone receptors (Sunahara & Taussig, 2002). Mammals also express another AC isoform (AC10 or sAC) that lacks any transmembrane domains and is not directly activated by G_s, yet is also implicated in signaling from endosomes (Inda et al., 2016). It is not known if the same AC isoforms that mediate sustained endosomal responses also mediate transient cAMP elevation followed by a ligand-dependent plateau phase, which is characteristic of location-aware signaling by the B2AR. We also do not know if there exist other proteins, besides the core cascade components studied here, needed at the endosome membrane to confer signaling specificity to the nucleus. For example, signaling specificity downstream of GPCR-Gs activation at the plasma membrane critically depends on scaffolding by A-kinase anchoring proteins (AKAPs), and AKAPs are known that localize to endosomes (Søberg & Skålhegg, 2018; Taylor et al., 2012). What function(s) such scaffold proteins have in determining signaling specificity from endosomes, and what other

scaffold-associated proteins might also contribute, are additional questions raised by the present results that merit future investigation.

The ability of the cAMP cascade to mediate location-aware signaling from endosomes also raises interesting biophysical questions, particularly with regard to the diffusible nature of cAMP and PKAcat. At presently estimated rates of free diffusion, both cAMP and PKAcat would be expected to equilibrate throughout the cytoplasm within several seconds or less. This is advantageous for endosomal responses that are conveyed to the nucleus by a sustained elevation of overall cytoplasmic cAMP concentration, but is problematic for location-aware responses conveyed by nuclear accumulation of PKAcat. Whereas cAMP generated from endosomes is already known to locally activate PKA in the perinuclear region through enforced proximity and membrane tethering, locally unleashed PKAcat must then accumulate in the nucleus. Based on previous studies indicating that PKAcat enters the nucleus by diffusion and is then actively exported (Harootunian et al., 1993; Wen et al., 1995), we assume that endocytosis-dependent nuclear accumulation of PKAcat reflects an increase in unleashed PKAcat entry; this would require an increased free concentration at the outer nuclear membrane to drive nuclear entry by mass action. Endosomes in which B2AR-Gs activation has been shown are readily resolved from the nucleus using diffraction-limited confocal microscopy, indicating that they are at least 200 nm away. However, local concentration gradients around sites of diffusible mediator production typically dissipate within a distance scale of tens of nanometers. These considerations reveal a distance 'gap' that we presently cannot explain, as we do presently do not detect an obvious effect of endocytosis on PKAcat localization or dynamics in the perinuclear region.

One possible explanation is that we are missing a population of endosomes that are located closer to the nucleus than we are presently able to resolve, and are the actual sites of location-aware signaling to the nucleus. Another possibility is that we are missing an additional endocytosis-dependent protein (such as a regulator of nuclear import or export) that conveys a longer-range effect on nuclear PKAcat. A third possibility is suggested by the present FRAP data, revealing a rate of PKAcat fluorescence recovery 10-100 fold slower than expected from free diffusion. In principle, this could reflect slow equilibration of a rapidly diffusing protein pool due to limited availability of binding sites, or it could reflect slowed effective diffusion due to rapid binding of PKAcat and 'hopping' from one site to another. We suggest that the latter behavior is possible because PKA regulatory subunits are present at high concentration in the cytoplasm and in substantial excess to PKAcat that they bind, and because the rate of PKAcat:PKAreg association approaches the diffusion limit *in vitro*. If slow FRAP kinetics indeed reflect an effective diffusion regime during the plateau signaling phase, this by itself could significantly increase the distance scale over which local unleashing of PKAcat is propagated in the plateau phase. Future studies, using additional biochemical and biophysical approaches, will be required to test this hypothesis, and to further elucidate other aspects of the discrete cellular mechanism of location-aware signaling to the nucleus that the present results delineate.

2.5 Acknowledgements

2.6 Materials and methods

Cell culture

Human HEK293 and HEK293T cells were grown in DMEM (Gibco, 11965) supplemented with 10%

fetal bovine serum (UCSF Cell Culture Facility). Cells were grown at 37°C and 5% CO_2 in a

humidified incubator. HEK293 stable cell lines, FLAG-β2AR (Cao et al., 1999) and GloSensor20F-

IRES-Rluc, were generated from the parent cell line by transfection of the plasmid of interest

followed by antibiotic selection.

DNA transfections

Cells were seeded at 70% confluency in a well of a 6 well plate (Corning) or a 35 mm imaging dish

(MatTek, P35G-1.5-14-C) and transfected overnight with 4 μL Lipofectamine 2000 (Invitrogen).

Media was changed the next day and cells were used within 24-48 hours post transfection for

experimentation.

Table 2.1 Amounts of transfected DNA constructs

Plasmid	Amount (ng)
pcDNA3	300
pcDNA3 mCherry-Dyn1	300
pcDNA3 mCherry-Dyn1-K44E	300
pcDNA3.1+ 2x NLS mNG21-10 IRES TagBFP	400
pcDNA3.1+ SSF-B2AR	1000

siRNA transfections

Cells were seeded at 30% confluency in a 10 cm dish and transfected overnight with 200 pmol

siRNA (Qiagen) with 24 μL RNAiMax Lipofectamine (Invitrogen). Media was changed the next day

and cells recovered for another 48 hours before experimentation. If DNA transfection was

performed, cells were transfected with DNA and Lipofectamine 2000 (Invitrogen) 24 hours before

experimentation. The siRNAs used were All Star Negative (Control; Qiagen, SI03650318) and *CHC17* siRNA (Qiagen, 5'-AAGCAATGAGCTGTTTGAAGA-3').

Endocytic blockade by Dyngo-4A

Cells treated with Dyngo-4A were first changed to serum free media. Then DMSO (control) or 30 µM Dyngo-4A was added to cells for 15 minutes to block endocytosis prior to the experiment.

DNA constructs

cAMP luminescence biosensor with renilla luciferase

pSF CMV GloSensor20F IRES Rluc was made from pSF CMV EMCV Rluc (Boca Scientific) and pGloSensor-20F (Promega). GloSensor20F DNA was PCR amplified, and 5' EcoRI and 3' EcoRV sites were added. The vector, pSF CMV EMCV Rluc, was digested with EcoRI and EcoRV and an InFusion (Clontech) reaction was used to insert GloSensor20F into the vector.

Nuclear localized mNG2$_{1-10}$

pcDNA3.1+ 2xNLS mNG2$_{1-10}$ IRES TagBFP was made by a multiple insert ligation with QuickLigase (NEB) put all inserts into pcDNA3.1+ (Clontech). A gBlock (IDT) of 2x NLS (SV40) mNG2$_{1-10}$ was ordered and PCR amplified with 5' BamHI and 3' XhoI AgeI NotI. An IRES fragment was PCR amplified from pSF CMV EMCV Rluc (Boca Scientific) with 5' AgeI and 3' XhoI. Lastly, TagBFP was amplified with 5' XhoI and 3' XbaI.

cAMP fluorescence biosensor

The cAMP fluorescence biosensor was generated from a human Epac2 cAMP FRET sensor with the cpGFP from Green GECO 1.0 (Zhao et al., 2011). H4 and H6 helix-containing fragments of the

Epac2-derived cAMP-binding module were inserted in place of the M13 peptide and EF hand-containing calcium binding modules in GCaMP6f, respectively, using a variable linker strategy in E. coli.

cAMP fluorescent biosensor development

Primary screening was carried out by assay of isoproterenol-dependent fluorescence changes in HEK293 cells transiently transfected with plasmid DNA minipreps using Lipofectamine 2000 (Invitrogen) per the manufacturer's instructions, imaged by epifluorescence microscopy and selecting for an upward-deflecting fluorescence response. Primary screening was performed by imaging of living cells in HEK293 cells 24 hours after transfection in MatTek dishes using a custom-built 37℃ incubation chamber fit to an inverted epifluorescence microscope (Nikon TE2000) equipped with a 20X NA 0.5 Plan Fluor objective and custom-built LED illuminator with 485/20x bandpass emission filter (Chroma). Images were collected through a 504 nm dichroic mirror and 525/30m bandpass filter (Chroma) using a cooled CCD camera (Roper CoolSNAP HQ), with LED illumination and fluorescence acquisition controlled using Micromanager and ImageJ. Kinetic analysis was carried out on serial image stacks collected in the linear range of detection using Plot Profile in ImageJ.

HEK293T mNG2-PKAcat cells

Cells were obtained from the Huang lab at UCSF. Briefly, HEK293T cells expressing mNG2$_{1-10}$ were electroporated with Cas9/sgRNA RNP complexes and the HDR template for the PKAcat gene, PRKACA. Electroporated cells were cultured for 5-10 days before FACS selection for 488-GFP positive cells. Next, genomic DNA was extracted from the knock-in cell line and the genomic DNA

was amplified with three primer sets around the knock-in site. The amplified products were sent for sequencing to verify knock-in of mNG2$_{11}$ at the N-terminus of PKAcat.

RNA extraction

RNA was isolated from cells using the QIAshredder and RNeasy Mini kit (Qiagen, 79654 and 74104, respectively). Briefly, after treatment, cells in a 6 well plate were placed on ice and washed once with cold PBS. Then cells were lysed, and RNA was extracted by following the manufacturer's protocol. RNA was eluted in 30-50 µL of DEPC H$_2$O, and the concentration of each sample was determined.

Reverse transcription reaction

cDNA was generated from RNA using the SuperScript III First-strand synthesis system (Invitrogen, 18080-051). Briefly, 2 µg of RNA was used per reaction primed with oligo dT. The reverse transcription reaction was performed according to the manufacturer's protocol.

qRT-PCR

qRT-PCR was performed using a StepOnePlus (Applied Biosystems) instrument. cDNA generated from extracted RNA was used as the input for the qRT-PCR, with amplification by Power SYBR Green PCR master mix (Applied Biosystems, 4367659). Levels of transcripts were normalized to *GAPDH*. The primer pairs used is in **Table 2.2**.

Table 2.2 qRT-PCR primer sequences

Primer	Sequence
GAPDH forward	5'-CTGCCCAAGATCTTCCATGT-3'
GAPDH reverse	5'-GACAAGCTTCCCGTTCTCAG-3'
PCK1 forward	5'-CTGCCCAAGATCTTCCATGT-3'
PCK1 reverse	5'-CAGCACCCTGGAGTTCTCTC-3'
CHC17 forward	5'-ACTTAGCCGGTGCTGAAGAA-3'
CHC17 reverse	5'-AACCGACGGATAGTGTCTGG-3'

cAMP luminescence assay

HEK293 cells stably expressing a cAMP luciferase-based biosensor (GloSensor20F-IRES-Rluc) were lifted and resuspended in imaging media (DMEM without phenol red (Gibco, 31053) supplemented with 30 mM HEPES). These cells were then incubated with 1.6 mM D-luciferin (Gold Biotechnology, LUCNA-1g) for one hour at 37°C and 5% CO_2 in a humidified incubator and distributed into a 24 well plate (200 μL/well). Immediately before imaging, cells were treated with 200 μL imaging media only (DMEM without phenol red supplemented with 30 mM HEPES; Gibco 31053 and 15630 respectively) or imaging media with isoproterenol (100 nM final; Sigma, I6504) and placed into a 37°C heated light-proof chamber, then imaged every 10 seconds for 20 minutes. When the cAMP luminescence image series finished, 100 μL of 5x stop buffer (to eliminate firefly luciferase luminescence) with 10 μM coelenterazine (Gold Biotechnology, CZ2.5) was added to each well. Renilla luciferase luminescence was immediately imaged at 10 second intervals for one minute.

Images were acquired by a 512×512 pixel electron multiplying CCD sensor (Hamamatsu C9100-13) using Micro-Manager. Using Fiji, ROIs were drawn around each well, and corresponding background ROIs were placed in an area without cells. Intensity over time was measured and corrected for background luminescence for both firefly and renilla luciferase values. The renilla

luminescence values over the time series was averaged (renilla$_{avg}$). A ratio (i$_{f/r}$) of firefly to renilla$_{avg}$ luminescence was calculated per well over time. Next, each time series was initialized to the average of the first 5 time points (i$_{new}$ = i$_{f/r}$ - i$_{savg}$). The max (average of the top 5 proximal values) of each isoproterenol treated condition was determined, and each condition was normalized to the max of the control isoproterenol treated sample.

Spinning disk confocal imaging

Imaging was performed on a Nikon Ti inverted spinning disk confocal microscope (Yokogawa CSU-W1) with 405-, 488-, 561- and 640-solid-state lasers (Andor) and an Andor Zyla 4.2 sCMOS camera controlled by μManager (2.1 beta) software. Cells were kept in imaging media (DMEM without phenol red supplemented with 30 mM HEPES) and were maintained in a temperature- and humidity-controlled chamber (Okolab) during imaging.

cAMP fluorescence imaging assay

Images were acquired with the spinning disk confocal microscope previously described using a Plan Apo λ 20x 0.75 NA objective (Nikon). Cells were imaged every 20 seconds for 45 minutes at 37°C. Cells were treated with 100 nM isoproterenol (Iso) at 5 minutes, 10 μM alprenolol (Alp) at 35 minutes, and 10 μM FSK and 500 μM isobutylmethylxanthine (IBMX) at 40 minutes.

ROIs were drawn around the entire cell, with corresponding ROIs of the same size were placed in an area nearby without cells to determine the background signal. Each cell fluorescence intensity was background subtracted. Next, the reference fluorescence was set to be the fluorescence at 5 minutes right as 100 nM isoproterenol was to be added. The change in fluorescence over the reference fluorescence was then determined for all time points.

Perinuclear PKAcat redistribution assay

Images were acquired with the spinning disk confocal microscope previously described using a Plan Apo VC 60x 1.4 NA objective (Nikon). Cells were imaged every 5 minutes for 35 minutes, except for additional time points at 30 seconds and one minute. Cells were treated with imaging media only (untreated) or 100 nM Iso in imaging media immediately after the initial image (~t=5s).

ROIs were drawn around perinuclear PKAcat with corresponding ROIs of the same size placed in a nearby area without cells to determine the background signal. The perinuclear fluorescence intensity was background subtracted. Each time point was normalized to the initial intensity for each condition.

Fixed imaging of nuclear PKAcat

HEK293T mNG2-PKAcat cells were either Untransfected or transfected with 2x NLS mNG2$_{1-10}$ IRES TagBFP were plated on poly-L-lysine (Sigma, P8920) coated coverslips (Fisher, 12-545-100) in 12 well plates. Cells untreated or treated with 100 nM isoproterenol for 45 minutes at 37°C. Cells were then washed 3 times with PBS and fixed with 3.7% formaldehyde (Fisher, F79) in PBS for 20 minutes. Cells were washed again with PBS followed by a TBS wash. Cells were stained with 1 µM DRAQ5 (Invitrogen, 62251) in PBS for 5 minutes. Cells were washed with PBS and mounted on glass slides with ProLong Gold Antifade mounting media (Invitrogen, P10144). Slides were stored for a minimum of 24 hours to allow mounting media to dry before imaging. Cells were imaged on the previously described spinning disk confocal microscope using a Plan Apo VC 60x 1.4 NA objective (Nikon).

First, the 647 nm channel was selected to draw ROIs in nuclei of all cells in the field of view. Next,

for cells transfected with 2x NLS mNG2$_{1-10}$ IRES TagBFP, ROIs were retained for cells positive in the

405 nm channel. Then, for cells transfected with mCherry-Dyn1-K44E, ROIs were retained for cells

positive in the 561 nm channel. Lastly, ROIs were checked that they only contained the nucleus of

mNG2-PKAcat expressing cells by checking the 488 nm channel. Corresponding background

ROIs were taken in an area without any cells, and the intensity of the nuclear ROI was background

subtracted. Intensities of each condition were averaged, and the 45 minute treated samples were

normalized to the corresponding untreated samples.

Nuclear PKAcat accumulation live imaging assay

HEK293T mNG2-PKAcat cells transfected with 2x NLS mNG2$_{1-10}$ IRES TagBFP were imaged with

the spinning disk confocal microscope previously described using a Plan Apo VC 60x 1.4 NA

objective (Nikon). Cells were initially imaged at 0, 0.5, 1 and 5 minutes, then were imaged every 5

minutes for 45 minutes at 37°C. Cells were treated with 100 nM isoproterenol (Iso) immediately

after the time lapse started (within ~5 s).

Transfected cells were first identified by checking the 647 nm channel. ROIs marking transfected

cells were first draw then adjusted to mark the nucleus of each transfected cell. Corresponding

background ROIs were not used as background intensity was not always less than the intensity

from the nuclear ROI. The change in fluorescence over the initial fluorescence was then determined

for all time points.

Fluorescence recovery after photobleaching of perinuclear PKAcat

Images were acquired with the spinning disk confocal microscope previously described using a Plan Apo VC 100x 1.4 NA objective (Nikon). A Rapp Optoelectronic UGA-40 photobleaching system was used to photobleach mNG$_2$-PKAcatα in an ROI primarily containing the Golgi with a 473 nm laser (Vortran). Cells were imaged at 10 second intervals for 5.5 minutes (except for an added interval of 5 seconds before photobleaching) and photobleached at 30 seconds to monitor fluorescence recovery after photobleaching.

Quantitative image analysis was performed on unprocessed images using Fiji software by drawing ROIs around the bleach spot and taking the fluorescence intensity from each frame. Corresponding ROIs in areas without cells were used for background subtraction. Intensity frame immediately following photobleaching was set to zero, then the intensity at each time point was normalized to the initial intensity.

CREB phosphorylation

After treatment with isoproterenol, cells in a 6 well plate were lysed on ice with 200 μL/well RIPA buffer (50 mM Tris, 150 mM NaCl, 1% Triton X-100, 0.5% Sodium Deoxycholate, 0.1% Sodium Dodecyl Sulfate) containing Complete Mini, EDTA-free (Roche, 11836170001) and PhosSTOP (Roche, 04906837001) for 25 minutes. Lysates were then transferred to microcentrifuge tubes and spun for 10 minutes at 14,000 rpm at 4°C. The supernatant was then saved and used for immunoblot experiments. Protein concentration was determined by BCA Protein Assay (Thermo Fisher, 23225).

Protein samples were mixed with NuPage LDS Sample Buffer (Invitrogen, NP0007) and 1 mM dithiothreitol (DTT) (Sigma, D0632). Samples were loaded into a NuPAGE 4-12% Bis-Tris Protein gel (Invitrogen, NP0335BOX) and transferred to nitrocellulose prior to immunoblot analysis.

Nuclear cytoplasmic separation

Nuclear-cytoplasmic separation was performed using the NE-PER Nuclear and Cytoplasmic Extraction Reagents (Thermo Scientific, 78833) and according to the manufacturer's protocol. Briefly, after treatment with isoproterenol, cells were washed with PBS then lifted with TrypLE Select (Gibco, 12563) from a 6 cm dish. Cells were transferred to a microcentrifuge tube and spun down at 500 g for 5 minutes. The cell pellet was washed with PBS and spun again at 500 g for 3 minutes. Then cell pellets were placed on ice and resuspended with 200 µL CER I, vortexed and placed back on ice for 10 minutes. Next, 11 µL of CER II was added to each tube and vortexed briefly and put on ice for 1 minute. The tubes were then spun at 20,000 g for 5 minutes. The supernatant was removed and saved as the cytoplasmic fraction. To obtain the nuclear fraction, 100 µL NER was added to the pellet and the pellet was vortexed briefly 5 times with 10 minute incubations on ice in between. Then the samples were spun down at 20,000 g for 10 minutes, and the supernatant was saved as the nuclear fraction.

Protein samples were mixed with NuPage LDS Sample Buffer (Invitrogen, NP0007) and 1 mM dithiothreitol (DTT) (Sigma, D0632). Samples were loaded into a NuPAGE 4-12% Bis-Tris Protein gel (Invitrogen, NP0336BOX) and transferred to nitrocellulose prior to immunoblot analysis.

Immunoblot analysis

After transfer onto nitrocellulose, membranes were stained with Ponceau S solution (Sigma, P7170-1L) to check for transfer quality. Membranes were washed with PBS to remove the Ponceau S solution before blocking with Odyssey blocking buffer. For blots where phosphorylated CREB was to be detected, Odyssey TBS blocking buffer (LI-COR Biosciences, 927-50000) was used, otherwise all other blots used Odyssey PBS blocking buffer (LI-COR Biosciences, 927-40000). The following primary antibodies were used to probe for proteins with interested with the corresponding secondary antibodies. The blots were imaged on an Odyssey Infrared Imaging System (LI-COR Biosciences) and bands were analyzed by ROI analysis with background subtraction in Fiji.

Table 2.3 Antibodies used for immunoblot detection of proteins

Antibody	Manufacturer	Catalog #
Mouse anti CREB (86B10)	Cell Signaling Technologies	9104
Rabbit anti pCREB (S133) (87G3)	Cell Signaling Technologies	9198
Rabbit anti PKA C-α	Cell Signaling Technologies	4782
Mouse anti HDAC2 (3F3)	Cell Signaling Technologies	5113
Mouse anti α-tubulin (DM1A)	Cell Signaling Technologies	3873
IRDye 680RD Donkey anti-Mouse IgG	LI-COR Biosceinces	926-68072
IRDye 800CW Donkey anti-Rabbit IgG	LI-COR Biosceinces	926-32213

Supplemental Materials and Methods

Flow cytometry

Cell surface fluorescence of HEK293 cells stably expressing FLAG-β2AR was measured to determine receptor endocytosis. Cells were incubated with 100 nM isoproterenol for 30 minutes at 37°C to internalize receptors to steady state. After treatment, cells were washed with cold PBS three times, then incubated with 1 µg/ml AlexaFluor647-conjugated (Invitrogen, A20173) M1 mouse anti Flag monoclonal (Sigma, F-3040) antibody at 4°C for one hour on a shaker. Cells were mechanically lifted and mean fluorescence was read by flow cytometry for each sample on a FACSCalibur (BD). Each condition had three technical replicates per biological replicate.

cAMP fluorescence sensor secondary screen

Secondary screening and cAMP concentration-response determination were carried out in vitro using a cytoplasmic fraction prepared from transiently transfected HEK293 cells by Dounce homogenization in 100 mM KCl 30 mM HEPES pH7.4 and PMSF followed by centrifugation at 40,000 g for 10 minutes. The supernatant was maintained on ice, adjusted to 1 mg/mL total protein concentration and then supplemented with 100 µM isobutylmethylxanthine (IBMX; Sigma, I5879) before assays. Fluorescence was monitored using 100 µL aliquots in a 96-well plate, at room temperature and in the presence of added cAMP as indicated, using a Gemini XPS fluorimeter (Molecular Dynamics) set to 488 nm excitation and 510 nm emission. Mean values derived from duplicate fluorescence determinations were analyzed according to a single-site binding model ($F / Fo = max * [cAMP] / \{[cAMP] + K_D\}$) fit by a non-linear regression method (sigmoidal, 4PL, least squares fit) using Prism (GraphPad).

HEK293T immunoblot for PKAcat

The parent cell line, HEK293T mNG2$_{1-10}$ and the knock-in cell line, HEK293T mNG2-PKAcat were both lysed with RIPA buffer containing Complete Mini, EDTA-free protease inhibitor. Cells were collected in microcentrifuge tubes and spun down at 14,000 rpm for 10 minutes at 4°C. The supernatant was removed and saved for immunoblot analysis. Protein concentrations were determined by BCA protein assay.

Detection of nuclear PKAcat in HEK293T mNG2-PKAcat cells by live imaging

HEK293T mNG2-PKAcat cells were imaged either untreated or treated with 10 µM FSK and 100 µM IBMX for 60 minutes. Images at 0 minutes and 60 minutes were acquired on a Nikon Ti inverted spinning disk confocal microscope (Yokogawa CSU-22) with a custom 405-, 488-, 561- and 640-laser launch, with an Apo TIRF 100x/1.49 NA Oil objective (Nikon) and a Photometrics Evolve Delta EMCCD camera controlled by Nikon Elements software. Cells were kept in a temperature- and humidity-controlled chamber (Okolab) during imaging.

Photobleaching recovery non-linear curve fit

Photobleaching data was replotted to set the time of bleaching at 0 seconds. Non-linear regression (sigmoidal, 4PL) was then performed on each condition using Prism (GraphPad) to determine half-time and plateau values.

2.7 References

Agarwal, S. R., Clancy, C. E., & Harvey, R. D. (2016). Mechanisms Restricting Diffusion of

　　Intracellular cAMP. *Scientific Reports*, *6*(1), 19577. https://doi.org/10.1038/srep19577

Allen, J. A., & Roth, B. L. (2011). Strategies to Discover Unexpected Targets for Drugs Active at G

　　Protein–Coupled Receptors. *Annual Review of Pharmacology and Toxicology*, *51*(1), 117–

　　144. https://doi.org/10.1146/annurev-pharmtox-010510-100553

Brindle, P. K., & Montminy, M. R. (1992). The CREB family of transcription activators. *Current

　　Opinion in Genetics & Development*, *2*(2), 199–204. Retrieved from

　　http://www.ncbi.nlm.nih.gov/pubmed/1386267

Calebiro, D., Nikolaev, V. O., Gagliani, M. C., De Filippis, T., Dees, C., Tacchetti, C., … Lohse, M.

　　J. (2009). Persistent cAMP-signals triggered by internalized G-protein-coupled receptors.

　　PLoS Biology, *7*(8). https://doi.org/10.1371/journal.pbio.1000172

Cao, T. T., Deacon, H. W., Reczek, D., Bretscher, A., & von Zastrow, M. (1999). A kinase-

　　regulated PDZ-domain interaction controls endocytic sorting of the β2-adrenergic receptor.

　　Nature, *401*(6750), 286–290. https://doi.org/10.1038/45816

Clister, T., Greenwald, E. C., Baillie, G. S., Zhang, J., & Zhang Correspondence, J. AKAP95

　　Organizes a Nuclear Microdomain to Control Local cAMP for Regulating Nuclear PKA _

　　Elsevier Enhanced Reader.pdf. , 26 Cell Chemical Biology § (2019).

Esseltine, J. L., & Scott, J. D. (2013). AKAP signaling complexes: pointing towards the next

　　generation of therapeutic targets? *Trends in Pharmacological Sciences*, *34*(12), 648–655.

　　https://doi.org/10.1016/j.tips.2013.10.005

Feng, S., Sekine, S., Pessino, V., Li, H., Leonetti, M. D., & Huang, B. (2017). Improved split

　　fluorescent proteins for endogenous protein labeling. *Nature Communications*, *8*(1), 370.

　　https://doi.org/10.1038/s41467-017-00494-8

Ferrandon, S., Feinstein, T. N., Castro, M., Wang, B., Bouley, R., Potts, J. T., … Vilardaga, J.-P. (2009). *Sustained cyclic AMP production by parathyroid hormone receptor endocytosis*. *5*(10), 734–742. https://doi.org/10.1038/nchembio.206

Gonzalez, G. A., & Montminy, M. R. (1989). Cyclic AMP stimulates somatostatin gene transcription by phosphorylation of CREB at serine 133. *Cell*, *59*(4), 675–680. https://doi.org/10.1016/0092-8674(89)90013-5

Goulding, J., May, L. T., & Hill, S. J. (2018). Characterisation of endogenous A2A and A2B receptor-mediated cyclic AMP responses in HEK 293 cells using the GloSensor™ biosensor: Evidence for an allosteric mechanism of action for the A2B-selective antagonist PSB 603. *Biochemical Pharmacology*, *147*, 55–66. https://doi.org/10.1016/J.BCP.2017.10.013

Hagiwara, M., Brindle, P., Harootunian, A., Armstrong, R., Rivier, J., Vale, W., … Montminy2, M. R. *Coupling of Hormonal Stimulation and Transcription via the Cyclic AMP-Responsive Factor CREB is Rate Limited by Nuclear Entry of Protein Kinase A.* , 13 § (1993).

Harootunian, A. T., Adams, S. R., Wen, W., Meinkoth, J. L., Taylor, S. S., & Tsien, R. Y. (1993). Movement of the free catalytic subunit of cAMP-dependent protein kinase into and out of the nucleus can be explained by diffusion. *Molecular Biology of the Cell*, *4*(10), 993–1002. https://doi.org/10.1091/mbc.4.10.993

Hauser, A. S., Attwood, M. M., Rask-Andersen, M., Schiöth, H. B., & Gloriam, D. E. (2017). Trends in GPCR drug discovery: new agents, targets and indications. *Nature Reviews Drug Discovery*, *16*(12), 829–842. https://doi.org/10.1038/nrd.2017.178

Inda, C., Claro, P. A. dos S., Bonfiglio, J. J., Senin, S. A., Maccarrone, G., Turck, C. W., & Silberstein, S. (2016). Different cAMP sources are critically involved in G protein-coupled receptor CRHR1 signaling. *Journal of Cell Biology*, *214*(2), 181–195. https://doi.org/10.1083/jcb.201512075

Irannejad, R., Pessino, V., Mika, D., Huang, B., Wedegaertner, P. B., Conti, M., & von Zastrow, M. (2017). Functional selectivity of GPCR-directed drug action through location bias. *Nature Chemical Biology*, *13*(7), 799–806. https://doi.org/10.1038/nchembio.2389

Irannejad, R., Tomshine, J. C., Tomshine, J. R., Chevalier, M., Mahoney, J. P., Steyaert, J., … von Zastrow, M. (2013). Conformational biosensors reveal GPCR signalling from endosomes. *Nature*, *495*(7442), 534–538. https://doi.org/10.1038/nature12000

Kamiyama, D., Sekine, S., Barsi-Rhyne, B., Hu, J., Chen, B., Gilbert, L. A., … Huang, B. (2016). Versatile protein tagging in cells with split fluorescent protein. *Nature Communications*, *7*, 11046. https://doi.org/10.1038/ncomms11046

Kotowski, S. J., Hopf, F. W., Seif, T., Bonci, A., & von Zastrow, M. (2011). Endocytosis Promotes Rapid Dopaminergic Signaling. *Neuron*, *71*(2), 278–290. https://doi.org/10.1016/j.neuron.2011.05.036

Leonetti, M. D., Sekine, S., Kamiyama, D., Weissman, J. S., Huang, B., Fig, D., & Gfp, F. (2016). A scalable strategy for high-throughput GFP tagging of endogenous human proteins. *Proceedings of the National Academy of Sciences*, *113*(25), 10–12. https://doi.org/10.1073/pnas.1606731113

Lobingier, B. T., & von Zastrow, M. (2019). When trafficking and signaling mix: How subcellular location shapes G protein-coupled receptor activation of heterotrimeric G proteins. *Traffic*, *20*(2), 130–136. https://doi.org/10.1111/tra.12634

Lohse, C., Bock, A., Maiellaro, I., Hannawacker, A., Schad, L. R., Lohse, M. J., & Bauer, W. R. (2017). Experimental and mathematical analysis of cAMP nanodomains. *PLOS ONE*, *12*(4), e0174856. https://doi.org/10.1371/journal.pone.0174856

Lyga, S., Volpe, S., Werthmann, R. C., Gotz, K., Sungkaworn, T., Lohse, M. J., … Calebiro, D. (2016). Persistent cAMP Signaling by Internalized LH. *Endocrinology*, *157*(April), 1613–1621.

https://doi.org/10.1210/en.2015-1945

Mayr, B., & Montminy, M. (2001). Transcriptional regulation by the phosphorylation-dependent factor CREB. *Nature Reviews Molecular Cell Biology*, *2*(8), 599–609. https://doi.org/10.1038/35085068

Mccluskey, A., Daniel, J. A., Hadzic, G., Chau, N., Clayton, E. L., Mariana, A., … Robinson, P. J. (2013). Building a better dynasore: The dyngo compounds potently inhibit dynamin and endocytosis. *Traffic*, *14*(12), 1272–1289. https://doi.org/10.1111/tra.12119

Montminy, M. R., & Bilezikjian, L. M. (1986). Binding of a nuclear protein to the cyclic-AMP response element of the somatostatin gene. In *28. Murashige, T. & Skoog, F. Physiol. Pl. IS* (Vol. 322). Retrieved from Plenum website: https://www.nature.com/articles/328175a0.pdf

Nigg, E. A., Hilz, H., Eppenberger, H. M., & Dutly, F. (2000). *Rapid and reversible translocation of the catalytic subunit of cAMP-dependent protein kinase type II from the Golgi complex to the nucleus*. *4*(l), 2801–2806.

Slessareva, J. E., Routt, S. M., Temple, B., Bankaitis, V. A., & Dohlman, H. G. (2006). Activation of the Phosphatidylinositol 3-Kinase Vps34 by a G Protein α Subunit at the Endosome. *Cell*, *126*(1), 191–203. https://doi.org/10.1016/J.CELL.2006.04.045

Søberg, K., & Skålhegg, B. S. (2018). The Molecular Basis for Specificity at the Level of the Protein Kinase a Catalytic Subunit. *Frontiers in Endocrinology*, *9*, 538. https://doi.org/10.3389/fendo.2018.00538

Sunahara, R. K., & Taussig, R. (2002). Isoforms of mammalian adenylyl cyclase: multiplicities of signaling. *Molecular Interventions*, *2*(3), 168–184. https://doi.org/10.1124/mi.2.3.168

Taylor, S. S., Ilouz, R., Zhang, P., & Kornev, A. P. (2012). Assembly of allosteric macromolecular switches: lessons from PKA. *Nature Reviews Molecular Cell Biology*, *13*. https://doi.org/10.1038/nrm3432

Tsvetanova, N. G., Irannejad, R., & von Zastrow, M. (2015). G protein-coupled receptor (GPCR) signaling via heterotrimeric G proteins from endosomes. *The Journal of Biological Chemistry*, *290*(11), 6689–6696. https://doi.org/10.1074/jbc.R114.617951

Tsvetanova, N. G., & von Zastrow, M. (2014). Spatial encoding of cyclic AMP signaling specificity by GPCR endocytosis. *Nature Chemical Biology*, *10*(12), 1061–1065. https://doi.org/10.1038/nchembio.1665

van der Bliek, A. M., Redelmeier, T. E., Damke, H., Tisdale, E. J., Meyerowitz, E. M., & Schmid, S. L. (1993). Mutations in human dynamin block an intermediate stage in coated vesicle formation. *The Journal of Cell Biology*, *122*(3), 553–563. https://doi.org/10.1083/jcb.122.3.553

Vassilopoulos, S., Esk, C., Hoshino, S., Funke, B. H., Chen, C.-Y., Plocik, A. M., … Brodsky, F. M. (2009). A Role for the CHC22 Clathrin Heavy-Chain Isoform in Human Glucose Metabolism. *Science*, *324*(5931), 1192–1196. https://doi.org/10.1126/science.1171529

Violin, J. D., DiPilato, L. M., Yildirim, N., Elston, T. C., Zhang, J., & Lefkowitz, R. J. (2008). beta2-adrenergic receptor signaling and desensitization elucidated by quantitative modeling of real time cAMP dynamics. *The Journal of Biological Chemistry*, *283*(5), 2949–2961. https://doi.org/10.1074/jbc.M707009200

von Zastrow, M., & Kobilka, B. K. (1992). Ligand-regulated internalization and recycling of human beta 2-adrenergic receptors between the plasma membrane and endosomes containing transferrin receptors. *Journal of Biological Chemistry*, *267*(5), 3530–3538.

Wen, W., Meinkotht, J. L., Tsien, R. Y., & Taylor, S. S. (1995). Identification of a signal for rapid export of proteins from the nucleus. *Cell*, *82*(3), 463–473. https://doi.org/10.1016/0092-8674(95)90435-2

Zhang, J., Ferguson, S. S., Barak, L. S., Ménard, L., & Caron, M. G. (1996). Dynamin and beta-

arrestin reveal distinct mechanisms for G protein-coupled receptor internalization. *The Journal of Biological Chemistry*, *271*(31), 18302–18305. https://doi.org/10.1074/jbc.271.31.18302

Zhao, Y., Araki, S., Wu, J., Teramoto, T., Chang, Y.-F., Nakano, M., … Campbell, R. E. (2011). An Expanded Palette of Genetically Encoded Ca2+ Indicators. *Science*, *333*(6051), 1888–1891. https://doi.org/10.1126/science.1208592

2.8 Figures
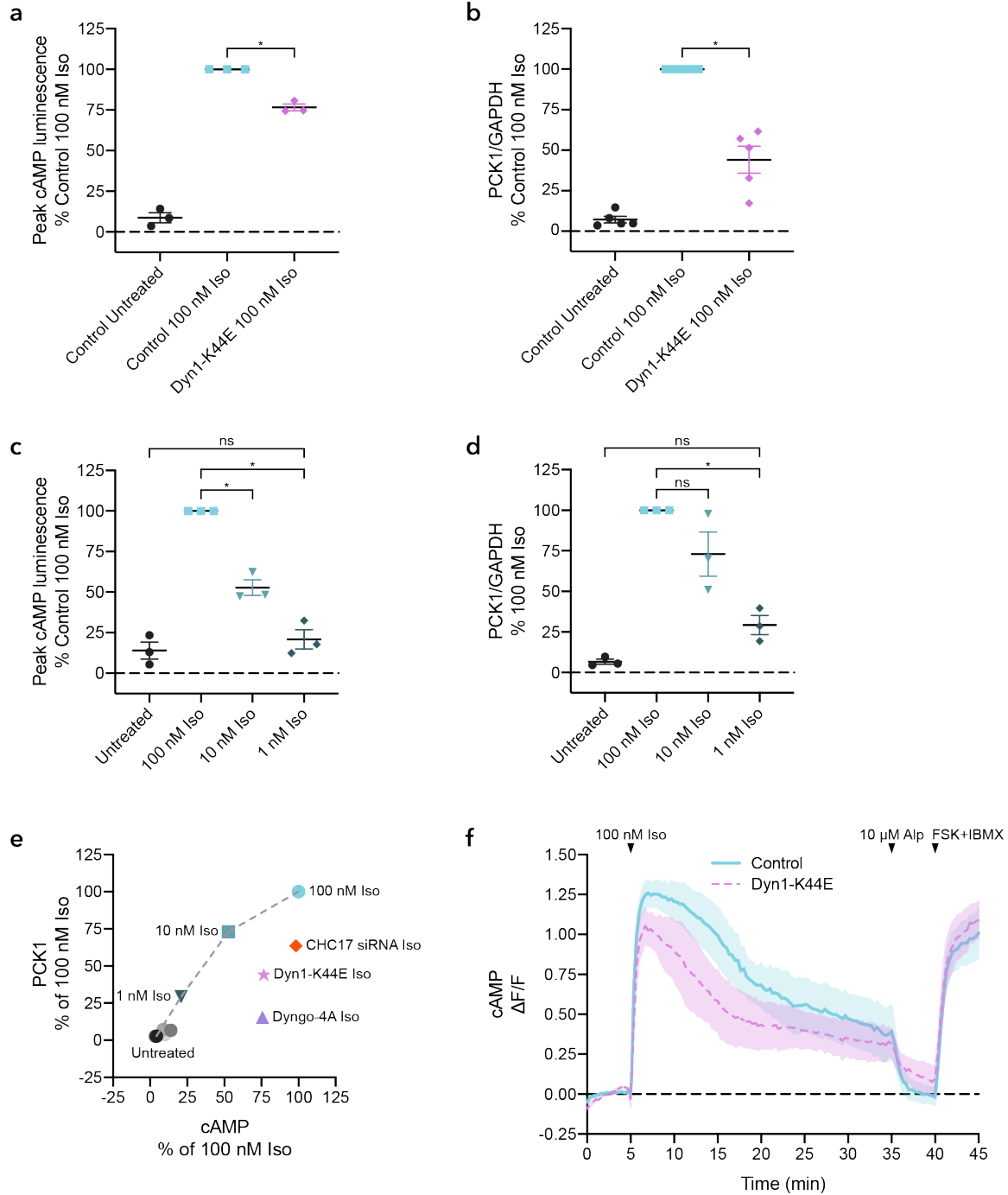
Figure 2.1 Magnitude and kinetics of cAMP signaling
Amount. **a**. Endocytic blockade by dominant negative dynamin (Dyn1-K44E) reduces β2AR-stimulated cAMP. HEK293 cells expressing a cAMP luciferase biosensor was coexpressed with either pcDNA3 (control) or mCherry-Dyn1-K44E. Cells were untreated or treated with 100 nM Iso. The maximum luminescence value (using a window averaging 5 proximal values) of each sample was determined and normalized to the control iso condition. (n = 3, P = 0.0038, two-tailed unpaired t-test.) **b**. Endocytic blockade by dominant negative dynamin (Dyn1-K44E) reduces β2AR-stimulated induction of PCK1. qRT-PCR was performed on samples from HEK293 cells transfected with pcDNA3 (control) or mCherry-Dyn1-K44E followed by two hours of 100 nM Iso. (n = 5, P < 0.0001, two-tailed unpaired t-test.) **c**. Production of cAMP increases with concentration of Iso. HEK293 cells expressing a cAMP luciferase biosensor were untreated or treated with 100 nM Iso, 10 nM Iso and 1 nM Iso. The maximum luminescence value (using a window averaging 5

71

proximal values) of each sample was determined and normalized to the 100 nM iso condition. (n = 3, 100 nM vs 10 nM Iso P = 0.0003, 100 nM vs 1 nM Iso P < 0.0001, Untreated vs 1 nM Iso P = 0.6885; ordinary one-way ANOVA Sidak's multiple comparisons test.) **d**. Induction of PCK1 increases with concentration of Iso. qRT-PCR was performed HEK293 cells untreated and treated with 100 nM, 10 nM, and 1 nM Iso for two hours (n = 3, 100 nM vs 10 nM Iso P = 0.0969, 100 nM vs 1 nM Iso P = 0.0004, Untreated vs 1 nM Iso P = 0.1798; ordinary one-way ANOVA Sidak's multiple comparisons test.) **e**. Endocytic inhibition results in a smaller reduction in overall cAMP than PCK1 induction. Different endocytic inhibition methods (mutant dynamin1, siRNA depletion of clathrin, pharmacological inhibitor of dynamin) have a greater degree of reduction in PCK1 induction than in overall cAMP when compared to the control 100 nM Iso condition. Isoproterenol treated cells (10 nM, 1 nM doses) have a greater degree of reduction in overall cAMP than in PCK1 induction when compared to the 100 nM Iso condition. **Timing**. **f**. Kinetics of cAMP production over time. HEK293 cells transiently co-expressing a cpGFP cAMP sensor and pcDNA3 (control) or mCherry-Dyn1-K44E were imaged and treated with 100 nM Iso for 30 minutes followed by 5 minutes of 10 µM Alp and 5 minutes of 500 µM IBMX with 10 µM FSK (Control, n = 4, Dyn1-K44E n = 3, P < 0.0001 for Time and Transfection, two-way ANOVA.) All data are mean ± sem.

a

HEK293T mNG2$_{1-10}$
mNG2$_{1-10}$

mNG2$_{11}$-PKAcatα

HEK293T mNG2-PKAcat
mNG2$_{1-10}$
mNG2$_{11}$-PKAcat

b

Control

| | 0 min | 0.5 min | 1 min | 15 min | 30 min |

mNG2-PKAcatα

Untreated

100 nM Iso

c

Dyn1-K44E

| | 0 min | 0.5 min | 1 min | 15 min | 30 min |

mNG2-PKAcatα

Untreated

100 nM Iso

d

% Initial intensity vs Time (min)

- Control Untreated
- Control 100 nM Iso
- Dyn1-K44E Untreated
- Dyn1-K44E 100 nM Iso
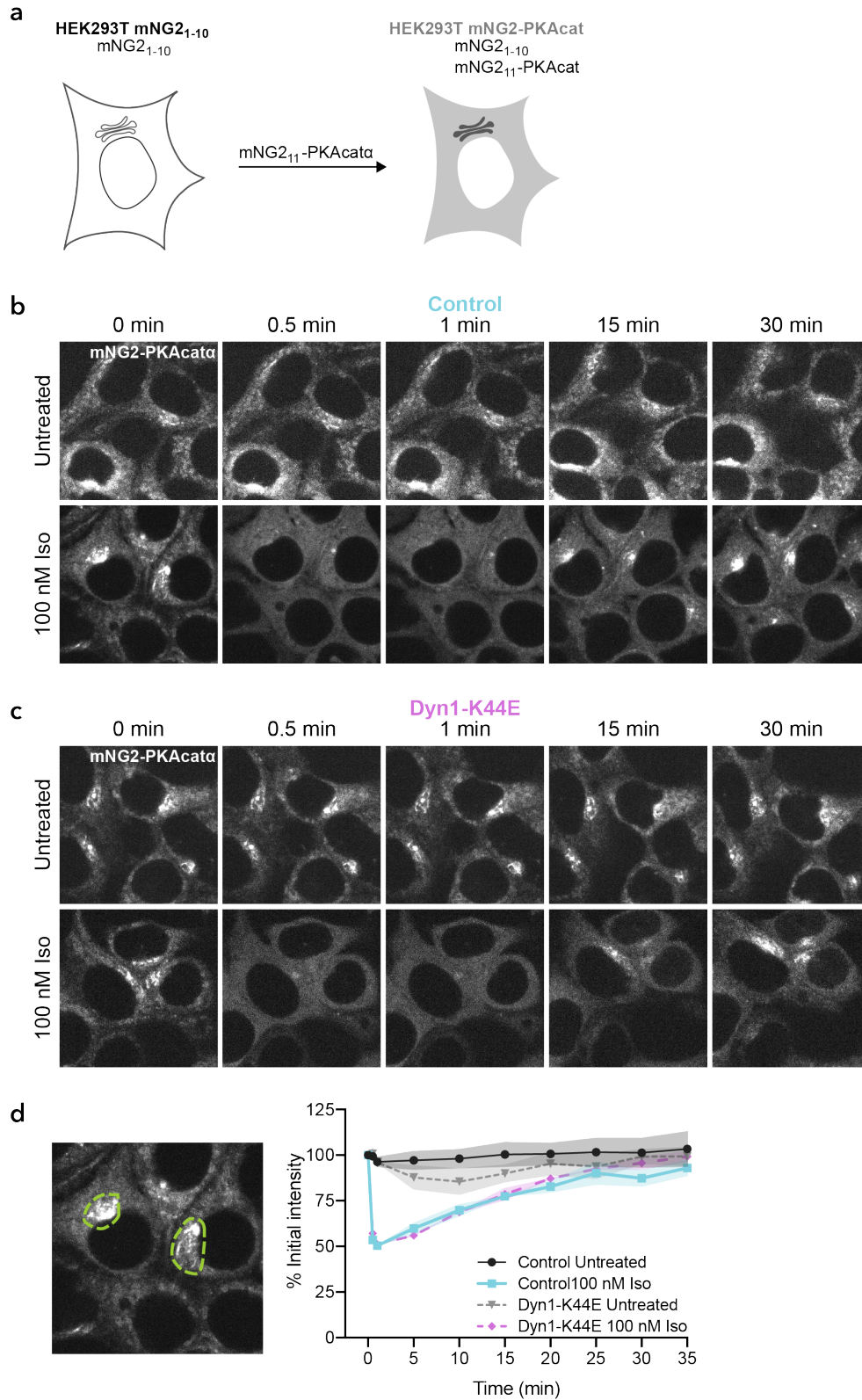
Figure 2.2 Perinuclear PKAcat initially redistributes in the cell after Iso stimulation followed by reconcentration
a. Cartoon of split mNG2$_{1-10}$:mNG2$_{11}$-PKAcat CRISPR knock-in strategy. **b-c**. Representative live cell spinning disk confocal images of endogenously tagged mNG2-PKAcat HEK293T cells. Cells transiently expressing pcDNA3 (**b**, control) or mCherry-Dyn1-K44E (**c**) were untreated (top) or treated with 100 nM Iso (bottom) at 0 minutes. **d**. Quantification of

experiments described in b and c. Examples of ROIs drawn around the perinuclear region in green. (n = 3, Control untreated vs Control Iso P = 0.0014, Dyn1-K44E untreated vs Dyn1-K44E Iso P = 0.0381, Control Iso vs Dyn1-K44E Iso P = 0.9933, Control untreated vs Dyn1-K44E untreated P = 0.8681; ordinary one-way ANOVA Sidak's multiple comparisons test.) Data are mean ± sem.
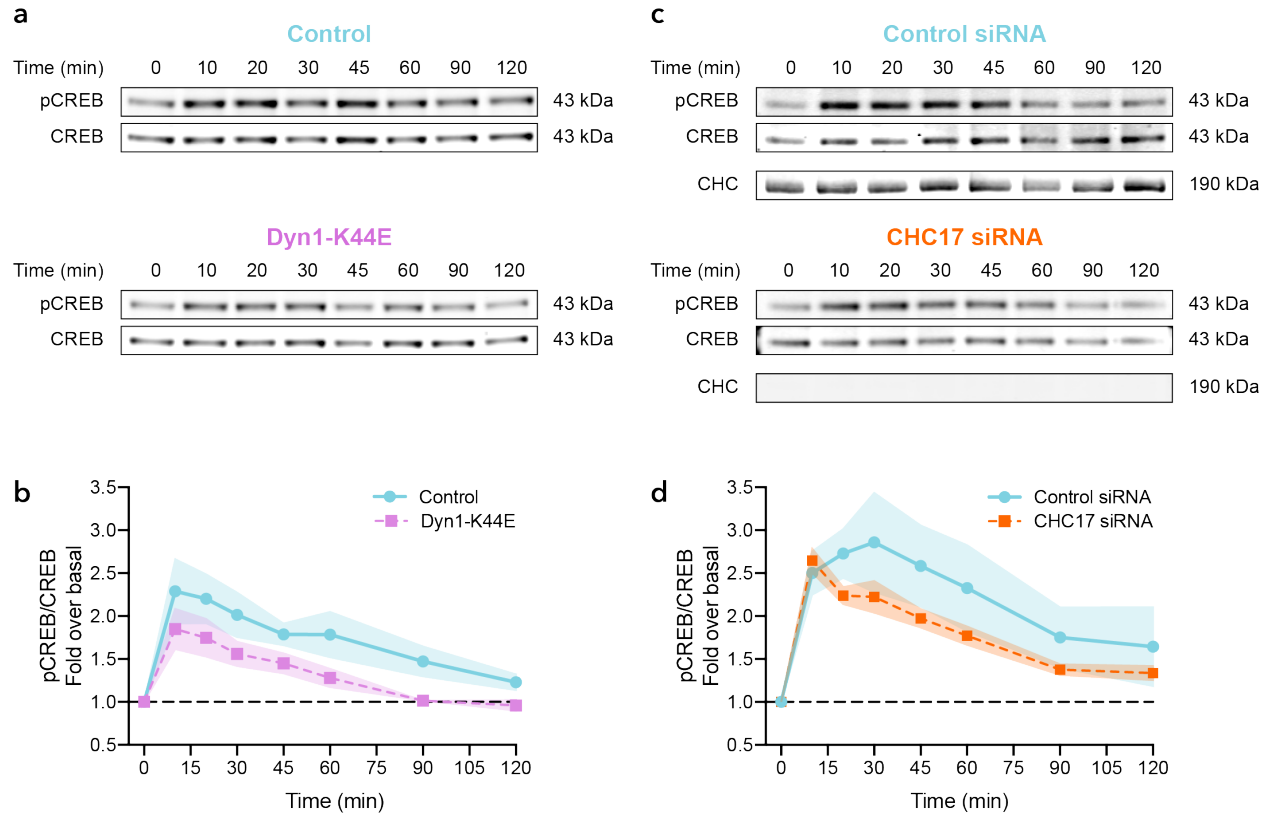
Figure 2.3 Endocytic blockade reduces Iso-stimulated CREB phosphorylation over time
Western blot analysis of CREB phosphorylation (Ser133) on HEK293 cells untreated and treated with 100 nM Iso for 10, 20, 30, 45, 60, 90, and 120 minutes. Cells transiently expressing mCherry-Dyn1 (control) or mCherry-Dyn1-K44E (**a**), scramble (control) or clathrin (CHC17) siRNA (**c**). **b** and **d**. Quantification of Western blots in a (n = 3, Time P < 0.0001, Transfection P = 0.0005; two-way ANOVA) and c (n = 7, Time P < 0.0001, Transfection P = 0.0181; two-way ANOVA.) Data are mean ± sem.
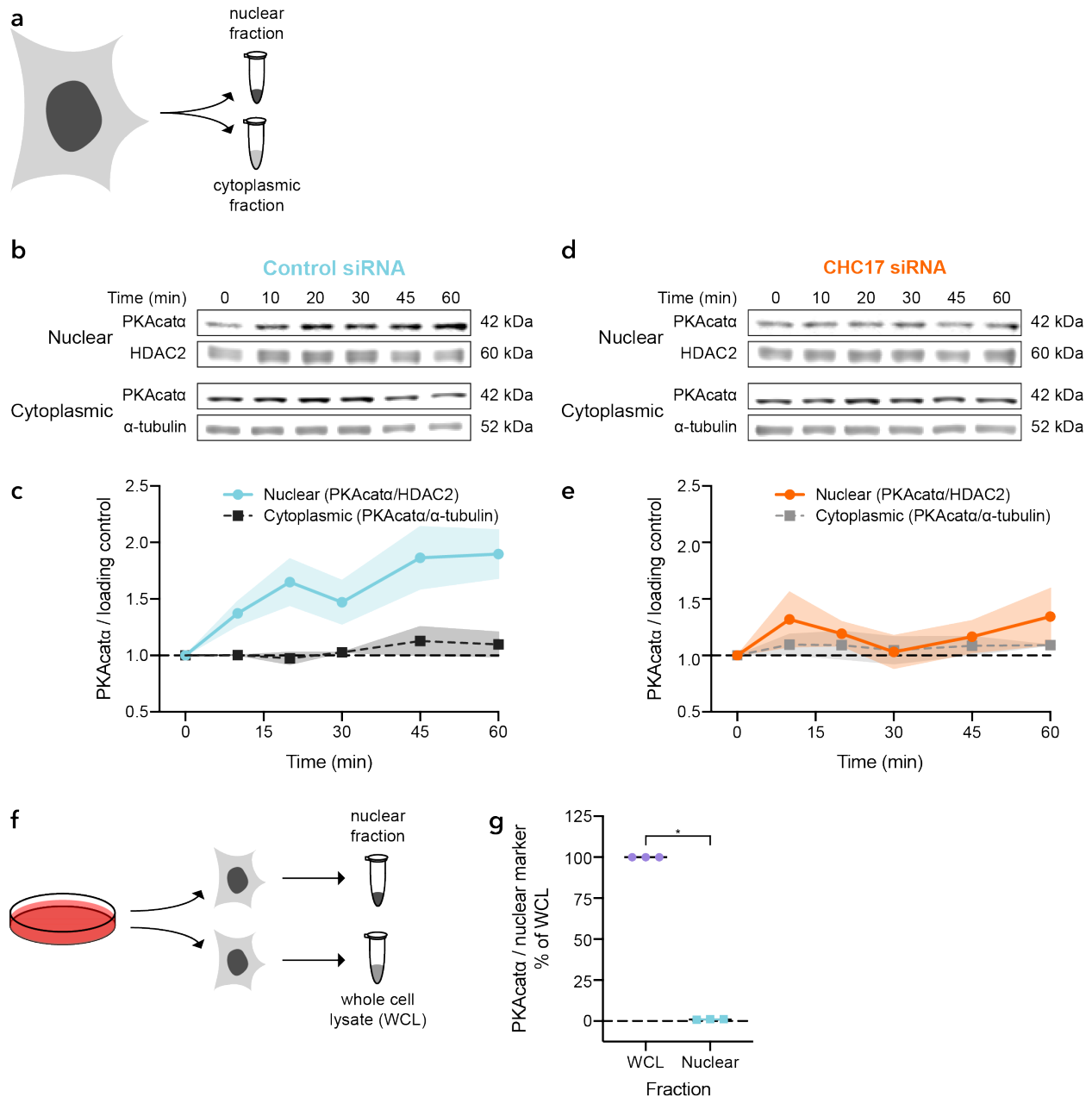
Figure 2.4 β2AR endosomal signaling promotes nuclear PKAcat accumulation
Nuclear and cytoplasmic fractions were collected from HEK293 cells untreated and treated with 100 nM Iso for 10, 20, 30, 45 and 60 minutes. Western blot analysis of PKAcat on nuclear and cytoplasmic fractions. **a**. Cartoon of nuclear and cytoplasmic fractionation. Cells transiently expressing scramble siRNA (**b**, control) or clathrin siRNA (**c**, CHC17). **d** and **e**. Quantification of Western blots in **b** (nuclear n = 3, cytoplasmic n = 4; Time P = 0.0100 and Fraction P < 0.0001; two-way ANOVA) and **c** (n = 4, ns, Time P = 0.5095 and Fraction P = 0.1782; two-way ANOVA.) **f**. Cartoon of nuclear fraction samples and whole cell lysate samples extracted from the same plate. **g**. Western blot quantification of PKAcat from whole cell lysate and nuclear samples (n = 3, P < 0.0001, two-tailed unpaired t-test.) All data are mean ± sem.
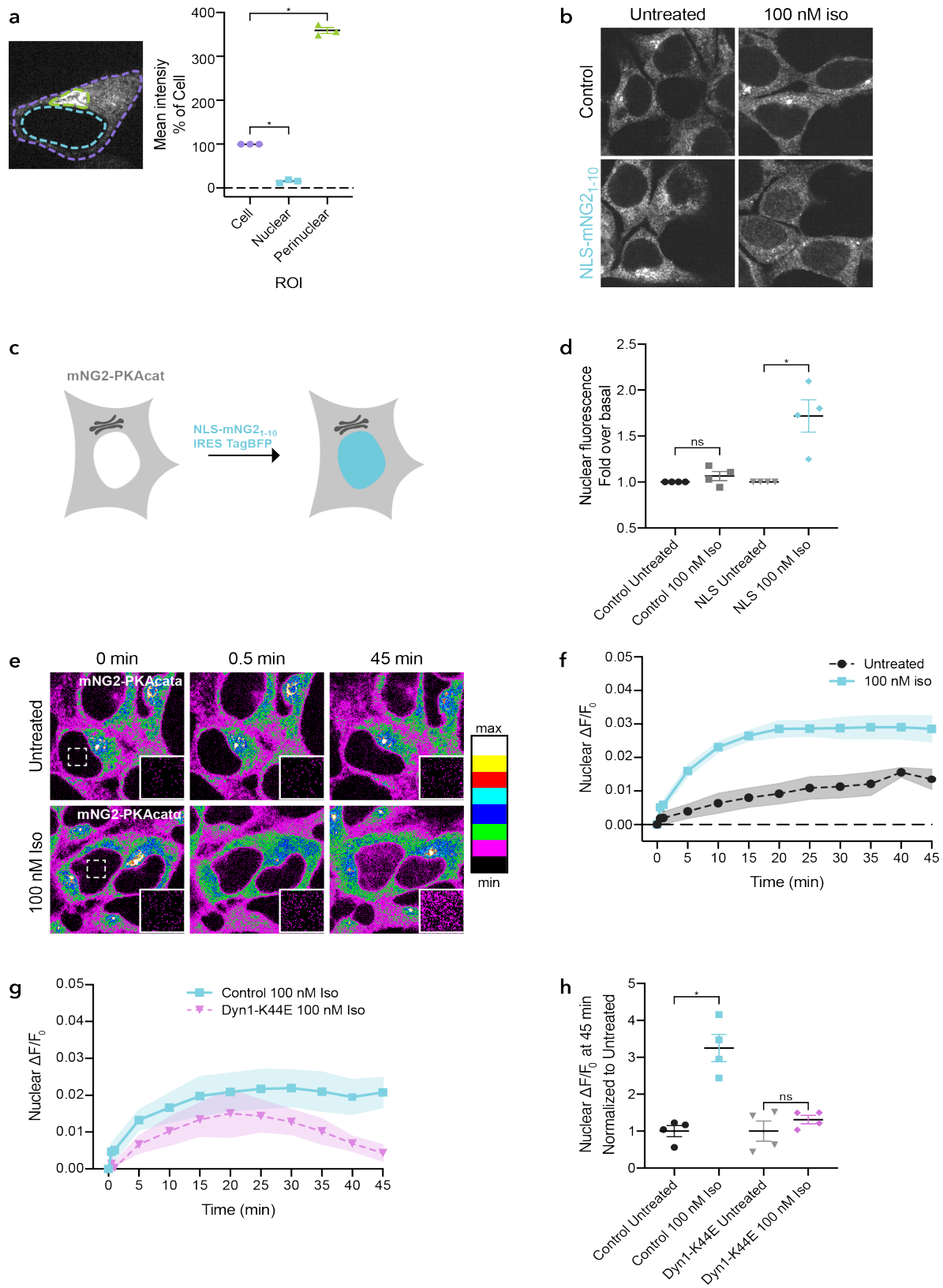
Figure 2.5 Endocytic blockade reduces amount of nuclear PKAcat after Iso stimulation
a. mNG2-PKAcat mean intensities of ROIs relative to whole cell. Mean intensities from ROIs drawn around the whole cell (purple), nucleus (teal) and perinuclear (green) were measured and calculated as a percentage of mean ROI

intensity of the whole cell (n = 3, P < 0.0001 for Cell vs Nuclear and Cell vs Perinuclear; ordinary one-way ANOVA Sidak's multiple comparisons test.) **b.** Schematic of imaging-based assay to detect nuclear PKAcat. Cells co-expressing $mNG2_{1-10}$ and endogenously-tagged $mNG2_{11}$-PKAcat are untransfected or transfected with nuclear (2x NLS) localized $mNG2_{1-10}$. **c.** Representative spinning disk confocal images of fixed cells untransfected (control, top) and transfected with nuclear localized $mNG2_{1-10}$ (bottom). Cells were untreated or stimulated with 100 nM Iso for 45 minutes. **d.** Quantification of fixed cells in **c** (n = 4, cells ≥ 74 per experiment; Control 0 min vs 45 min P = 0.8625, NLS 0 min vs 45 min P = 0.0003; ordinary one-way ANOVA.) **e.** Representative spinning disk confocal images of live cells expressing $mNG2_{11}$-PKAcat, $mNG2_{1-10}$ and nuclear localized (2x NLS) $mNG2_{1-10}$.) Cells were untreated (top) or treated with 100 nM Iso (bottom) at 0 minutes. High contrast images of cells at 45 minutes on the right. **f.** Quantification of cells untreated or stimulated with 100 nM Iso at 0 minutes in **e** (n = 3, Interaction P = 0.0012, Time and Treatment P < 0.0001, P < 0.05 untreated vs Iso time = 5-45 minutes, two-way ANOVA, Sidak's multiple comparisons test.) **g.** Quantification of cells transiently expressing pcDNA3 (control) or mCherry-Dyn1-K44E (n = 4, Time and Transfection P < 0.0001, two-way ANOVA.) Data are mean ± sem. **h.** Quantification of cells transiently expressing pcDNA3 (control) or mCherry-Dyn1-K44E from **g**, data normalized to 45 minute 100 nM Iso time point (n = 4, Control untreated vs Iso P < 0.0001, Dyn1-K44E untreated vs Iso P = 0.7726, Control Iso vs Dyn1-K44E Iso P = 0.0004; ordinary one-way ANOVA, Sidak's multiple comparisons test.) All data are mean ± sem.
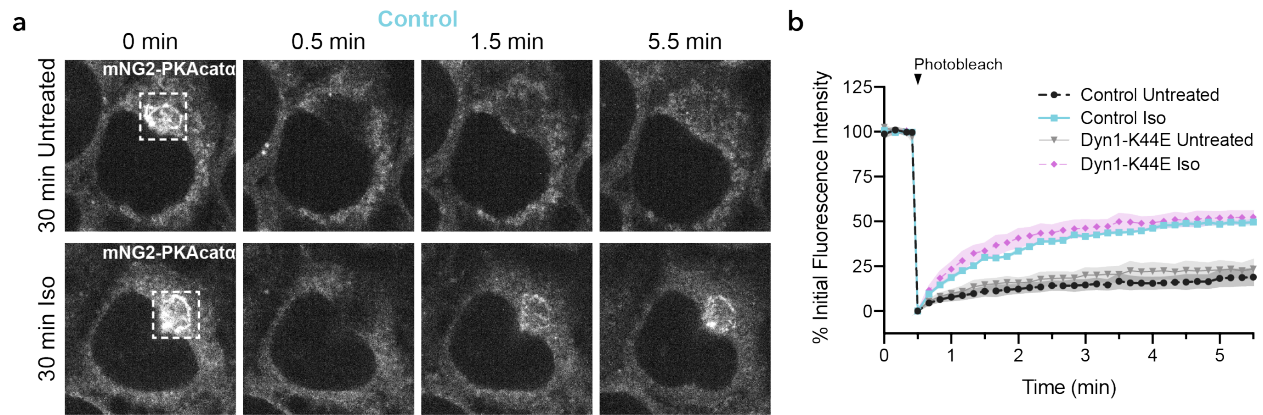
Figure 2.6 Fluorescence recovery after photobleaching of perinuclear PKAcat
a. Fluorescence recovery after photobleaching. Untransfected cells (control) were untreated (top) or treated with 100 nM isoproterenol (bottom) for 30 minutes before live imaging. Then cells were photobleached (white box) at 0.5 min and fluorescence recovery was monitored for 5 minutes after photobleaching. **b**. Quantitation of photobleaching. Fluorescence in the region of interest (white box in **a**) was measured over 5.5 minutes (before and after photobleaching). Fluorescence over time was normalized to the pre-photobleached fluorescence intensity. (n = 3; Control untreated vs Iso P = 0.0027; Dyn1-K44E untreated vs Iso P = 0.0030; Control untreated vs Dyn1-K44E untreated, P = 0.9502; Control Iso vs Dyn1-K44E Iso, P = 0.9569; ordinary one-way ANOVA, Sidak's multiple comparisons test.) All data are mean ± sem.
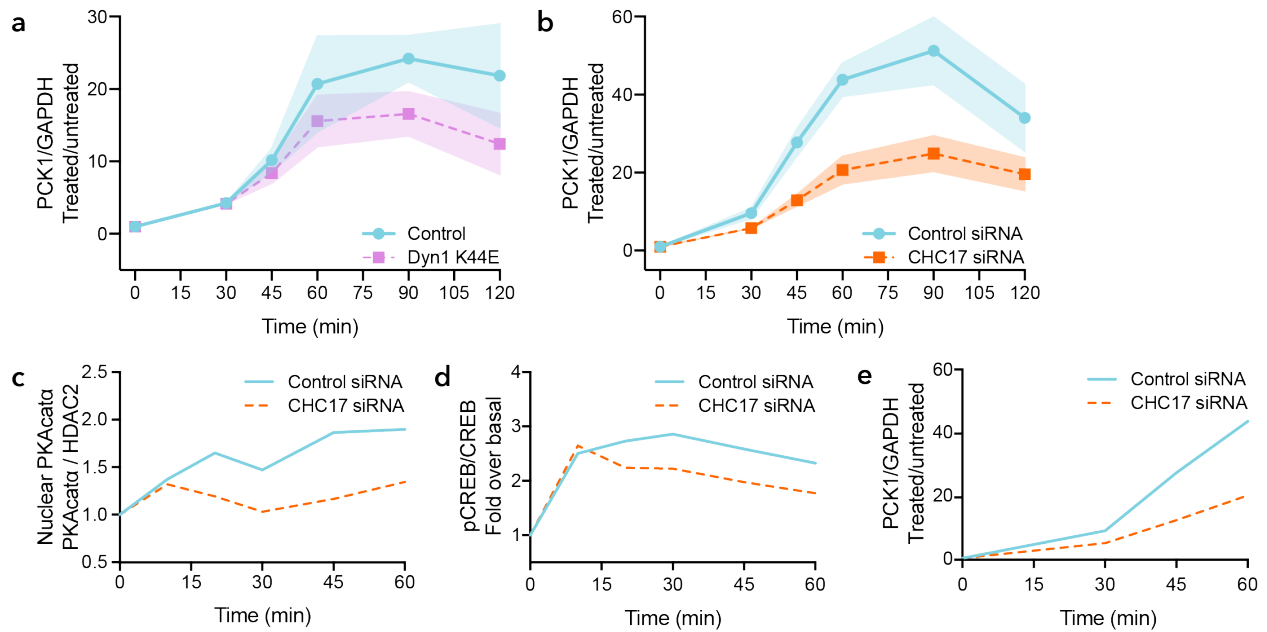
Figure 2.7 Endocytosis blockade reduces β2AR-stimulated *PCK1* transcription
Cells were transfected with either **a**. mCherry-Dyn1 (Control) or mCherry-Dyn1-K44E, or **b**. Control siRNA or CHC17 siRNA, then untreated or treated with 100 nM isoproterenol up to two hours. qRT-PCR was performed on these samples for *PCK1* and *GAPDH*. (Dyn1 vs Dyn1K44E n = 6, Time P < 0.0001, Transfection P = 0.0476, two-way ANOVA.) (Control siRNA vs CHC17 siRNA n = 6, Interaction P = 0.0260, Time P < 0.0001, Transfection P < 0.0001, P < 0.005 for time = 60 and 90 min; two-way ANOVA, Sidak's multiple comparisons test.) All data are mean ± sem. Nuclear cAMP signaling cascade responses are shown in the same time scale (up to 60 minutes) in cells transfected with control siRNA or CHC17 siRNA. **c**. Immunoblot analysis of PKAcat from nuclear samples treated with 100 nM Iso. **d**. Immunoblot analysis of CREB phosphorylation from whole cell lysates after 100 nM Iso treatment. **e**. qRT-PCR quantitation of cells treated with 100 nM Iso.
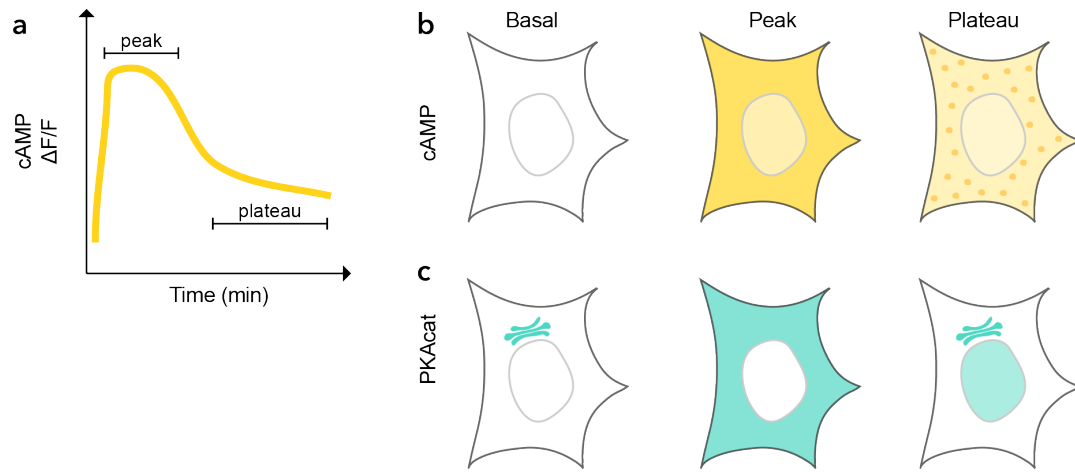
Figure 2.8 Summary model
a, **b**. The profile of overall cellular cAMP signaling after β2AR activation can be described by two distinct phases - an initial peak phase characterized by high levels of cAMP subsequently followed by a plateau phase distinguished by a low level of constant cAMP. **c**. Corresponding changes with PKAcat occur during these distinct cAMP phases. At basal state, PKAcat is non-uniformly distributed throughout the cytoplasm, and highly concentrated at a perinuclear region. During the peak phase, PKAcat is released from the perinuclear region and redistributed throughout the cytoplasm. During the plateau phase, PKAcat returns to the perinuclear region and has begun to enter the nucleus.
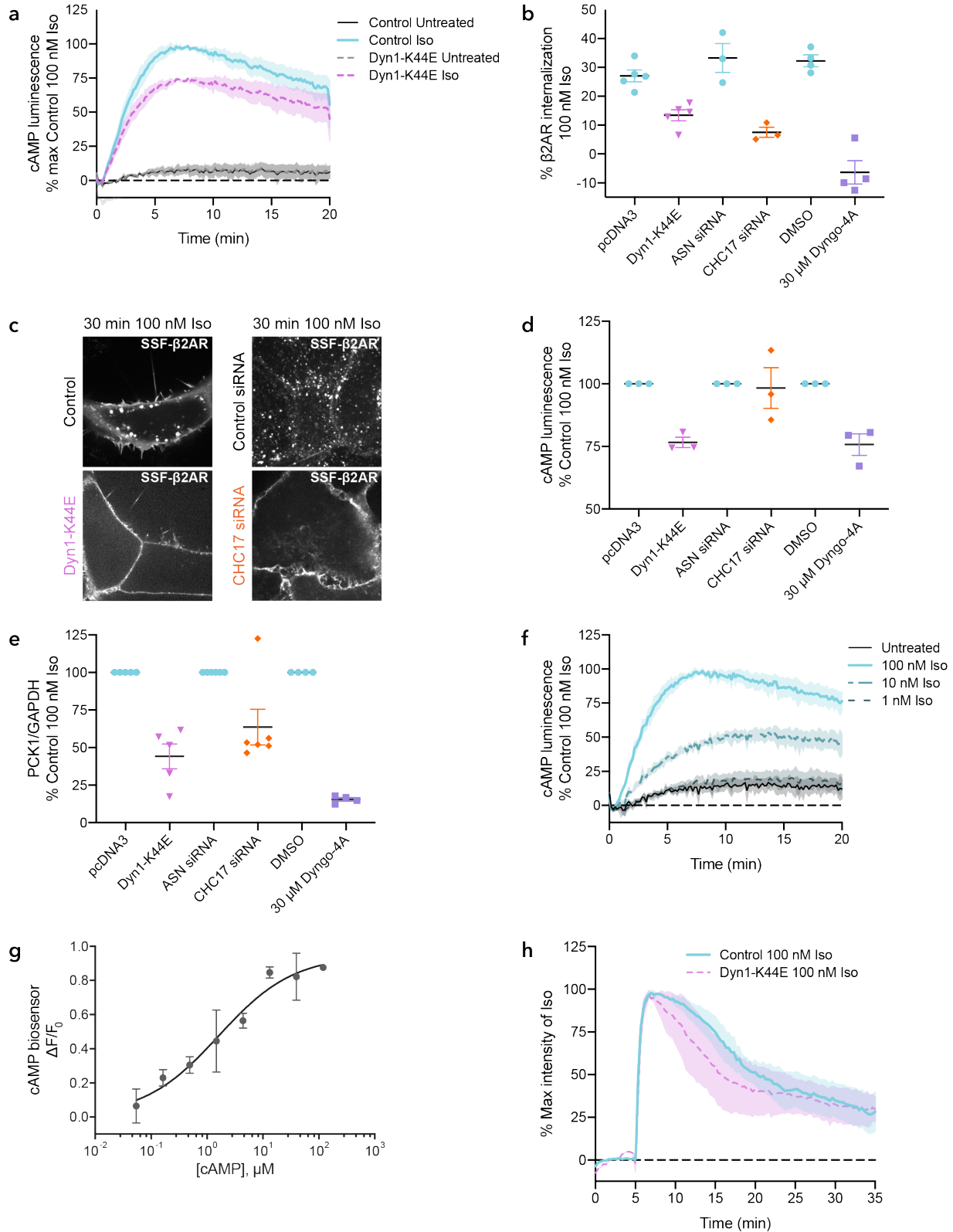
Supplemental Figure 2.1 Effects of endocytic blockade on the cAMP signaling pathway
a. Endocytic blockade by dominant negative dynamin (Dyn1-K44E) reduces cAMP over time. Cells stably expressing cAMP luminescence biosensor (GloSensor-IRES-Rluc) were transiently transfected with pcDNA3 (Control) and mCherry-Dyn1-K44E. Cells were untreated or treated with 100 nM Isoproterenol at 0 minutes and imaged for 20 minutes. All

conditions are normalized to the max of the Control 100 nM Iso condition (window averaging 5 proximal values). **b.** Endocytic blockade effects on β2AR internalization. Three methods of endocytic inhibition are assayed by β2AR internalization. Prior to 100 nM Iso addition, cells stably expressing FLAG-β2AR are either transiently transfected with pcDNA3 (Control) or mCherry-Dyn1-K44E, ASN siRNA (Control) or CHC17 siRNA, or pretreated with DMSO (Control) and 30 μM Dyngo-4A for 15 minutes. Then, cells were untreated or treated with 100 nM Iso for 30 minutes. Surface cell receptor was determined by M1-FLAG-647 antibody and internalization was subsequently calculated per condition. **c.** Images of endocytic blockade methods on β2AR internalization. Cell surface B2ARs were labeled using M1-FLAG-647 in cells stably expressing FLAG-β2AR. After 30 minutes of 100 nM Iso, cells were imaged by spinning disk confocal microscopy. Images of representative single slices are shown depicting the amount of β2AR internalization after 30 minutes isoproterenol. **d.** Effects of endocytic blockade on peak cAMP luminescence. Cells stably expressing cAMP luminescence biosensor (GloSensor-IRES-Rluc) were transiently transfected with pcDNA3 (Control) or mCherry-Dyn1-K44E, ASN siRNA (Control) or CHC17 siRNA, or pretreated with DMSO (Control) and 30 μM Dyngo-4A for 15 minutes. The peak luminescence value (window averaging 5 proximal values) of each sample was determined and normalized to the corresponding control iso condition. **e.** Endocytic blockade by multiple methods reduces β2AR-stimulated PCK1 transcription. We employed three methods of endocytic inhibition are assayed by β2AR internalization. Cells were either transiently transfected with pcDNA3 (Control) or mCherry-Dyn1-K44E, ASN siRNA (Control) or CHC17 siRNA, or pretreated with DMSO (Control) and 30 μM Dyngo-4A for 15 minutes. qRT-PCR was performed on cells untreated or treated with 100 nM iso for two hours. **f.** Isoproterenol stimulates cAMP luminescence over time. Cells stably expressing cAMP luminescence biosensor (GloSensor-IRES-Rluc) were untreated or treated with 100 nM, 10 nM, or 1 nM isoproterenol at 0 minutes and imaged for 20 minutes. All conditions are normalized to the max of the 100 nM Iso condition (window averaging 5 proximal values. **g.** cAMP fluorescence biosensor characterization in vitro. Cytoplasmic fraction prepared from HEK293 cells transiently expressing cpGFP-cAMP biosensor was treated with 100 μM IBMX, and different concentrations of cAMP. Fluorescence was recorded and the data was fit to a non-linear regression model (Sigmoidal, 4PL). Data are mean ± stdev, from one independent experiment. **h.** Kinetics of cpGFP-cAMP biosensor response. Cells transiently transfected with the cpGFP-cAMP biosensor and pcDNA3 (Control) or mCherry-Dyn1-K44E were imaged with 100 nM Iso added at 5 minutes. Each cAMP response was normalized to the peak response within 30 minutes after iso addition. All data are mean ± sem, and from at least three independent experiments. *exception **g.**

a

HEK293T

mNG2$_{1\text{-}10}$	+	+
mNG2$_{11}$-PKAcatα	−	+

PKAcatα ▭ 42 kDa

b

Dyn1-K44E   mNG2-PKAcatα

Untreated

100 nM Iso
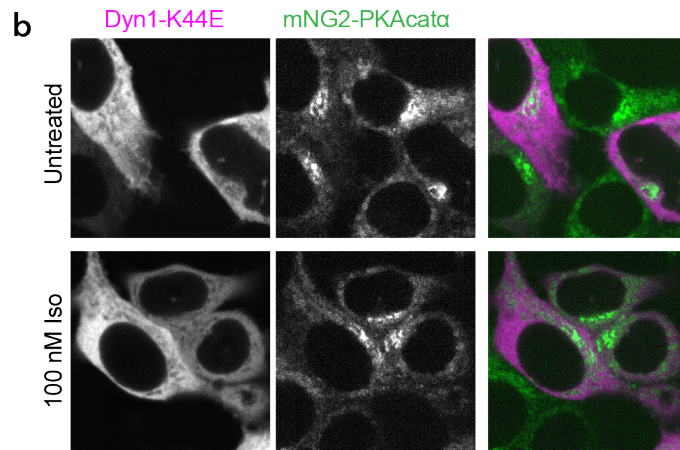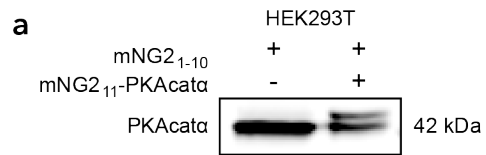
Supplemental Figure 2.2 Gene-edited mNG2-PKAcat HEK293T cells
a. Immunoblot of cells expressing unlabeled and labeled PKAcat. Immunoblot analysis on PKAcat (~42 kDa) was performed on samples from HEK293T cells stably expressing mNG2$_{1\text{-}10}$ only or mNG2$_{1\text{-}10}$ and mNG2$_{11}$-PKAcat. **b**. Identifying cells expressing mCherry-Dyn1-K44E. Cells expressing mCherry-Dyn1-K44E were identified to determine which cells would be used for analysis.

a

0 min   60 min FSK+IBMX

mNG2-PKAcatα

b

NLS-mNG2$_{1-10}$ mNG2-PKAcat

Untreated

100 nM Iso
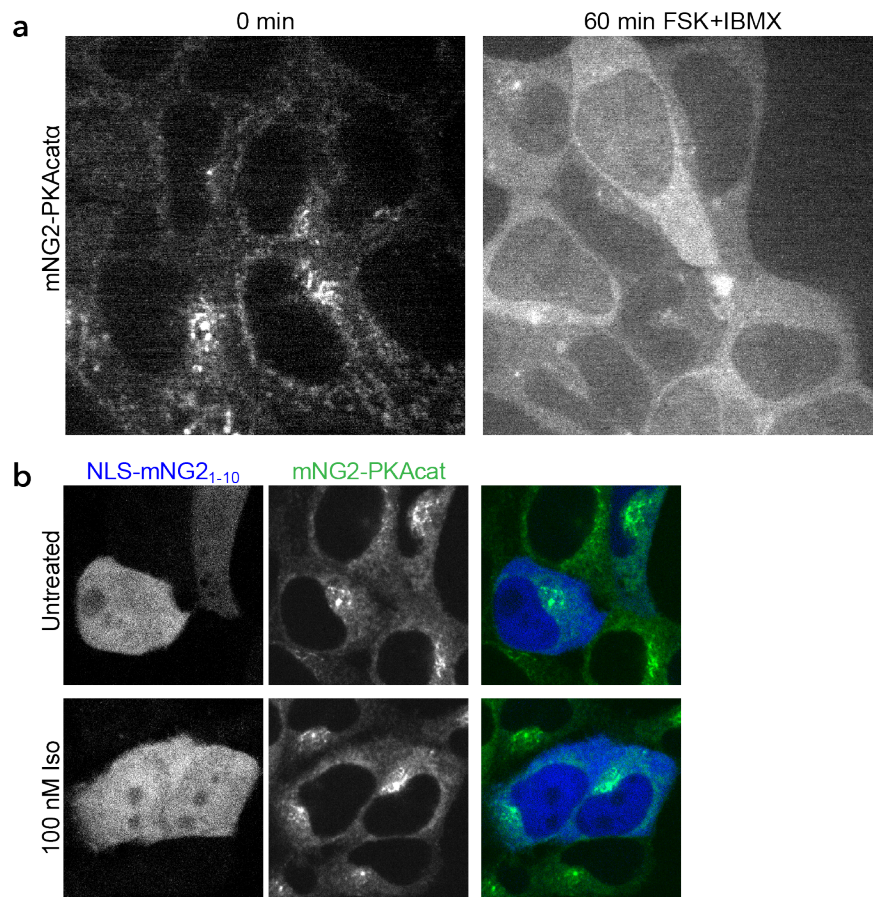
Supplemental Figure 2.3 Detection of nuclear PKAcat by live microscopy
a. Visualizing PKAcat in the nucleus with live imaging. Gene-edited cells expressing endogenous mNG2-PKAcat were treated with 10 µM FSK and 500 µM IBMX for 60 minutes. **b**. Identifying cells expressing NLS-mNG2$_{1-10}$ IRES TagBFP. Cells expressing NLS-mNG2$_{1-10}$ IRES TagBFP were identified to determine which cells would be used for analysis.
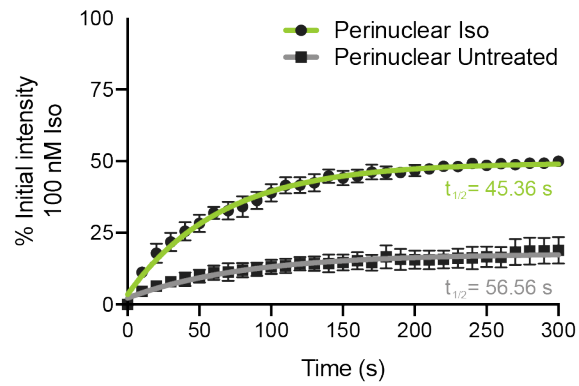
Supplemental Figure 2.4 Fluorescence recovery after photobleaching curve fit
Photobleaching recovery curves with non-linear fit. Recovery curves from **Figure 2.6b** are replotted so recovery begins a 0 seconds. Each recovery curve was fit using non-linear regression and an exponential one-phase association model. The perinuclear iso condition (green) has a half-time of 45.36 s and fractional recovery of 49.45%. The perinuclear untreated condition (gray) has a half-time of 56.56 s and a fractional recovery of 17.67%. All data are mean ± sem.

Chapter 3: M2R inhibits β2AR-stimulated *PCK1* trasncription from the plasma membrane

Grace Peng conceived of this project, generated constructs, conducted all experiments, and analysis, and wrote the manuscript presented in this chapter. Mark von Zastrow contributed to project development and data analysis.

3.1 Abstract

Cardiac G protein-coupled receptors (GPCRs) are important in regulating heart function. These GPCRs detect extracellular stimuli (agonists) and generate an intracellular signaling response crucial to controlling heart rate and cardiac muscle contractility. Disordered signaling is observed in pathologies including congestive heart failure, cardiomyopathy and hypertension. β2-adrenergic receptors (β2ARs) and M2 muscarinic acetylcholine receptors (M2Rs) are GPCRs that are co-expressed in cardiac muscle cells and operate to exert largely opposing modulatory effects. β2ARs stimulate cardiac excitability primarily by coupling to the heterotrimeric G protein G_s. Conversely, M2Rs reduce excitability by coupling to G_i. Both GPCRs internalize after agonist-induced activation. Recent work has shown that some GPCRs, including β2ARs, initiate a second phase of signaling by coupling to G_s on endosomes. Here we find that M2Rs, are capable of entering the same endosomes as β2ARs and are also able to inhibit the β2AR endosomal signal. These findings provide insight into a fundamentally new aspect of cellular GPCR signaling, namely whether endocytosis facilitates functional coordination between these GPCRs or, alternatively, if endocytosis isolates a subset of β2AR signaling actions from M2R modulation, which is fundamental to understanding the physiological relevance of cardiac endosomal signaling.

3.2 Introduction

Cells sense their extracellular environment via external stimuli and transmit signals to mediate a proper response. Many of these responses are controlled by G protein-coupled receptors (GPCRs). GPCRs are responsible for the signal transmission of many processes including cell motility and migration, vision, taste and smell. Classically, a stimulus known as an agonist binds to activate the receptor and trigger intracellular signaling (Sorkin & von Zastrow, 2002).

In the heart, adrenaline and acetylcholine are agonists for β-adrenergic and muscarinic acetylcholine receptors, respectively. These G protein-coupled receptors (GPCRs) are co-expressed in cardiac muscle cells (myocytes) and trigger physiologically opposing actions through intracellular G protein signaling cascades (Brodde & Michel, 1999). β2ARs and M2Rs predominantly couple to two distinct classes of heterotrimeric G proteins, G_s and G_i respectively. Historically, these G proteins were classified based on their ability to stimulate (G_s) or inhibit (G_i) the adenylyl cyclase (AC) enzymes that generate the intracellular second messenger cAMP (Alberts et al., 2002). In the heart, β2AR-G_s activation of AC increases cAMP concentration to enhance the strength of cardiac contraction (Brodde & Michel, 1999; Dzimiri, 1999; Nikolaev et al., 2006; Rochais et al., 2006). M2R-G_i activation inhibits AC and activates G-protein activated inwardly rectifying K^+ (GIRK) channels, to effectively antagonize the β2AR effects physiologically (Aprigliano et al., 1997; Brodde & Michel, 1999; Harvey, 2012; Harvey & Belevych, 2003; Nikolaev et al., 2006). In cardiac cells, GIRK channels contribute to setting resting membrane potential and increase the rate of cardiac repolarization after an action potential (Brodde & Michel, 1999; Harvey, 2012).

For β2AR and M2R to maintain their antagonistic relationship, both receptors must be present at the same membrane. However, both the β2AR and M2R internalize rapidly after agonist-induced activation (Robin Pals-Rylaarsdam et al., 1997; Reiner & Nathanson, 2012; von Zastrow & Kobilka, 1992), which redistributes each receptor and potentially disrupts this required functional interaction at the plasma membrane. Endocytosis has well known effects in modulating GPCR number and activity after prolonged or repeated exposure to agonist, but it is not traditionally thought to impact the signal itself because internalized GPCRs were believed to be functionally inactive. Recent results suggest, in contrast, that the β2AR and some other G_s-coupled GPCRs mediate a discrete, second phase of GPCR and G_s activation from endosomes (Calebiro et al., 2009; Ferrandon et al., 2009; Irannejad et al., 2013; Kotowski et al., 2011).

Endosomal signaling of GPCRs is a new area cell biology that has grown vastly in the last decade. The majority of the evidence support signaling from endosomes by G_s-coupled receptors, however other subtypes (G_i, G_q) have also been found capable as well. Yet, how endosomal signaling affects the integrative cellular response remains unexplored. The antagonistic relationship between β2AR and M2R remains a particularly interesting example to study as the β2AR is known to signal from the endosome, and β2AR and M2R act through a common effector protein, adenylyl cyclase, to modulate the cellular signaling response.

On first principles, we reason that both receptors must be in the same membrane for their antagonist relationship to exist. Both β2AR and M2R localize to early endosomes marked by early endosome antigen 1 (EEA1) (Robin Pals-Rylaarsdam et al., 1997; Reiner & Nathanson, 2012; von Zastrow & Kobilka, 1992), therefore we think it likely that both receptors internalize to the same endosomes. To further investigate how endocytosis affects the functional relationship between

β2AR and M2R, we utilize a real time cAMP assay useful for detecting rapid effects, as it can provide time resolution on the order of seconds. In the heart, β2ARs mediate acute actions that fall well within this time window, but β2ARs also mediate important long-term effects. Many of these are mediated by control of downstream transcription. Recent work suggests that β2AR-G_s cAMP production from endosomes is particularly important to these long-term effects, and particular transcripts have been defined that are selectively induced by cAMP generated from endosomes (Tsvetanova & von Zastrow, 2014). *PCK1* is robustly induced after ~2 hours of β2AR activation and is a sensitive detector of cAMP generated from endosomes relative to the plasma membrane (Tsvetanova & von Zastrow, 2014).

Here we investigate how endocytosis changes the functional relationship between the β2AR and M2R by looking at endocytosis-dependent cAMP-transcription. We start with the hypothesis that M2Rs function in endosomes to inhibit β2AR-G_s-AC signaling. This study uses HEK293 cells as an experimentally advantageous model based on known occurrence of β2AR-G_s-AC activation in both the plasma membrane and endosomes (Irannejad et al., 2013), and the availability of well-defined manipulations for perturbing receptor trafficking (Hausdorff et al., 1991; McCluskey et al., 2013; Seibold et al., 2000; Vassilopoulos et al., 2009). HEK293 cells are also a useful experimental model because they express β2ARs as the major endogenous beta-adrenergic receptor (Violin et al., 2008), lack endogenous M2R activity (no detectable carbachol response without expression of recombinant M2Rs), and recombinant M2Rs confer both acute and long-term modulation of endogenous β2AR signaling in these cells. We additionally seek to determine whether M2Rs mediate a long-term effect on β2AR signaling from endosomes through cAMP-dependent transcriptional control, using the previously established target gene, *PCK1*, as a readout. This

assay will complement the acute cAMP accumulation, is more specific to endosomal cAMP

signaling.

3.3 Results

β2AR and M2R transit a shared population of endosomes

We posit that for M2R to modulate the β2AR signal, both receptors need to be on the same membrane, in the case of endosomal signaling, this requires both receptors to be in the same endosome. Here we test whether β2AR and M2R redistribute to different endosomes or converge at the same endosomes after agonist addition of both receptors.

β2AR and M2R are both known to internalize to early endosome antigen 1 (EEA1) positive endosomes (Robin Pals-Rylaarsdam et al., 1997; Reiner & Nathanson, 2012; von Zastrow & Kobilka, 1992), but whether they internalize to the same EEA1 positive endosomes is not known. We first determined whether both β2ARs and M2Rs internalize to the same endosomes. In HEK293 cells, we overexpressed HA-β2AR and FLAG-M2R and used fluorescently conjugated anti-HA and anti-FLAG antibodies to label each receptor. We found that both β2ARs and M2Rs colocalize on the same endosomes after agonist induced internalization with saturating amounts of isoproterenol and carbachol (agonists for β2AR and M2R respectively; **Figure 3.1a**).

We next assessed this overlap between β2AR and M2R in the cell qualitatively by identifying subpopulations of endosomes (early, late and recycling) with fluorophore-tagged endosomal markers (EEA1, Rab7, Rab4 and Rab11, respectively) (Grant & Donaldson, 2009; Rink et al., 2005). Using the same method to label and detect β2AR and M2R, we additionally overexpressed each endosomal marker and looked at cells before and after isoproterenol and carbachol treatment (**Figures 3.1b-f**). Before agonist addition, both receptors are primarily detected at the plasma membrane (**Figure 3.1b**). After agonist-induced internalization with isoproterenol and carbachol, both receptors internalized to EEA1 positive endosomes (**Figure 3.1c**). β2AR and M2R

colocalize together with Rab4 early/recycling endosomes (**Figure 3.1d**) but not late (Rab7) or

Rab11 recycling endosomes (**Figures 3.1e-f**) after 30 minutes of isoproterenol and carbachol

addition. These results show that M2R transits a shared population of endosomes as β2AR. This

initial result allows for the possibility that M2R could affected β2AR endosomal signaling by being

at the same endosome.

β2ARs are in an active conformation in a subpopulation of endosomes and, in these endosomes,

they can also activate G_s (Irannejad et al., 2013). We used established conformationally sensitive

nanobody biosensors a new class of reagents derived from nanobodies, which selectively

recognize particular conformational states of the GPCR or G protein. We expressed Nb80-EGFP

and Nb37-mCherry to detect activated β2AR and G_s, respectively, and examined whether the

β2AR and M2R population of endosomes also contain activated β2AR and G_s. Using our previous

strategy to image epitope-tagged HA-β2AR and FLAG-M2R, we expressed each nanobody

biosensor and imaged cells in the presence and absence of isoproterenol and carbachol (**Figures**

3.2a-c). Before agonist addition, Nb80-EGFP is in diffuse in the cytoplasm, and β2AR and M2R

remain on the plasma membrane (**Figure 3.2a**). After addition of isoproterenol and carbachol, β2AR

and M2R internalize to endosomes which also contain Nb80-EGFP (**Figure 3.2b**). To detect

activated G_s, we used Nb37-mCherry, which like Nb80-EGFP is also diffusely in the cytoplasm

before agonist addition. After stimulation of β2AR with isoproterenol, Nb37-mCherry localized to

both the plasma membrane and endosomes (**Figure 3.2c**). β2AR and M2R additionally localized to

the locations as Nb-37-mCherry. These data suggest that M2R colocalizes with activated β2AR

and activated G_s, therefore M2R localizes to endosomes which allows for the possibility it to

modulate the β2AR signal.

Characterization of M2R internalization

Though M2R has been found at early endosomes, the components involved in the internalization pathway remain unclear. Many of the previous studies conflict in determining which components are required in this pathway. Some reports claim a caveolin-independent, clathrin-independent and dynamin-independent pathway, and thus a very non-traditional pathway distinct from β2AR (Delaney et al., 2002; Roseberry & Hosey, 2001). More recent reports contradict these earlier findings and determine a necessity for clathrin and dynamin (Jones et al., 2006). With the advancement of siRNAs and pharmacological inhibitors, a new look at the M2R internalization pathway will help elucidate the important components of this pathway. Furthermore, to determine the importance of endocytosis on the signaling by M2R, we will need the ability to block endocytosis.

First, we used a previously established flow cytometry-based assay to determine the number of surface-labeled receptors in the presence and absence of agonist to determine the amount of internalization under different conditions. Using a cell line stably expressing FLAG-M2R, we found that M2R internalization begins within 5 minutes after carbachol treatment and reaches steady state after 30 minutes of carbachol treatment (**Figure 3.3a**). Next, to test whether M2R internalization is truly clathrin- and dynamin- independent in HEK293 cells, we blocked endocytosis by using siRNA against clathrin heavy chain (CHC17) and a chemical inhibitor against dynamin (Dyngo-4A) (McCluskey et al., 2013; Vassilopoulos et al., 2009). We found endocytosis of M2R was greatly reduced when clathrin and dynamin were perturbed (**Figures 3.3b&c**), suggesting that M2R internalization is clathrin- and dynamin-dependent.

β2AR internalization is well established and also clathrin- and dynamin-dependent. This poses a problem, if both receptors internalize using the same components, we cannot selectively block the internalization of one receptor to determine how endocytosis affects their functional relationship. We focused on M2R internalization mutants because it is known that β2AR signals from the endosome. We can use M2R internalization mutants to determine whether endosomal M2R modulates the β2AR endosomal signal.

Intracellular loop 3 of the M2R contains two Ser/Thr clusters that are phosphorylated by GRK2, which are important for desensitization and internalization (R. Pals-Rylaarsdam & Hosey, 1997; R. Pals-Rylaarsdam et al., 1995). We obtained an intracellular loop 3 deletion mutant (M2R Δi3, residues 232-372; **Figure 3.3d**) previously used in obtaining the crystal structure of activated M2R. We also generated a previously described mutant where the two Ser/Thr clusters are mutated to Ala to prevent internalization (M2R NC8, **Figure 3.3d**). We generated stable cell lines of these mutants and confirmed internalization deficiency by microscopy. We imaged cells overexpressing Rab5-EGFP to mark early endosomes, and FLAG-M2R, FLAG-M2R Δi3, or FLAG-M2R NC8 before and after a 30 minutes carbachol treatment (**Figure 3.3e**). In all cases, M2R was found at the endosome before carbachol treatment. As expected, wildtype M2R was primarily found at early endosomes marked by Rab5 after carbachol addition. In contrast, both M2R Δi3 and M2R NC8 were found primarily at the plasma membrane. These images suggest that the M2R Δi3 and M2R NC8 mutants do not internalize efficiently. We additionally performed flow cytometric analysis to characterize internalization of the M2R mutants. First, we compared the receptor expression levels of each M2R stable cell line, and found them to be similar (**Figure 3.3f**). Next, we found that after 30 minutes of carbachol treatment, both the M2R Δi3 and M2R NC8 mutants had greatly reduced internalization (**Figure 3.3g**), consistent with our imaging results. Here, we verified that M2R

internalization is clathrin- and dynamin-dependent. Additionally, we validated two M2R

internalization mutants for use in our functional experiments investigating the impact of M2R

endocytosis on β2AR signaling.

M2R inhibits β2AR acute cAMP signaling

Functional antagonism between β2AR and M2R signaling has been well described (Aprigliano et

al., 1997; Brodde & Michel, 1999), but how much of M2R inhibition β2AR occurs from the plasma

membrane or the endosome is unknown. First, we verified that M2R impacts β2AR signaling in

HEK293 cells by measuring cAMP production when β2AR and β2AR and M2R are stimulated. To

do so, we express a cAMP luminescence biosensor that increases in luminescence as more cAMP

is detected. We stimulated endogenous β2ARs only and simultaneously with overexpressed M2Rs

to determine how much cAMP inhibition M2R caused. We found that M2R caused a moderate

inhibition (**Figure 3.4a**) in β2AR-stimulated cAMP.

To understand how much inhibition M2R imparts at endosomes, we first confirmed that endocytic

blockade by the chemical inhibitor Dyngo-4A, moderately reduced the amount of cAMP produced

by β2AR using the same cAMP luminescence biosensor as before (**Figure 3.4b**, blue circles and

triangles). We reasoned that if M2R inhibits β2AR-stimulated cAMP production at the endosome,

then blocking both β2AR and M2R endocytosis would reduce the degree of M2R inhibition on

β2AR-stimulated cAMP.

Here, we find that M2R inhibition of β2AR-stimulated cAMP is approximately 30% (**Figure 3.4b**,

blue circles and gray squares). We tested how M2R inhibition of β2AR-stimulated cAMP was

impacted by endocytic blockade, and found that M2R reduced β2AR-stimulated cAMP by

approximately 20% when endocytosis of both receptors was blocked (**Figure 3.4b**, blue and gray triangles). This would initially suggest that M2R does inhibit β2AR at the endosome given our previously stated rationale, however when tested and compared by one-way ANOVA, this difference is not significant.

Our assay may not be sensitive enough to detect M2R inhibition in the endosome or M2R inhibition of β2AR-G_s-AC signaling primarily occurs from the plasma membrane. To determine which of these were the case, we sought other methods to investigate the effect of M2R inhibition on β2AR-G_s-AC signaling. Next, we used a biochemical homogenous time resolved fluorescence assay, and measured the amount of cAMP produced per sample after 30 minutes of agonist addition. The addition of isoproterenol increased the amount of cAMP compared to untreated cells as expected (**Figure 3.4c**, blue circles). Co-stimulation with carbachol led to about a 55% reduction in cAMP production (**Figure 3.3c** blue circles and gray squares). When endocytosis was blocked, M2R inhibition of β2AR-stimulated cAMP was approximately 50% (**Figure 3.4c** blue and gray triangles). While these data are consistent with the luminescence assay, they also lacked significance by one-way ANOVA.

Lastly, we used the M2R internalization mutants that we previously validated to determine whether we could detect a difference in the amount of inhibition between M2R wildtype and internalization mutant on β2AR-G_s-AC signaling. We first checked the amount of cAMP produced when β2AR and M2R were concomitantly activated (**Figure 3.4d**). We find that the max amount of cAMP produced is relatively similar across all M2R types (wildtype and internalization mutants). Wildtype M2R inhibited β2AR-stimulated cAMP production by about 30%, but the M2R internalization

mutants inhibited β2AR-stimulated cAMP by about 25% (**Figure 3.4e**). Again, these data were not found to be significant by one-way ANOVA.

Even if our assays were not sensitive enough to detect how much M2R affects endosomal β2AR-stimulated cAMP production, our data do suggest that most, if not all, M2R inhibition on the β2AR-G_s-AC signal occurs at the plasma membrane. Though we could not concretely determine whether M2R modulates the endosomal β2AR-G_s-AC signal, we next used a more sensitive read out to test the role of M2R in its impact on downstream β2AR signaling.

M2R intracellular loop 3 is required for inhibition of cAMP-dependent transcription

Previous work found a set of genes that are specifically induced when the β2AR-G_s-AC pathway was activated when endocytosis was allowed. The transcription of one gene, *PCK1*, is significantly induced when endocytosis of the β2AR is allowed compared to when endocytosis of β2AR is blocked, indicating that *PCK1* is strongly tied to cAMP produced from the endosome (Tsvetanova & von Zastrow, 2014). Here, we use *PCK1*, to interrogate whether M2R inhibits the endocytic-sensitive β2AR transcriptional target. We verified by quantitative PCR (qRT-PCR) that *PCK1* significantly induced when endocytosis was allowed, but greatly reduced when endocytosis was blocked (**Figure 3.5a**). Next, we determined the effect of M2R activation the β2AR-stimulated *PCK1* induction. When stably expressing M2R was coactivated with β2AR, *PCK1* induction was reduced greatly, by about 40% (**Figure 3.5b**). Because *PCK1* is an endocytosis-sensitive target, these data suggest that M2R is capable of inhibiting β2AR-G_s-AC signaling.

We do not have direct evidence for activated M2R in the endosome and from the endosome inhibit β2AR-G_s-AC signaling at the endosome, we used our internalization mutants to help characterize

the inhibition of *PCK1* by M2R. We performed qRT-PCR in cell lines stably expressing M2R

wildtype and internalization mutants (Δi3 or NC8). We found that M2R reduced β2AR-stimulated

PCK1 induction by approximately 50% (**Figures 3.5c&d**; red), while M2R Δi3 and M2R NC8

reduced β2AR-stimulated *PCK1* induction by approximately 10% and 40% respectively (**Figures

3.5c&d**; dark and light gray). These results suggest that wildtype M2R is most capable in inhibiting

β2AR-stimulated *PCK1* induction, as M2R NC8 has reduced inhibition comparatively. These results

also suggest that M2R intracellular loop 3 is required for the inhibition of β2AR-stimulated *PCK1*

induction, as the removal of intracellular loop 3 severely reduced the ability of M2R Δi3 to modulate

the induction of *PCK1* by the β2AR.

Dynamin is required for M2R-mediated inhibition of β2AR-stimulated *PCK1* transcription

We further investigated what was required of this M2R-mediated inhibition of *PCK1* transcription.

While of β2AR-stimulated *PCK1* induction is primarily associated with the endosomal signal, we

assume that there is some amount that is attributed to the plasma membrane, as inhibition of

endocytosis does not completely eliminate *PCK1* transcription (**Figure 3.5a**). Though there are

unclear differences between the two M2R internalization mutants, they both have reduced

inhibition of *PCK1* transcription compared to wildtype M2R. We hypothesized that there may be

continued inhibition of *PCK1* transcription through the plasma membrane signal, because the M2R

internalization mutants are unable to desensitize and will consequently generate a stronger

inhibitory effect at the plasma membrane.

To determine whether the inhibitory effect by the M2R internalization mutants were on the β2AR

plasma membrane or endosomal signal, we tested the effects of endocytic blockade when both

β2AR and M2R were stimulated. When endocytosis was inhibited by the chemical inhibitor of

dynamin, Dyngo-4A, wildtype M2R had no effect on the β2AR-stimulated *PCK1* transcriptional

response (**Figure 3.6a**). This would suggest that endocytosis is important for M2R inhibition of

PCK1 transcription. To confirm this result, we next tested the effect of endocytic blockade on both

M2R internalization mutants. In both cases, we found that when endocytosis was blocked, M2R

Δi3 and M2R NC8 both did not have any effect on β2AR-stimulated *PCK1* transcription (**Figures**

3.6b&c). This result was contrary to the idea that endocytosis of M2R is important for its inhibition

of *PCK1* transcription.

Our results here show that the M2R has been found with β2AR at both the plasma membrane and

the endosome, and is therefore advantageously positioned to for β2AR signaling inhibition. M2R

receptor inhibits the β2AR cAMP signaling response at different levels and at different locations.

M2R inhibition of β2AR signaling occurs at the acute level of the overall cAMP response, and at the

long-term level of cAMP-dependent transcriptional response. The propagation of these signaling

events occur at different places within the cell, the overall cellular cAMP response primarily occurs

at the plasma membrane while cAMP production tied to *PCK1* transcription is specific to the

endosome.

3.4 Discussion

Functional antagonism between β2AR and M2R signaling was previously described when GPCR signaling was thought to occur primarily from the plasma membrane. The new area of GPCR endosomal signaling has opened up many questions including whether this well described functional antagonism occurs at the endosome as well as the plasma membrane. The present study stably overexpressed M2Rs in HEK293 cells (which endogenously express β2AR) investigated whether M2R endosomal signaling exists, and whether it contributes to the integrated cellular response by modulating the effects of the β2AR at the endosome.

Our data shows that M2Rs exist in the same endosomes as activated β2AR and G_s protein. This suggested that M2Rs may be capable of inhibiting β2AR from the endosome in addition to the plasma membrane. We investigated whether M2Rs are active at the endosome and inhibit the β2AR signaling cascade at the endosome. Consistent with previous studies, we found that M2Rs inhibit β2AR-elicited cAMP production using a live cAMP production assay. To determine whether M2R inhibited the β2AR-stimulated endosomal cAMP, we inhibited the internalization of either both β2AR and M2R or M2R only. Endocytic blockade of both receptors using a chemical inhibitor for dynamin showed that the inhibitory effect of M2R was slightly reduced or had no significant change. Work with the M2R internalization mutants also showed a similar degree of inhibition on β2AR-stimulated cAMP production. Together, these results suggested that the inhibitory effect on β2AR-stimulated cAMP by M2R is similar at the plasma membrane and the endosome.

β2AR-dependent *PCK1* induction was also markedly (but not completely) reduced by carbachol-induced activation of wildtype M2Rs. Previous work indicated that β2ARs induce *PCK1* in HEK293 cells primarily though generating cAMP from endosomes (Tsvetanova & von Zastrow, 2014). Taken

together, these results suggest that M2Rs modulate the β2AR signal at endosomes. M2R internalization mutants also inhibited β2AR-stimulated *PCK1* transcription to a lesser degree than wildtype M2R. This result suggested that M2Rs (wildtype and internalization mutants) were all capable of inhibiting the β2AR endosomal signal, however the mechanism of M2R inhibition remains unanswered.

The initial imaging results showed that M2R exists at endosomes with activated β2AR and G_s protein was promising. Though M2R was found to inhibit the β2AR endosomal signal, there was no direct or conclusive evidence to suggest that M2Rs are active at the endosome. What seems to be difficult to reconcile is the data where the two M2R internalization mutants have different abilities to inhibit β2AR-stimulated *PCK1* transcription. This would suggest that M2R can inhibit the β2AR endosomal signal from a different membrane, contrary to our original assumption. This is formally possible and therefore more experiments will need to be done to test this hypothesis.

We have come up with a few possible explanations with how M2R inhibition of β2AR-stimulated *PCK1* transcription does not require both receptors to exist at the same membrane. M2R at the plasma membrane may greatly inhibit the global cAMP levels required to allow PKAcat to effectively diffuse into the nucleus (**Figure 3.7a**). As previously described in Chapter 2, we hypothesize that the β2AR endosomal signal is promoted through the combined efforts of low global cAMP and high local endosomal cAMP to allow for small but significant concentrations of PKAcat to diffuse into the nucleus. Our results weakly support a stronger M2R inhibitory effect at the plasma membrane than at the endosome (**Figure 3.4**). We hypothesize here, that the M2R inhibitory effect at the plasma membrane is great, and reduces the global cAMP level significantly during the 'plateau phase' (see Chapter 2, **Figure 2.1f**). Without this low global cAMP level, slowed

effective diffusion of PKAcat cannot exist, and PKAcat cannot travel far enough to enter the nucleus.

Another possibility is for M2R to affect the localization of endosomal adenylyl cyclases (AC). Previous work investigating the D1 dopamine receptor indicated that AC5 reside intracellularly at internal vesicles (Kotowski et al., 2011). AC5/6 has been previously described to reside at plasma membrane and internally in the cell, though the trafficking of AC5/6 is not known. Recent work suggests that G_s proteins can promote the trafficking of certain ACs after G_s activation (Lazar, 2019). If AC5/6 or another AC traffics to the endosome through G_s protein activation, could $G\alpha_i$ protein activation prevent this trafficking as an inhibitory mechanism (**Figure 3.7b**)?

Lastly, we describe the necessity of the intracellular loop 3 for M2R inhibition on β2AR-stimulated *PCK1* transcription. Without the third loop, *PCK1* transcription is not inhibited (**Figure 3.6b**). The M2R intracellular loop 3 is a major regulatory domain known to to be important for internalization and desensitization. Additionally, because of its large size (residues 210-387), there may reside multiple motifs important in the regulation of signaling. One such way M2R intracellular loop 3 may play a role in the inhibition of β2AR-stimulated *PCK1* transcription is to recruit an additional protein that regulates cytoplasmic or endosomal cAMP (either through reduced synthesis or promotion of degradation, **Figure 3.7c**). This would reduce intracellular / endosomal cAMP and consequently reduce the cAMP-dependent *PCK1* transcriptional response.

Much future work needs to be done to determine if M2R inhibits β2AR signaling through any of these possibilities. Additionally, an inherent problem with interpreting signaling experiments based on cAMP is that is that the results are correlative. Development of biosensors that detect activation

of receptors and G proteins, as an independent and more incisive approach together with the cAMP signaling experiments will also help determine whether M2R is capable of endosomal signaling.

Further open questions include 1) how the endosome signal is influenced by receptor complexes such as β1AR/β2AR heterodimers (Lavoie et al., 2002), 2) the relationship between endosome activity and β2AR localization to caveolae at the plasma membrane (Odley et al., 2004; Rybin et al., 2000), and 3) whether β2ARs, capable of G_i-coupling (Daaka et al., 1997; Xiao et al., 1995), do so in endosomes.

3.5 Acknowledgements

3.6 Materials and methods

Cell Culture

Human HEK293 cells were grown in DMEM (Gibco, 11965) supplemented with 10% fetal bovine serum (UCSF Cell Culture Facility). Cells were grown at 37°C and 5% CO_2 in a humidified incubator. HEK293 stable cell lines (FLAG-M2R, FLAG-M2R Δi3, FLAG-M2R NC8) were generated by transfection of the plasmid of interest followed by antibiotic selection.

Imaging

Cells were plated on 35 mm imaging dishes (MatTek, P35G-1.5-14-C) coated with poly-L-lysine (Sigma, P8920) and transfected with 4 μL Lipofectamine 2000 (Invitrogen, 11668) and DNA 24 hours before imaging.

Table 3.1 Amounts of transfected DNA constructs for imaging experiments

Plasmid	Amount (ng)
pcDNA3.1+ FLAG-β2AR	1000
pcDNA3 HA-β2AR	1000
pcDNA3.1+ zeo FLAG-M2R	1000
pcDNA3.1+ zeo FLAG-M2R Δi3	1000
pcDNA3.1+ zeo FLAG-M2R NC8	1000
EEA1-DsRed	300
Rab4-mCherry	300
Rab5-EGFP	300
Rab7-EGFP	300
Rab11-EGFP	300
Nb80-EGFP	100
Nb37-mCherry	100
$G\alpha_s$	600
myc-Gβ	300
Gγ	100

First, surface receptors (HA-β2ARs and/or FLAG-M2Rs) were labeled with fluorescently conjugated HA (Invitrogen, A21287 or MBL international, M180-A64) or M1-FLAG antibodies Sigma, F-3040 with Invitrogen, A20173 or A20174) antibody.

Images were acquired on a Nikon Ti inverted spinning disk confocal microscope (Yokogawa CSU-22) with a custom 405-, 488-, 561- and 640-laser launch, with an Apo TIRF 100x/1.49 NA Oil objective (Nikon) and a Photometrics Evolve Delta EMCCD camera controlled by Nikon Elements software. Cells were kept in a temperature- and humidity-controlled chamber (Okolab) during imaging.

Fixed cell imaging

After labeling surface receptors, cells were untreated or treated with 10 µM isoproterenol (Sigma, I6504) and 10 µM carbachol (Sigma, C4382) at 37°C to induce β2AR and M2R internalization, respectively. After 30 minutes of agonist treatment, cells were placed on ice and washed 3 times with cold. Then cells were fixed with 3.7% formaldehyde (Fisher, F79) in modified BRB80 buffer (80 mM sodium PIPES, 1 mM $MgCl_2$, 1 mM $CaCl_2$) for 20 minutes. Cells were washed with PBS, followed by a TBS wash. Cells were washed once more in PBS and mounted on glass slides with ProLong Gold Antifade mounting media (Invitrogen, P10144). Slides were stored for a minimum of 24 hours to allow mounting media to dry before imaging.

Live imaging

Cells were imaged in imaging media (DMEM without phenol red (Gibco, 31053) supplemented with 30 mM HEPES). Images were acquired before and after 30 minutes of agonist treatment.

Flow cytometry analysis of receptor internalization

Cell surface fluorescence of HEK293 cells stably expressing FLAG-M2R, FLAG-M2R Δi3, FLAG-M2R NC8, was measured to determine relative receptor expression and receptor endocytosis. Cells were incubated with 10 µM carbachol for 30 minutes at 37°C to internalize receptors to steady state. After treatment, cells were washed with cold PBS three times, then incubated with 1 µg/ml AlexaFluor647-conjugated (Invitrogen, A20173) M1 mouse anti Flag monoclonal (Sigma, F-3040) antibody at 4°C for 40 minutes on a shaker. Cells were mechanically lifted and mean fluorescence was read by flow cytometry for each sample on a FACSCalibur (BD). Each condition had three technical replicates per biological replicate.

Endocytic inhibition

Cells treated with Dyngo-4A were first changed to serum free media. Then DMSO (control) or 30 µM Dyngo-4A was added to cells for 15 minutes to block endocytosis prior to the experiment.

DNA constructs

pcDNA3.1(+) zeo FLAG-M2R was previously generated in the lab by James Hislop. M2R mutant construction used this construct as the parent vector. The M2R intracellular loop 3 deletion mutant (pcDNA3.1 hM2 Δi3) was a gift from the Kobilka lab (Kruse et al., 2013). The area proximal to the intracellular loop 3 deletion was amplified from this plasmid to generate pcDNA3.1(+) zeo FLAG-M2R Δi3. The M2R NC8 mutant has Ser/Thr to Ala in two phosphorylation clusters in intracellular loop 3, important for internalization (R. Pals-Rylaarsdam & Hosey, 1997). This mutant was generated using InFusion (Clontech) with gBlocks (IDT) containing the N cluster and C cluster of mutated phosphorylation sites and amplified pcDNA3.1(+) zeo FLAG-M2R.

cAMP luminescence assay

Cells were grown to 70% confluency in a 10 cm dish and transfected with 2 µg pGloSensor-20F (Promega, E1171) and 24 µL Lipofectamine 2000 (Invitrogen, 11668). The next day, cells were preincubated with 1.6 mM D-luciferin (Gold Biotechnology, LUCNA-1g) in imaging media (DMEM without phenol red supplemented with 30 mM HEPES; Gibco 31053 and 15630 respectively) for 40 minutes at 37°C and 5% CO_2 in a humidified incubator and distributed into the central 16 wells of a poly-L-lysine coated 24 well plate (250 µL/well). Immediately before imaging, cells were treated with 250 µL imaging media only or imaging media with isoproterenol (100 nM final) and placed into a 37°C heated light-proof chamber, then imaged every 10 seconds for 20 minutes.

Images were acquired by a 512×512 pixel electron multiplying CCD sensor (Hamamatsu C9100-13) using Micro-Manager. ROIs were drawn around each well, and corresponding background ROIs were placed in an area without cells. Additionally, a dark plate control (empty plate) was also imaged to remove background. Matlab was used to measure intensity of each wells, to background subtract from the dark plate control and background ROIs in each run, and to control for vignetting effects from the placement of the camera (Irannejad et al., 2013).

cAMP Homologous Time Resolved Fluorescence (HTRF)

The HTRF kit detecting cAMP levels from CisBio (62AM4PEB) was used. HEK293 cells stably expressing FLAG-M2R were seeded into a 6 well plate. Cells were lifted from 3 wells of the 6 well plate and resuspended in 10 mL of media. Cells were spun down and then resuspended in 2 mL media. The assay was performed according to the manufacturer's protocol.

Briefly, 25 µL of cells were plated in a in a white half-area 96 well plate. Then, 25 µL of media

containing no agonist, 10 µM isoproterenol and/or 10 µM carbachol was added to each sample

containing 500 µM isobutylmethylxanthine (IBMX; Sigma, I5879) and incubated for 30 minutes at

37°C and 5% CO_2 in a humidified incubator. After treatment, cells were lysed with first the addition

of 25 µL lysis buffer with cAMP-d2 conjugate followed by 25 µL anti-cAMP Eu^{3+} cryptate

conjugate. After lysis buffer was added, samples were incubated for one hour at room temperature

and read on a Tecan M200 Infinite Pro controlled with Tecan i-control software.

Initial analysis was done in Excel (Microsoft):

1. Determine ratio of 665 to 620 signal.

$$\text{ratio} = \frac{665_{\text{nm}} \times 10^4}{620_{\text{nm}}}$$

2. Background correct the ratio.

$$\Delta \text{ ratio} = \text{ratio}_{\text{std}} - \text{ratio}_{\text{neg}} \qquad \text{or} \qquad \Delta \text{ ratio} = \text{ratio}_{\text{sample}} - \text{ratio}_{\text{cellneg}}$$

3. For interassay comparison, calculate ΔF and ΔF_{max}.

$$\Delta F = \frac{\text{ratio}_{\text{sample}} - \text{ratio}_{\text{cellneg}}}{\text{ratio}_{\text{cell neg}}}$$

Use $\frac{\Delta F}{\Delta F_{\text{max}}}$ to compare assay to assay.

For actual concentrations, open a tutorial in Prism (GraphPad) "RIA or ELISA: Interpolate unknowns

from sigmoidal curve."

The log concentration of cAMP, and background corrected ratios for the standard curve and the

unknowns were entered. Then using Prism, unknowns from the standard curve were interpolated

using a 4PL sigmoidal model.

RNA extraction

RNA was isolated from cells using the QIAshredder and RNeasy Mini kit (Qiagen, 79654 and 74104, respectively). Briefly, after treatment, cells in a 6 well plate were placed on ice and washed once with cold PBS. Then cells were lysed, and RNA was extracted by following the manufacturer's protocol. RNA was eluted in 30-50 µL of DEPC H_2O, and the concentration of each sample was determined.

Reverse transcription reaction

cDNA was generated from RNA using the SuperScript III First-strand synthesis system (Invitrogen, 18080-051). Briefly, 2 µg of RNA was used per reaction primed with oligo dT. The reverse transcription reaction was performed according to the manufacturer's protocol.

Quantitative Real Time PCR

qRT-PCR was performed using a StepOnePlus (Applied Biosystems) instrument. cDNA generated from extracted RNA was used as the input for the qRT-PCR, with amplification by Power SYBR Green PCR master mix (Applied Biosystems, 4367659). Levels of transcripts were normalized to *GAPDH*. The primer pairs used were:

Table 3.2 qRT-PCR primer sequences

Primer	Sequence
GAPDH forward	5'-CTGCCCAAGATCTTCCATGT-3'
GAPDH reverse	5'-GACAAGCTTCCCGTTCTCAG-3'
PCK1 forward	5'-CTGCCCAAGATCTTCCATGT-3'
PCK1 reverse	5'-CAGCACCCTGGAGTTCTCTC-3'

3.7 References

Alberts, B., Johnson, A., Lewis, J., Raff, M., Roberts, K., & Peter Walter. (2002). *Signaling through*

G-Protein-Linked Cell-Surface Receptors (4gh ed.). Retrieved from

http://www.ncbi.nlm.nih.gov/books/NBK26912/

Aprigliano, O., Rybin, V. O., Pak, E., Robinson, R. B., & Steinberg, S. F. (1997). Beta 1-and Beta 2-

Adrenergic Receptors Exhibit Differing Susceptibility To Muscarinic Accentuated Antagonism.

The American Journal of Physiology, *272*(6 Pt 2), H2726-35. Retrieved from

http://www.ncbi.nlm.nih.gov/pubmed/9227552

Brodde, O. E., & Michel, M. C. (1999). Adrenergic and muscarinic receptors in the human heart.

Pharmacological Reviews, *51*(4), 651–690. Retrieved from

http://www.ncbi.nlm.nih.gov/pubmed/10581327

Calebiro, D., Nikolaev, V. O., Gagliani, M. C., De Filippis, T., Dees, C., Tacchetti, C., … Lohse, M.

J. (2009). Persistent cAMP-signals triggered by internalized G-protein-coupled receptors.

PLoS Biology, *7*(8). https://doi.org/10.1371/journal.pbio.1000172

Daaka, Y., Luttrell, L. M., & Lefkowitz, R. J. (1997). Switching of the coupling of the beta2-

adrenergic receptor to different G proteins by protein kinase A. *Nature*, *390*(NOVEMBER), 88–

91. https://doi.org/10.1038/36362

Delaney, K. A., Murph, M. M., Brown, L. M., & Radhakrishna, H. (2002). Transfer of M2 muscarinic

acetylcholine receptors to clathrin-derived early endosomes following clathrin-independent

endocytosis. *Journal of Biological Chemistry*, *277*(36), 33439–33446.

https://doi.org/10.1074/jbc.M205293200

Dzimiri, N. (1999). Regulation of beta-adrenoceptor signaling in cardiac function and disease.

Pharmacological Reviews, *51*(3), 465–501. Retrieved from

http://www.ncbi.nlm.nih.gov/pubmed/10471415

Ferrandon, S., Feinstein, T. N., Castro, M., Wang, B., Bouley, R., Potts, J. T., … Vilardaga, J.-P. (2009). *Sustained cyclic AMP production by parathyroid hormone receptor endocytosis*. *5*(10), 734–742. https://doi.org/10.1038/nchembio.206

Grant, B. D., & Donaldson, J. G. (2009). Pathways and mechanisms of endocytic recycling. *Nature Reviews. Molecular Cell Biology*, *10*(9), 597–608. https://doi.org/10.1038/nrm2755

Harvey, R. D. (2012). *Muscarinic Receptor Agonists and Antagonists: Effects on Cardiovascular Function*. https://doi.org/10.1007/978-3-642-23274-9_13

Harvey, R. D., & Belevych, A. E. (2003). Muscarinic regulation of cardiac ion channels. *British Journal of Pharmacology*, *139*(6), 1074–1084. https://doi.org/10.1038/sj.bjp.0705338

Hausdorff, W. P., Campbell, P. T., Ostrowski, J., Yu, S. S., Caron, M. G., & Lefkowitz, R. J. (1991). A small region of the beta-adrenergic receptor is selectively involved in its rapid regulation. *Proceedings of the National Academy of Sciences of the United States of America*, *88*(8), 2979–2983. Retrieved from http://www.pubmedcentral.nih.gov/articlerender.fcgi?artid=51367&tool=pmcentrez&rendertype=abstract

Irannejad, R., Tomshine, J. C., Tomshine, J. R., Chevalier, M., Mahoney, J. P., Steyaert, J., … von Zastrow, M. (2013). Conformational biosensors reveal GPCR signalling from endosomes. *Nature*, *495*(7442), 534–538. https://doi.org/10.1038/nature12000

Jones, K., Echeverry, M., Mosser, V., Gates, A., & Jackson, D. (2006). Agonist mediated internalization of M2 mAChR is beta-arrestin-dependent. *Journal of Molecular Signaling*, *1*, 7. https://doi.org/10.1186/1750-2187-1-7

Kotowski, S. J., Hopf, F. W., Seif, T., Bonci, A., & von Zastrow, M. (2011). Endocytosis Promotes Rapid Dopaminergic Signaling. *Neuron*, *71*(2), 278–290. https://doi.org/10.1016/j.neuron.2011.05.036

Kruse, A. C., Ring, A. M., Manglik, A., Hu, J., Hu, K., Eitel, K., … Kobilka, B. K. (2013). Activation

and allosteric modulation of a muscarinic acetylcholine receptor. *Nature*, *504*(7478), 101–106.

https://doi.org/10.1038/nature12735

Lavoie, C., Mercier, J. F., Salahpour, A., Umapathy, D., Breit, A., Villeneuve, L. R., … Hébertl, T. E.

(2002). β1/β2-adrenergic receptor heterodimerization regulates β2-adrenergic receptor

internalization and ERK signaling efficacy. *Journal of Biological Chemistry*, *277*(38), 35402–

35410. https://doi.org/10.1074/jbc.M204163200

Lazar, A. M. (2019). *Elucidating the regulation of adenylyl cyclase type 9 by dynamic membrane*

trafficking.

McCluskey, A., Daniel, J. A., Hadzic, G., Chau, N., Clayton, E. L., Mariana, A., … Robinson, P. J.

(2013). Building a Better Dynasore: The Dyngo Compounds Potently Inhibit Dynamin and

Endocytosis. *Traffic*, *14*(12), 1272–1289. https://doi.org/10.1111/tra.12119

Nikolaev, V. O., Bünemann, M., Schmitteckert, E., Lohse, M. J., & Engelhardt, S. (2006). Cyclic

AMP imaging in adult cardiac myocytes reveals far-reaching β1-adrenergic but locally

confined β2-adrenergic receptor-mediated signaling. *Circulation Research*, *99*(10), 1084–

1091. https://doi.org/10.1161/01.RES.0000250046.69918.d5

Odley, A., Hahn, H. S., Lynch, R. A., Marreez, Y., Osinska, H., Robbins, J., & Dorn, G. W. (2004).

Regulation of cardiac contractility by Rab4-modulated 2-adrenergic receptor recycling.

Proceedings of the National Academy of Sciences, *101*(18), 7082–7087.

https://doi.org/10.1073/pnas.0308335101

Pals-Rylaarsdam, R., & Hosey, M. M. (1997). Two Homologous Phosphorylation Domains

Differentially Contribute to Desensitization and Internalization of the m2 Muscarinic

Acetylcholine Receptor. *Biochemistry*, *272*(22), 14152–14158.

https://doi.org/10.1074/jbc.272.22.14152

Pals-Rylaarsdam, R., Xu, Y., Witt-Enderby, P., Benovic, J. L., & Hosey, M. M. (1995). *Desensitization and internalization of the m2 muscarinic acetylcholine receptor are directed by independent mechanisms. 270*(48). https://doi.org/10.1074/jbc.270.48.29004

Pals-Rylaarsdam, Robin, Gurevich, V. V., Lee, K. B., Ptasienski, J. A., Benovic, J. L., & Hosey, M. M. (1997). Internalization of the m2 muscarinic acetylcholine receptor. Arrestin- independent and -dependent pathways. *Journal of Biological Chemistry*, *272*(38), 23682–23689. https://doi.org/10.1074/jbc.272.38.23682

Reiner, C., & Nathanson, N. M. (2012). Muscarinic Receptor Trafficking. In *Handbook of experimental pharmacology* (pp. 61–78). https://doi.org/10.1007/978-3-642-23274-9_4

Rink, J., Ghigo, E., Kalaidzidis, Y., & Zerial, M. (2005). Rab Conversion as a Mechanism of Progression from Early to Late Endosomes. *Cell*, *122*(5), 735–749. https://doi.org/10.1016/j.cell.2005.06.043

Rochais, F., Abi-Gerges, A., Horner, K., Lefebvre, F., Cooper, D. M. F., Conti, M., … Vandecasteele, G. (2006). A specific pattern of phosphodiesterases controls the cAMP signals generated by different Gs-coupled receptors in adult rat ventricular myocytes. *Circulation Research*, *98*(8), 1081–1088. https://doi.org/10.1161/01.RES.0000218493.09370.8e

Roseberry, A. G., & Hosey, M. M. (2001). Internalization of the M2 muscarinic acetylcholine receptor proceeds through an atypical pathway in HEK293 cells that is independent of clathrin and caveolae. *Journal of Cell Science*, *114*(Pt 4), 739–746. https://doi.org/10.1074/jbc.272.38.23682

Rybin, V. O., Xu, X., Lisanti, M. P., & Steinberg, S. F. (2000). Differential targeting of beta -adrenergic receptor subtypes and adenylyl cyclase to cardiomyocyte caveolae. A mechanism to functionally regulate the cAMP signaling pathway. *The Journal of Biological Chemistry*,

275(52), 41447–41457. https://doi.org/10.1074/jbc.M006951200

Seibold, A., Williams, B., Huang, Z. F., Friedman, J., Moore, R. H., Knoll, B. J., & Clark, R. B. (2000). Localization of the sites mediating desensitization of the beta(2)-adrenergic receptor by the GRK pathway. *Molecular Pharmacology*, *58*(5), 1162–1173. https://doi.org/10.1124/mol.58.5.1162

Sorkin, A., & von Zastrow, M. (2002). Signal transduction and endocytosis: close encounters of many kinds. *Nat Rev Mol Cell Biol*, *3*(8), 600–614. https://doi.org/10.1038/nrm883

Tsvetanova, N. G., & von Zastrow, M. (2014). Spatial encoding of cyclic AMP signaling specificity by GPCR endocytosis. *Nature Chemical Biology*, *10*(12), 1061–1065. https://doi.org/10.1038/nchembio.1665

Vassilopoulos, S., Esk, C., Hoshino, S., Funke, B. H., Chen, C.-Y., Plocik, A. M., … Brodsky, F. M. (2009). A Role for the CHC22 Clathrin Heavy-Chain Isoform in Human Glucose Metabolism. *Science*, *324*(5931), 1192–1196. https://doi.org/10.1126/science.1171529

Violin, J. D., DiPilato, L. M., Yildirim, N., Elston, T. C., Zhang, J., & Lefkowitz, R. J. (2008). beta2-adrenergic receptor signaling and desensitization elucidated by quantitative modeling of real time cAMP dynamics. *The Journal of Biological Chemistry*, *283*(5), 2949–2961. https://doi.org/10.1074/jbc.M707009200

von Zastrow, M., & Kobilka, B. K. (1992). Ligand-regulated internalization and recycling of human beta 2-adrenergic receptors between the plasma membrane and endosomes containing transferrin receptors. *Journal of Biological Chemistry*, *267*(5), 3530–3538.

Xiao, R. P., Ji, X., & Lakatta, E. G. (1995). Functional coupling of the beta 2-adrenoceptor to a pertussis toxin- sensitive G protein in cardiac myocytes. *Mol Pharmacol*, *47*(2), 322–329.

3.8 Figures
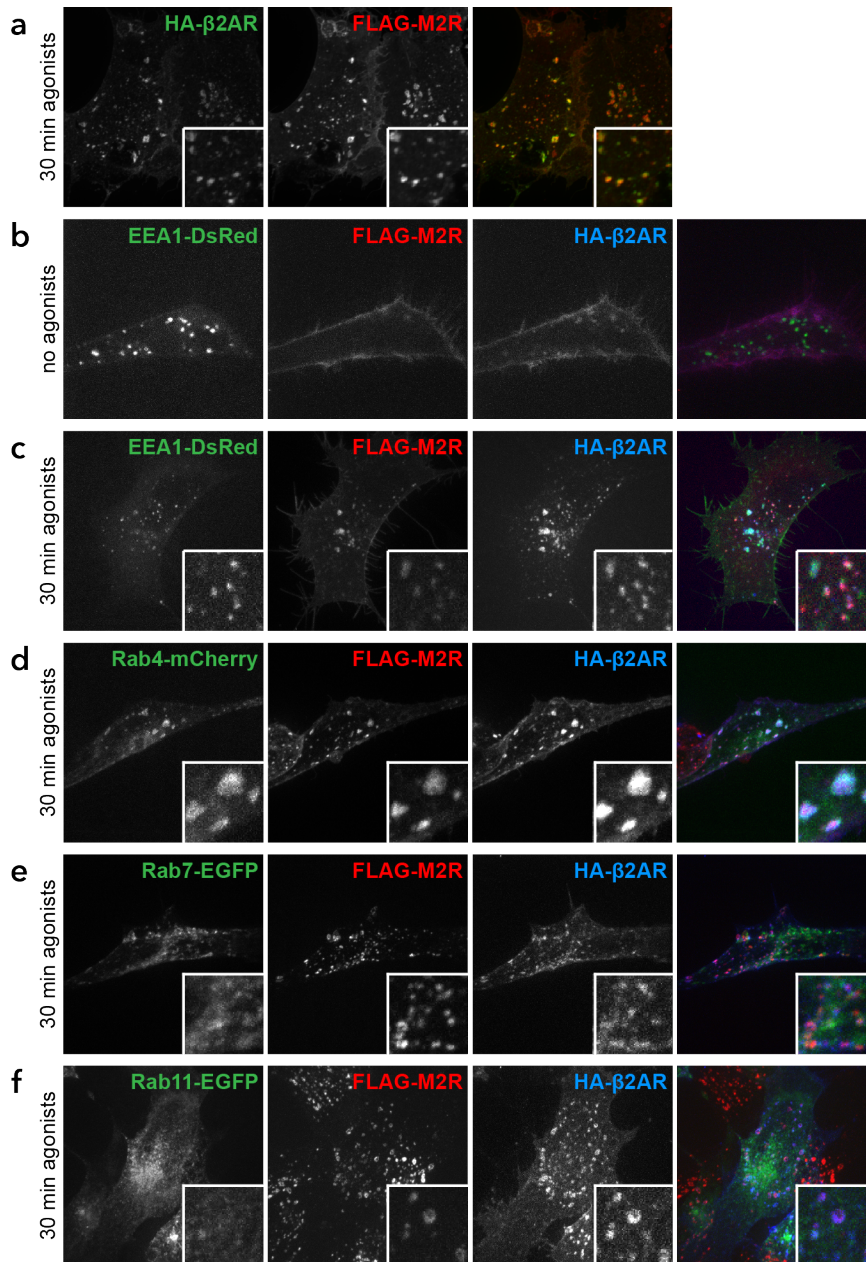
Figure 3.1 β2AR and M2R colocalize a shared population of endosomes
Cells co-expressing HA-β2AR and FLAG-M2R were labeled with fluorescently conjugated HA and FLAG antibodies.
a. Cells were treated with 10 μM Isoproterenol and 10 μM Carbachol for 30 minutes. **b & c**. Cells were also transfected with the early endosome marker, EEA1-DsRed. Cells untreated (**b**) and treated with 10 μM Isoproterenol and 10 μM Carbachol for 30 minutes (**c**). d-f. Cells transfected with markers for early recycling endosomes (**d**, Rab4-mCherry), late endosomes (**e**, Rab7-EGFP), and perinuclear recycling endosomes (**f**, Rab11-EGFP), were treated with 10 μM Isoproterenol and 10 μM Carbachol for 30 minutes.

118
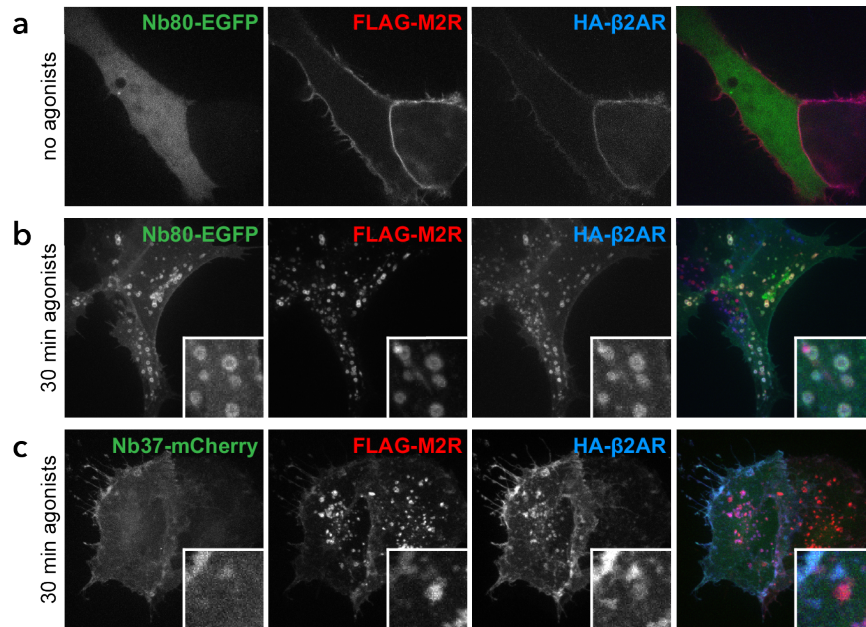
Figure 3.2 M2R colocalizes with activated β2AR and Gₛ at endosomes
Cells co-expressing HA-β2AR and FLAG-M2R were labeled with fluorescently conjugated HA and FLAG antibodies. Cells were additionally transfected with nanobodies that mark activated β2AR, Nb80-EGFP (**a & b**) and activated Gαₛ, Nb37-mCherry (**c**). Cells were either untreated (**a**) or treated with 10 µM Isoproterenol and 10 µM Carbachol for 30 minutes (**b & c**).
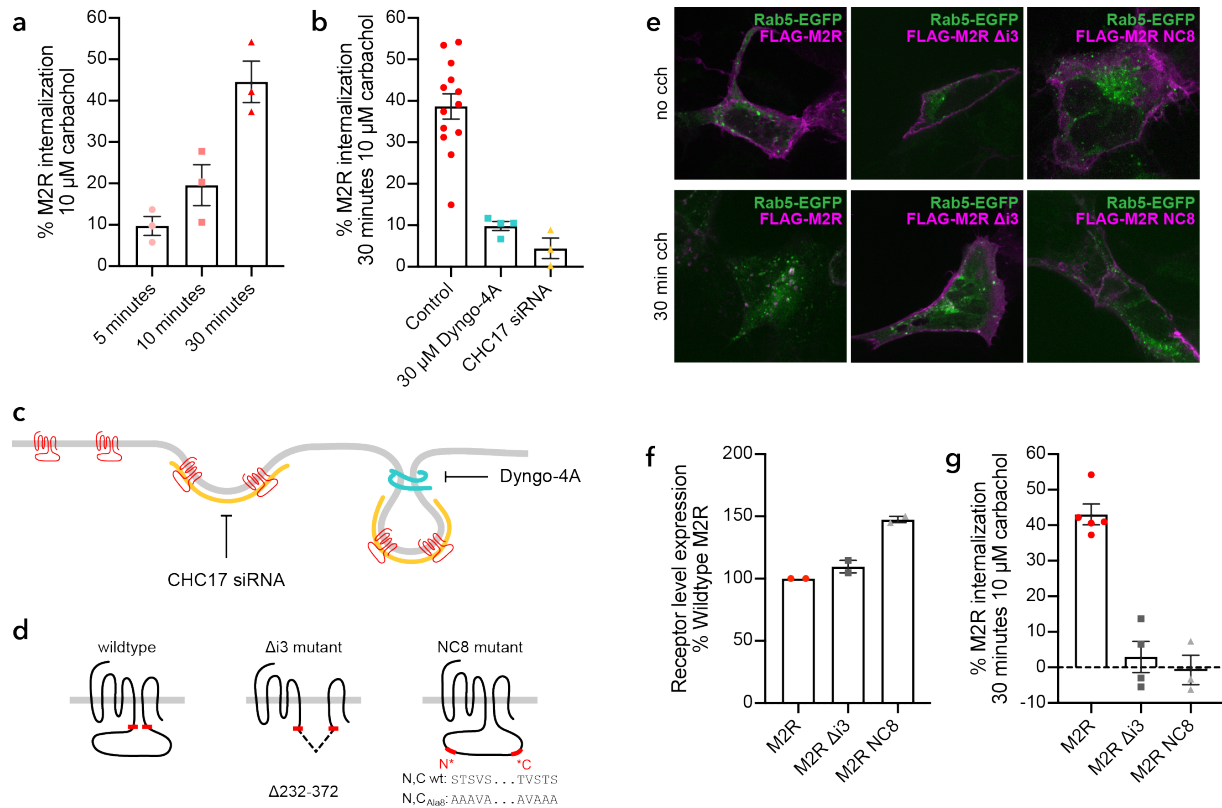
Figure 3.3 Characterization of M2R internalization
M2R internalization was characterized using a flow cytometric assay detecting cell surface receptors (**a, b, g**) and by spinning disk confocal imaging (**e**). **a**. Wildtype M2R internalization at 5, 10 and 30 minutes after 10 μM Carbachol addition. **b**. M2R internalization when endocytosis is blocked using either Dyngo-4A (dynamin inhibitor) or CHC17 siRNA (clathrin siRNA). p = 0.0002 for Control vs Dyngo-4A; p < 0.0001 for Control vs CHC17 siRNA; p = 0.8468, ns, for Dyngo-4A vs CHC17siRNA, by ordinary one-way ANOVA, Sidak's multiple comparisons test. **c**. Cartoon of methods of endocytic blockade used in **b**. **d**. Cartoons of M2R mutants, intracellular loop 3 is highlighted between the two red markers. M2R Δi3 mutant has residues 232-372 in intracellular loop 3 deleted. M2R NC8 mutant has two clusters that represent phosphorylation sites. Ser/Thr residues in these clusters are mutated to Ala. **f & g**. M2R wildtype and mutant stable cell line characterization. **f**. Receptor level expression is measured by labeling cell surface receptors and compared across wildtype M2R and internalization mutant M2R stable cell lines. data are mean ± stdev. **g**. M2R internalization of wildtype and internalization mutant stable cell lines are measured after 30 minute treatment with 10 μM Carbachol. p < 0.0001 for M2R wildtype vs both internalization mutantsl p = 0.9021, ns, for M2R Δi3 vs M2R NC8, by ordinary one-way ANOVA, Sidak's multiple comparison's test. Data are mean ± sem, except in **f**, data are mean ± stdev.
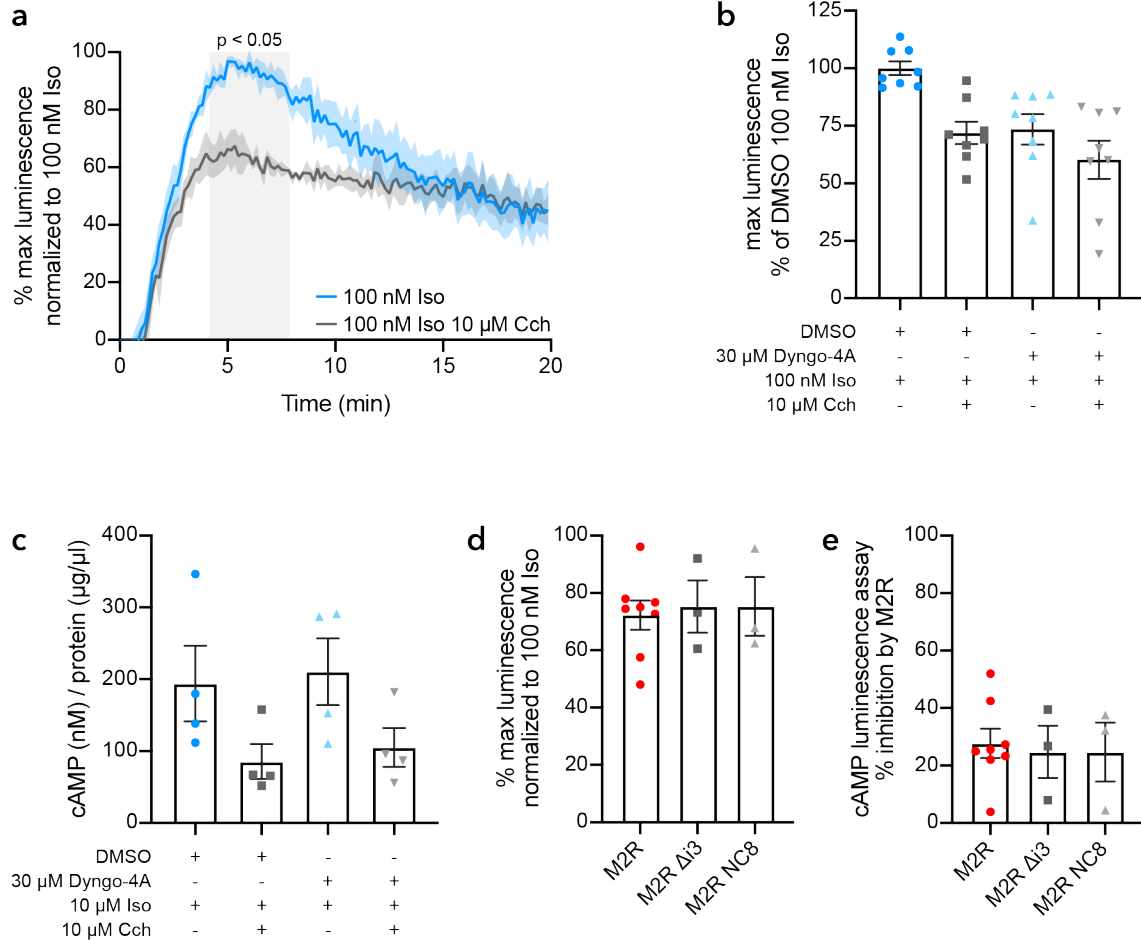
Figure 3.4 M2R inhibition of β2AR acute cAMP signaling
Cells stably expressing FLAG-M2R (wildtype and internalization mutants). **a & b**. cAMP was measured using the cAMP luminescence assay. **a**. Cells were treated with 100 nM Iso or 100 nM Iso and 10 μM Cch and imaged for 20 minutes. Gray region represents $p > 0.05$ by two way ANOVA, Sidak's multiple comparison's test. **b**. Cells were pretreated with DMSO or 30 μM Dyngo-4A, then cells were treated with 100 nM Iso or 100 nM Iso and 10 μM Cch. Maximum luminescence from each condition was normalized to the maximum luminescence from the Control (DMSO) 100 nM Iso condition. $p = 0.0052$ for DMSO Iso vs Iso Cch; $p = 0.2428$, ns, for Dyngo-4A Iso vs Iso Cch by ordinary one-way ANOVA, Sidak's multiple comparison test. **c**. cAMP was measured using a cAMP homogenous time resolved fluorescence assay. Cells were pretreated with DMSO or 30 μM Dyngo-4A, then cells were treated with 100 nM Iso or 100 nM Iso and 10 μM Cch for 30 minutes in IBMX. Amount of cAMP produced was normalized to the amount of protein per sample. **d & e**. cAMP was measured using the cAMP luminescence assay. Cells were treated with 100 nM Iso or 100 nM Iso and 10 μM Cch for 30 minutes. **d**. Maximum luminescence normalized to the maximum luminescence of 100 nM Iso. **e**. Inhibition by wildtype M2R and M2R internalization mutants are plotted. Data are mean ± sem.
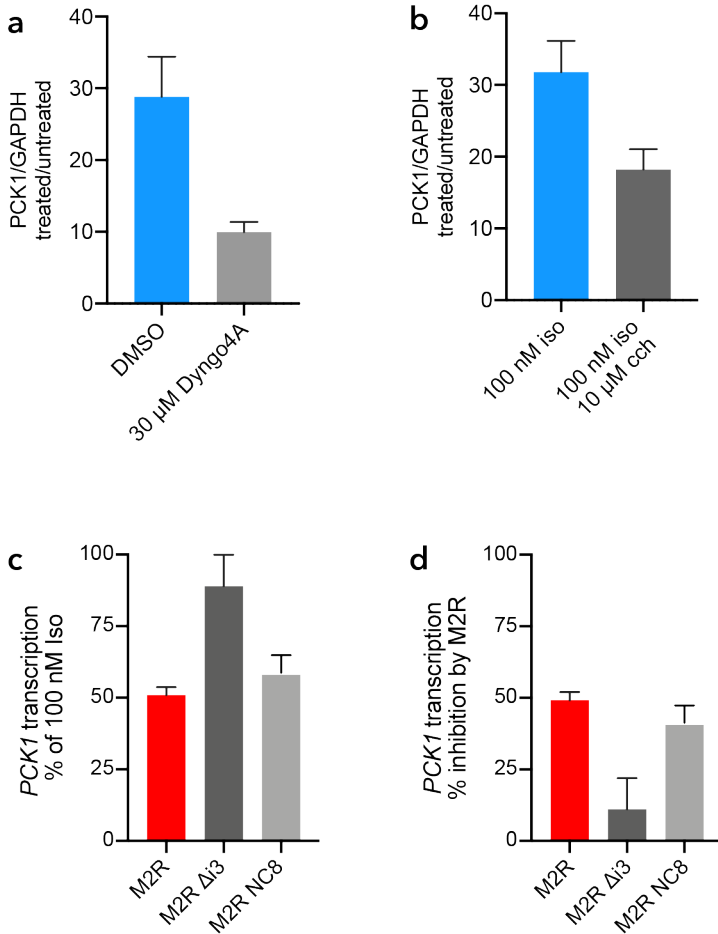
Figure 3.5 M2R inhibition of β2AR-induced *PCK1* transcription is dependent on the i3 loop
Cells were treated with agonists for 2 hours. qRT-PCR was performed on samples from these cells with primers for *PCK1* and *GAPDH*. **a**. Cells expressing FLAG-M2R were pretreated with DMSO or Dyngo-4A before 100 nM Iso treatment. p = 0.0147 by two-tailed, paired, t-test. **b**. Cells expressing FLAG-M2R were treated with 100 nM Iso or 100 nM Iso and 10 μM Cch. p = 0.0002 by two-tailed, paired, t-test. **c**. Cells expressing FLAG-M2R (wildtype, Δi3 or NC8) were treated with 100 nM Iso or 100 nM Iso and 10 μM Cch. p < 0.0001 for M2R vs M2R Δi3; p = 0.3895, ns, for M2R vs M2R NC8; p < 0.0001 for M2R Δi3 vs M2R NC8, by ordinary one-way ANOVA, Sidak's multiple comparisons test. Data are mean ± sem.
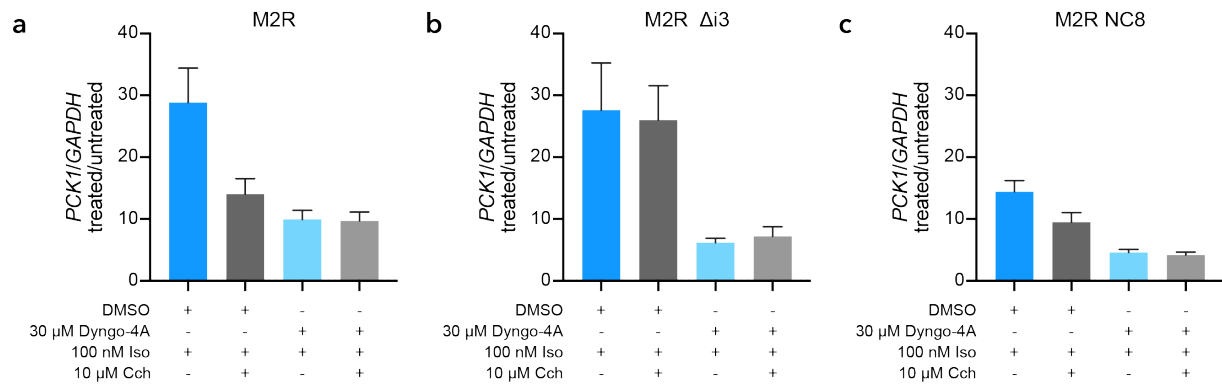
Figure 3.6 M2R inhibition of β2AR-induced *PCK1* transcription is endocytosis independent
Cells were stably expressing FLAG-M2R wildtype (**a**), M2R Δi3 (**b**), or M2R NC8 (**c**), were pretreated with DMSO or Dyngo-4A for 15 minutes and then treated with 100 nM Iso or 100 nM Iso and 10 μM Cch for 2 hours. qRT-PCR was performed on samples from these cells with primers for *PCK1* and *GAPDH*.
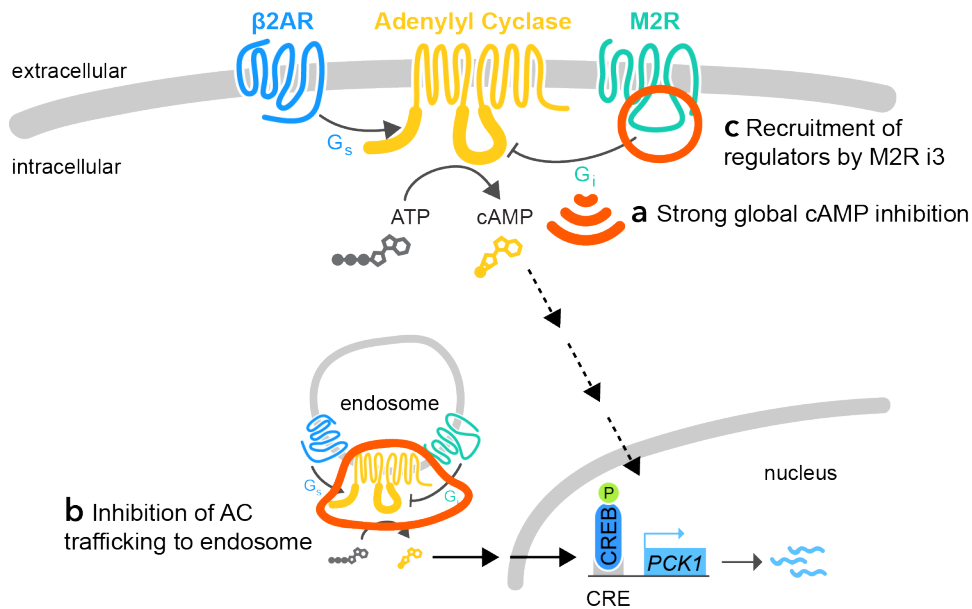
Figure 3.7 Model of functional antagonism between β2AR and M2R
β2AR stimulates the production of cAMP through adenylyl cyclase at the plasma membrane. After endocytosis, β2AR continues to produce cAMP. A downstream consequence of the β2AR cAMP signaling cascade is the phosphorylation of CREB and the induction of *PCK1* transcription. *PCK1* transcription is strongly induced when endocytosis is allowed (solid arrows) and weakly induced when endocytosis is inhibited (dashed arrows). M2R inhibits adenylyl cyclase production of cAMP at the plasma membrane. M2R is able to inhibit β2AR-stimulated *PCK1* transcription, however this inhibition does not require M2R to be at the plasma membrane. **a**. M2R strongly inhibits global cAMP from the plasma membrane. **b**. Adenylyl cyclase (AC) trafficking is inhibited through Gα$_i$ activation at the plasma membrane. **c**. M2R intracellular loop 3 (i3) is required for inhibition of β2AR-stimulated *PCK1* transcription. M2R i3 may recruit regulators of cAMP for inhibition of β2AR-stimulated *PCK1* transcription.

Chapter 4: Tools for studying GPCRs

4.1 Overview

As G protein-coupled receptor (GPCR) endosomal signaling through G proteins is a new area of cell biology, the field requires the development of new tools in order to study this localized signaling. Recent tools that have proven useful in studying GPCR endosomal signaling are conformation biosensors for use in detecting activated GPCRs and G proteins. Expansion of this tool set to other proteins involved signaling would be helpful in detecting where activated proteins are and locations important for this specialized signaling. Additionally, clever pharmacological strategies have been used to activate or turn off signaling from certain membranes by pairing agonists and antagonists with different membrane permeabilities. However, not all GPCRs have pairs of agonists and antagonists with these properties. Another way we can interrogate signaling is by targeting previously described biosensors to different locations in the cell. Lastly, caveats to my work are that they use overexpressed receptors and saturating amounts of agonists. We can easily decrease the amount of agonist used but decreasing receptor expression can be more difficult when strong promoters such as CMV generally are found and used in commercial plasmids. Here, we use a previously published method to easily introduce plasmids that have been optimized to reduce receptor expression by weak promoters and destabilization elements and briefly characterized these low expressing receptor plasmids in our assays.

4.2 Nanobody biosensors

Nanobodies are single chain and single domain camelid antibodies that are sensitive to specific protein conformations. Nanobodies have been previously used to stabilize ligand bound G protein-coupled receptors for structural studies (Rasmussen, Choi, et al., 2011; Rasmussen, DeVree, et al., 2011) and have been adapted as conformational biosensors with the addition of a fluorescent protein to detect activated GPCRs and G protein (Irannejad et al., 2013; Stoeber et al., 2018). Here, we aimed to adapt previously published nanobodies and nanobody biosensors to activated M2 muscarinic acetylcholine receptor (M2R) and Gα_i protein (Kruse et al., 2013).

4.2.1 Activated M2 muscarinic acetylcholine receptor nanobody biosensor (Nb9)

To begin development of an M2R nanobody biosensor, we received the nanobodies that detect activated M2R, Nb9-1, Nb9-8, and Nb9-20, from the Kobilka lab. All three nanobodies were amplified and cloned into pEGFP-N1 and pEGFP-C1.

We tested the nanobody biosensor's ability to detect M2R by transfecting cells with 1 µg FLAG-M2R and 100 ng Nb9-EGFP and looked for a redistribution of both receptor and nanobody after the addition of carbachol, an M2R agonist. We tested these nanobody biosensors using both total internal reflection fluorescent (TIRF) and spinning disk confocal microscopy, using β2AR and Nb80-EGFP as a positive control. Prior to imaging, receptors were labeled with fluorescent-conjugated anti-FLAG (M1) antibody. Before carbachol addition, the nanobody was diffuse in the cytoplasm and the receptor was primarily at the cell surface. After 10 µM carbachol addition, there was very little change in the distribution of Nb9 (**Figure 4.1**). Because there was no Nb9-EGFP detected at the plasma membrane where we know M2R functions, we suspected that Nb9-EGFP as a conformation biosensor was not working.
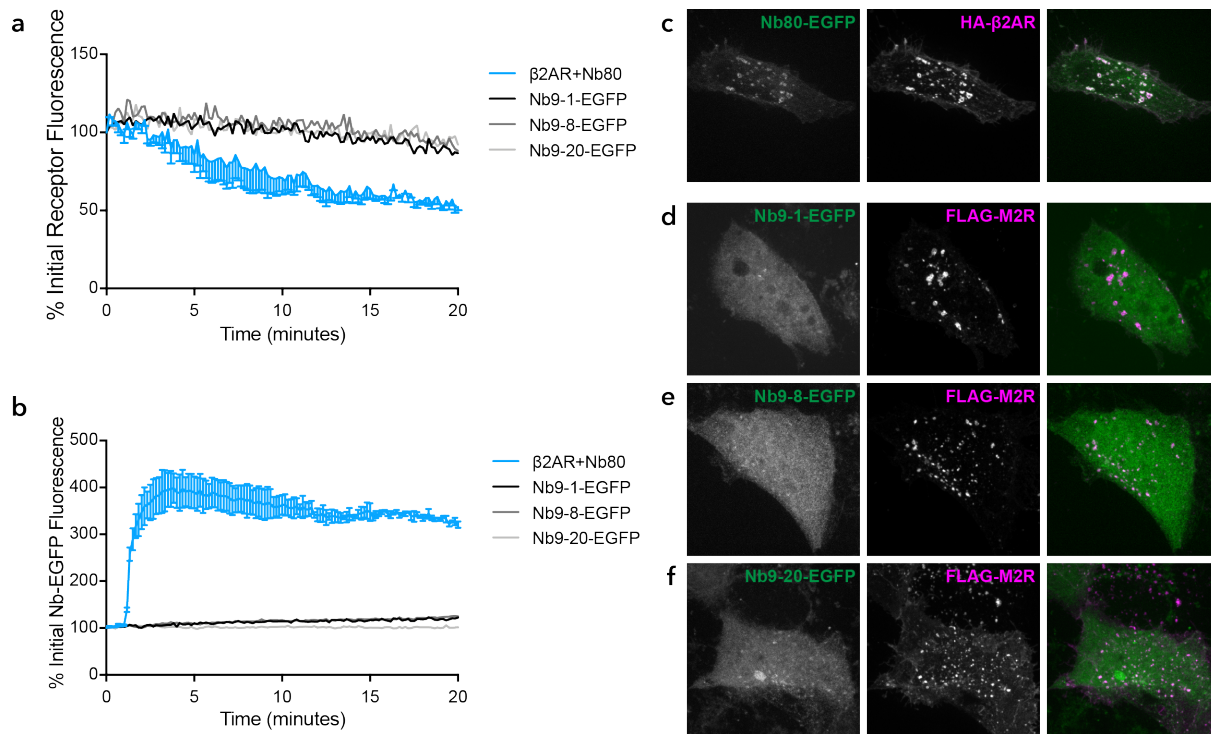
Figure 4.1 Development and results of activated M2R nanobody biosensors
a & b. TIRF analysis of receptor and Nb-EGFP after agonist addition. **c-f**. Cells overexpressing receptor and Nb-EGFP were treated with agonist (10 μM isoproterenol or 10 μM carbachol). Subcellular localization of both receptor and Nb-EGFP were qualitatively analyzed.

Some optimization of the nanobody biosensors, Nb9-1, Nb9-8, and Nb9-20 was attempted.

These strategies included switching the location of the EGFP to on the N-terminus, adding different

sized flexible linkers between Nb9 and EGFP (1x, 3x and 5x GGS), and the use of pertussis toxin.

With the change in location of EGFP and adding flexible linkers, our rational was that maybe EGFP

was somehow hindering Nb9 binding, and so changed the location and increased the distance

between Nb9 and EGFP to test this hypothesis. We chose to use pertussis toxin as a way to

hinder $G\alpha_i$ binding because 1) Nb9 binds similarly to M2R as $G\alpha_i$ and 2) pertussis toxin ADP-

ribosylates the fifth to last residue on $G\alpha_i$. This was our strategy to either decrease potentially

precoupled M2Rs, or to prevent $G\alpha_i$ from blocking available M2Rs to bind. Unfortunately, changes

either failed localize Nb9-EGFP to the plasma membrane (consistent with the initial generation of

Nb9-EGFP biosensors), or were not reproducible. We hypothesize that a disulfide bridge in Nb9 (all

variants) is important in the stabilization of the nanobody, and in the reducing environment of the cell, the disulfide bridge is broken and the structure of the nanobody is altered.

4.2.2 Adapting activated Gα$_s$ Nb37 as an activated Gα$_i$ nanobody biosensor

Heterotrimeric G proteins, first discovered decades ago, have since been well studied and characterized in their role and importance in signal transduction (Gilman, 1987). The G protein subtypes have different lipid modifications which are known to be important in regulating their cellular localization and function (Wedegaertner,
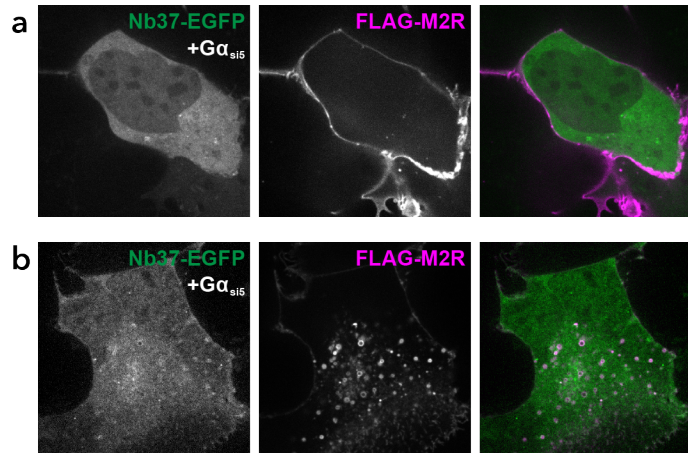
Figure 4.2 Adapting Nb37-EGFP for activated Gα$_i$ by using chimeric Gα$_{si5}$
Cells overexpressing FLAG-M2R, Nb37-EGFP, Gα$_{si5}$, Gβ and Gγ were imaged by spinning disk confocal. Cells were imaged before carbachol addition (**a**) and 30 minutes after (**b**) 10 μM carbachol treatment.

Wilson, & Bourne, 1995). The last five residues of a Gα protein is important in which GPCR it couples to (Liu, Conklin, Blin, Yun, & Wess, 1995). We used this characteristic in our strategy for adapting Nb37-EGFP as a Gα$_i$ nanobody biosensor. We generated a construct called Gα$_{si5}$, where we took the Gα$_s$ protein and replaced the last five residues with the last five residues from Gα$_i$. We then expressed this chimeric G protein along with Gβγ, Nb37-EGFP and M2R and looked at whether localization of Nb37-EGFP changed after carbachol activation of M2R (**Figure 4.2**).

4.3 Targeted cAMP FRET sensors

Previously, cAMP Förster Resonance Energy Transfer biosensors were developed using Epac or indicator of cAMP using Epac (ICUE) as the cAMP binding domain. Upon cAMP binding, FRET would decrease. Localized cAMP FRET sensors have been previously used to detect cAMP at the plasma membrane, in the nucleus and at the Golgi (DiPilato, Cheng, & Zhang, 2004; Godbole, Lyga, Lohse, & Calebiro, 2017; Sample et al., 2012). Our initial goal was to detect cAMP being produced from the endosome. We hypothesized that there would be a delay in endosomal cAMP production relative to plasma membrane cAMP production because the receptor and activated G protein would take time to traffic to the endosome.

To generate the constructs, we first started with the previously published CFP-ICUE2-Citrine construct (Violin et al., 2008). We used targeting sequences lyn11 and 2xFYVE (Hrs) that were previously used to target bacterial-derived photoactivatable adenylyl cyclase to the plasma membrane and
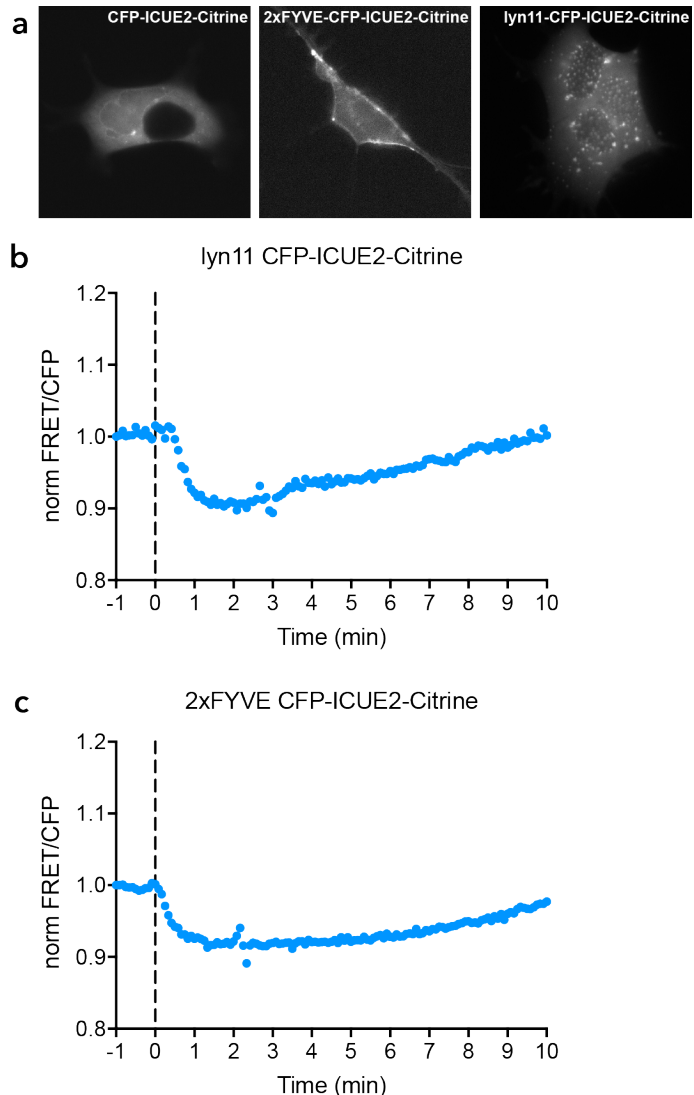
Figure 4.3 Targeting cAMP FRET sensors to the plasma membrane and the endosome
a. Cells transfected with CFP-ICUE2-Citrine, lyn11-CFP-ICUE2-Citrine or 2xFYVE-CFP-ICUE-Citrine and localization of each construct was checked by widefield epifluorescence microscopy. Quantitative analysis of the targeted cAMP FRET sensors in plasma membrane (lyn11-CFP-ICUE2-Citrine, **b**) and endosome (2xFYVE-CFP-ICUE2-Citrine, **c**) targeted cAMP FRET sensors.

130

the endosome (Tsvetanova & von Zastrow, 2014). We first compared the localization the targeted cAMP FRET sensors to the parent cytoplasmic cAMP FRET sensor by widefield epifluorescence microscopy (**Figure 4.3a**). We found that there was some diffuse fluorescence in the cytoplasm, but the targeted constructs did localize to the plasma membrane and the endosome.

Next, we investigated the dynamics of cAMP production in the plasma membrane and endosome targeted cAMP FRET sensors (**Figures 4.3b&c**). We found that both targeted cAMP FRET sensors behaved very similarly to the cytoplasmic cAMP FRET sensor (data not shown). We also did test these targeted sensors at room temperature and with saturating amounts of agonist and PDE inhibitor (10 µM isoproterenol and 100 µM IBMX). In both cases, we did see a larger FRET change after agonist was added, however the kinetics of each sensor remained similar.

Because we did not see a change in kinetics between the targeted sensor, we suspected this was due to the diffusibility of cAMP and the simplicity of the organization in our HEK293 cells. Previous studies in cardiomyocytes have shown spatial definition of cAMP (Nikolaev, Bünemann, Schmitteckert, Lohse, & Engelhardt, 2006). Cardiomyocytes are highly structured and organized cell in comparison to HEK293 cells, this could help explain the differences in our cAMP FRET sensor results.

4.4 Reducing overexpressed receptor levels

We used the ePiggyBac transposon gene delivery system to reduce protein expression by using a weak promoter (Ubiquitin C, UbC) and mRNA destabilizing elements (Alexander et al., 2019; Lacoste, Berenshteyn, & Brivanlou, 2009; Qin et al., 2010). Here, generated low expressing M2R receptor stables and show reduced expression compared to the original stable cell line, and conservation of M2R characteristics (internalization and inhibition of cAMP signaling).

To generate our M2R constructs, we first obtained destination vectors (pDEST ePiggyBac-UbC, pDEST ePiggyBac UbC-2xDE, pDEST ePiggyBac UbC-4xDE) from the Weiner lab. We cloned M2R IRES Neo and M2R NC8 IRES Neo into an entry vector, pENTR1A. Then using the Gateway cloning system, we switched our cassettes M2R IRES Neo or M2R NC8 IRES Neo into the destination vector to generate ePiggyBac UbC M2R IRES Neo and other variants. We then generated stable cell lines from these plasmids.

We tested these stable cell lines by first comparing their receptor expression levels to our previously generated M2R stable cell line (**Figure 4.4a**). We found that receptor expression was reduced in cells where M2R was promoted by UbC and expression was even further reduced with more destabilization elements (DE) and less ePiggyBac transposon expressed. These stable cell lines were also checked if they maintained expected internalization abilities. As expected, all the wildtype M2R cell lines were able to internalize to a significant degree after 30 minutes of 10 μM carbachol treatment (**Figure 4.4b**). Additionally, M2R NC8 cell lines behaved as expected with reduced internalization after 30 minutes of 10 μM carbachol treatment (**Figure 4.4b**). Lastly, the ability for these reduced expression cell lines to inhibit β2AR-stimualted *PCK1* transcription was examined. We found that M2R with four destabilization elements was still able to inhibt β2AR-

stimualted *PCK1* transcription, and that this was verified to be dependent on the activation of Gα$_i$

by the addition of pertussis toxin (**Figure 4.4c**). Similarly, M2R NC8 with four destabilization

elements also maintained the ability to inhibit β2AR-stimualted *PCK1* transcription that was Gα$_i$-

dependent (**Figure 4.4d**). Using the ePiggyBac gene delivery system in combination with elements

to reduce expression (weak promoter and destabilization elements) worked effectively to reduce

M2R expression levels without compromising function.
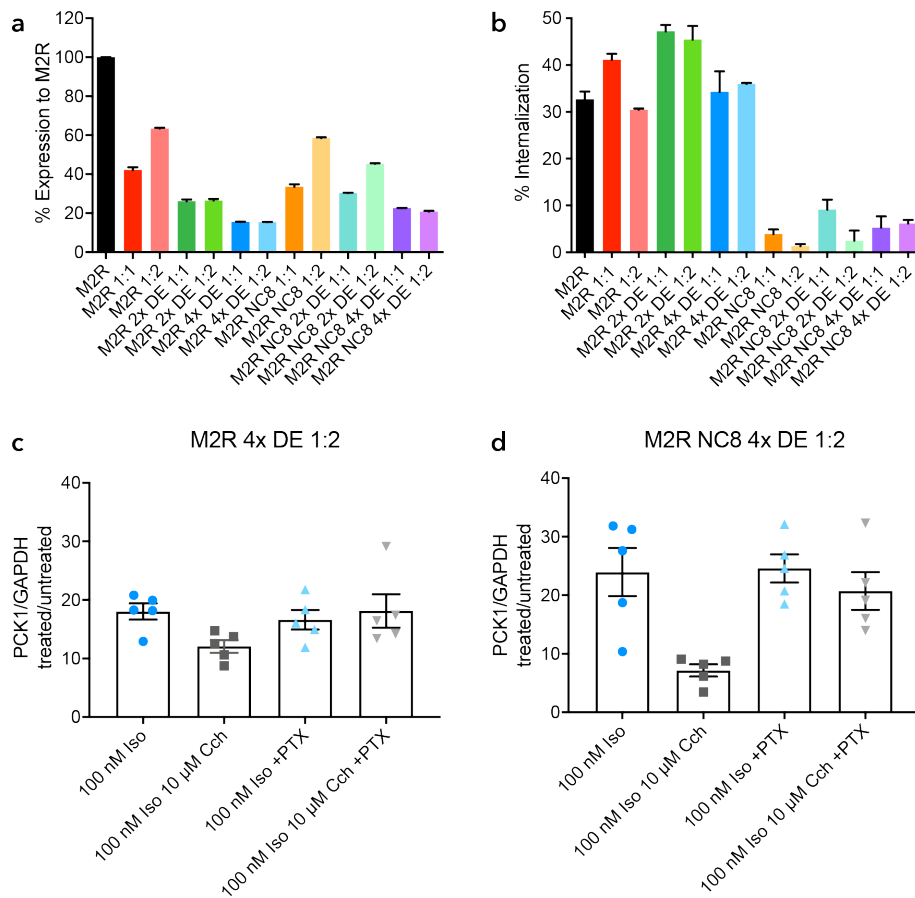
Figure 4.4 Characterization of stable cell lines with reduced receptor expression
a. Receptor expression of stable M2R cell lines generated using the ePiggyBac system. 1:1 and 1:2 ratios designates amount of receptor:ePiggyBac transposon constructs during transfection. **b.** M2R receptor internalization. Lowest expressors of M2R and M2R NC8 were both tested for inhibition on β2AR-stimulated *PCK1* transcription. Pertussis toxin added to check specificity of inhibition.

4.5 Detecting activated β2 adrenergic receptors in zebrafish

The recent studies using conformational biosensors has proven how powerful these nanobody

biosensor can be. These nanobody biosensors have been found to be rather specific, as they do

bind to other receptors of the same type - Nb80 does not detect other $G\alpha_s$ activated GPCRs, e.g.

D1 dopamine receptor (Irannejad et al., 2013). However, Nb80 detects human β1AR in addition to

β2AR, likely because they are approximately 66% homologous.

To expand the use of nanobody biosensors for study within organisms, we asked whether the

β2AR-specific Nb80 could detect zebrafish βARs. Zebrafish have one β1AR (*adrb1*) and two

β2ARs (*adrb2a* and *adrb2b*), and these βARs are 60% or more homologous to their human

analogs. Previous work has been done characterizing different βAR agonists by expressing

zebrafish βARs in HEK293 cells (Steele et al., 2011). Here, we generate FLAG-tagged zebrafish

βAR constructs (FLAG-zfβAR) by isolating genomic DNA from a zebrafish tail fin sample. Like many

GPCRs, none of the zebrafish βARs had introns, and so the cDNA was directly amplified from the

genomic DNA and cloned into pcDNA3 with an N-terminal FLAG tag. Only zfβ1AR and zfβ2ARb

were cloned, and mistakenly a stop codon was forgotten, resulting in a minorly larger protein.

These constructs were recloned by others and the same trafficking behavior was seen for both

receptors (personal communication, R. Irannejad 2019).

We transfected zfβARs and Nb80-EGFP and imaged their localizations in the cell after 30 minutes

of 10 µM isoproterenol by spinning disk confocal (**Figures 4.5a&b**). We found that zfβ1AR

internalized after isoproterenol addition and that Nb80-EGFP, instead of being diffuse in the

cytoplasm, exhibited puncta primarily at the perinuclear region that colocalized with some zfβ1ARs.

With zfβ2Arb, we found minimal internalization with zfβ2ARb primarily at the plasma membrane.

Nb80-EGFP in this case remained diffuse in the cytoplasm and did not seem to colocalize with Nb80-EGFP.
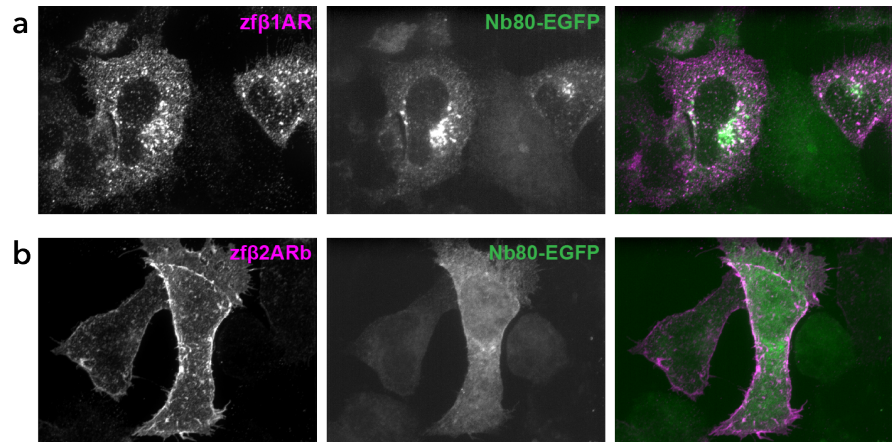
Figure 4.5 Detecting activated βARs in zebrafish
FLAG-tagged zfβARs, zfβ1AR (**a**) or zfβ2ARb (**b**), and Nb80-EGFP were transfected into HEK293 cells and imaged by spinning disk confocal after 30 minutes of 10 μM isoproterenol treatment.

Other work was also done to express Nb80-EGFP in zebrafish. We cloned a construct that put Nb80-EGFP under the cmlc2 zebrafish cardiac promoter and injected DNA into embryos. We found that the heart was faintly EGFP positive, but could not detect any changes after isoproterenol addition. Our major problems with this experiment were that 1) fish expressing Nb80-EGFP seemed to have development defects and 2) we had some issues with mounting larva and for imaging. Our rationale for our first problem was that high expression of Nb80 is known to be toxic and capable of blocking βAR signaling, overexpression of Nb80 in the heart may have caused development defects. To prevent this, we additionally generated a construct with a light inducible promoter for Nb80-EGFP. This system, TAEL, was previously described and used in zebrafish ((Motta-Mena et al., 2014; Reade et al., 2017). This construct yet to be tested.

4.6 References

Alexander, J. M., Guan, J., Li, B., Maliskova, L., Song, M., Shen, Y., … Weiner, O. D. (2019). Live-cell imaging reveals enhancer-dependent Sox2 transcription in the absence of enhancer proximity. *ELife*, *8*. https://doi.org/10.7554/eLife.41769

DiPilato, L. M., Cheng, X., & Zhang, J. (2004). Fluorescent indicators of cAMP and Epac activation reveal differential dynamics of cAMP signaling within discrete subcellular compartments. *Proceedings of the National Academy of Sciences*, *101*(47), 16513–16518. https://doi.org/10.1073/pnas.0405973101

Gilman, A. G. (1987). *G proteins: Tranducers of Receptor-Generated Signals*. Retrieved from www.annualreviews.org

Godbole, A., Lyga, S., Lohse, M. J., & Calebiro, D. (2017). Internalized TSH receptors en route to the TGN induce local Gs-protein signaling and gene transcription. *Nature Communications*, *8*(1), 23–42. https://doi.org/10.1038/s41467-017-00357-2

Irannejad, R., Tomshine, J. C., Tomshine, J. R., Chevalier, M., Mahoney, J. P., Steyaert, J., … von Zastrow, M. (2013). Conformational biosensors reveal GPCR signalling from endosomes. *Nature*, *495*(7442), 534–538. https://doi.org/10.1038/nature12000

Kruse, A. C., Ring, A. M., Manglik, A., Hu, J., Hu, K., Eitel, K., … Kobilka, B. K. (2013). Activation and allosteric modulation of a muscarinic acetylcholine receptor. *Nature*, *504*(7478), 101–106. https://doi.org/10.1038/nature12735

Lacoste, A., Berenshteyn, F., & Brivanlou, A. H. (2009). An efficient and reversible transposable system for gene delivery and lineage-specific differentiation in human embryonic stem cells. *Cell Stem Cell*, *5*(3), 332–342. https://doi.org/10.1016/j.stem.2009.07.011

Liu, J., Conklin, B. R., Blin, N., Yun, J., & Wess, J. (1995). Identification of a receptor/G-protein contact site critical for signaling specificity and G-protein activation. *Proceedings of the*

National Academy of Sciences of the United States of America, *92*(25), 11642–11646. https://doi.org/10.1073/pnas.92.25.11642

Motta-Mena, L. B., Reade, A., Mallory, M. J., Glantz, S., Weiner, O. D., Lynch, K. W., & Gardner, K. H. (2014). An optogenetic gene expression system with rapid activation and deactivation kinetics. *Nature Chemical Biology*, *10*(3), 196–202. https://doi.org/10.1038/nchembio.1430

Nikolaev, V. O., Bünemann, M., Schmitteckert, E., Lohse, M. J., & Engelhardt, S. (2006). Cyclic AMP imaging in adult cardiac myocytes reveals far-reaching β1-adrenergic but locally confined β2-adrenergic receptor-mediated signaling. *Circulation Research*, *99*(10), 1084–1091. https://doi.org/10.1161/01.RES.0000250046.69918.d5

Qin, J. Y., Zhang, L., Clift, K. L., Hulur, I., Xiang, A. P., Ren, B.-Z., & Lahn, B. T. (2010). Systematic Comparison of Constitutive Promoters and the Doxycycline-Inducible Promoter. *PLoS ONE*, *5*(5), e10611. https://doi.org/10.1371/journal.pone.0010611

Rasmussen, S. G. F., Choi, H.-J., Fung, J. J., Pardon, E., Casarosa, P., Chae, P. S., … Kobilka, B. K. (2011). Structure of a nanobody-stabilized active state of the β(2) adrenoceptor. *Nature*, *469*(7329), 175–180. https://doi.org/10.1038/nature09648

Rasmussen, S. G. F., DeVree, B. T., Zou, Y., Kruse, A. C., Chung, K. Y., Kobilka, T. S., … Kobilka, B. K. (2011). Crystal structure of the β2 adrenergic receptor-Gs protein complex. *Nature*, *477*(7366), 549–555. https://doi.org/10.1038/nature10361

Reade, A., Motta-Mena, L. B., Gardner, K. H., Stainier, D. Y., Weiner, O. D., & Woo, S. (2017). TAEL: a zebrafish-optimized optogenetic gene expression system with fine spatial and temporal control. *Development*, *144*(2), 345–355. https://doi.org/10.1242/dev.139238

Sample, V., DiPilato, L. M., Yang, J. H., Ni, Q., Saucerman, J. J., & Zhang, J. (2012). Regulation of nuclear PKA revealed by spatiotemporal manipulation of cyclic AMP. *Nature Chemical Biology*, *8*(4), 375–382. https://doi.org/10.1038/nchembio.799

Steele, S. L., Yang, X., Debiais-Thibaud, M., Schwerte, T., Pelster, B., Ekker, M., … Perry, S. F.

    (2011). In vivo and in vitro assessment of cardiac β-adrenergic receptors in larval zebrafish

    (Danio rerio). *Journal of Experimental Biology*, *214*(9), 1445–1457.

    https://doi.org/10.1242/jeb.052803

Stoeber, M., Jullié, D., Lobingier, B. T., Laeremans, T., Steyaert, J., Schiller, P. W., … von Zastrow,

    M. (2018). A Genetically Encoded Biosensor Reveals Location Bias of Opioid Drug Action.

    Neuron, *98*(5), 963-976.e5. https://doi.org/10.1016/J.NEURON.2018.04.021

Tsvetanova, N. G., & von Zastrow, M. (2014). Spatial encoding of cyclic AMP signaling specificity

    by GPCR endocytosis. *Nature Chemical Biology*, *10*(12), 1061–1065.

    https://doi.org/10.1038/nchembio.1665

Violin, J. D., DiPilato, L. M., Yildirim, N., Elston, T. C., Zhang, J., & Lefkowitz, R. J. (2008). beta2-

    adrenergic receptor signaling and desensitization elucidated by quantitative modeling of real

    time cAMP dynamics. *The Journal of Biological Chemistry*, *283*(5), 2949–2961.

    https://doi.org/10.1074/jbc.M707009200

Wedegaertner, P. B., Wilson, P. T., & Bourne, H. R. (1995). Lipid modifications of trimeric G

    proteins. *The Journal of Biological Chemistry*, *270*(2), 503–506.

    https://doi.org/10.1074/jbc.270.2.503

Chapter 5: Discussion

One day, in retrospect, the years of struggle will strike you as the most beautiful.
Sigmund Freud

5.1 Overview

The first papers describing G protein-coupled receptor signaling at the endosome through G protein activation were first published 10 years ago. In the past decade, much work has been done to understand more about the function and regulation of endosomal signaling by GPCRs. This dissertation explored how the endosome can promote such a specific and selective signal through cAMP-dependent transcription and investigated the consequences integrative cellular signaling from multiple receptors active at multiple locations. From Chapter 2, we identify that the key point in the cAMP signaling cascade in promoting cAMP-dependent transcription is nuclear PKAcat accumulation. In Chapter 3, we find that the M2R can inhibit β2AR-stimulated cAMP-dependent transcription but it is not necessary for M2R to be at the same membrane as β2AR. Together, our work in understanding endocytic control of cAMP-dependent transcription provides insight into how the cAMP signaling cascade is propagated and the importance of endocytosis.

5.2 Mechanism of nuclear accumulation of PKAcat

The role that PKAcat plays in the cAMP signaling cascade is to phosphorylate substrates in the cytoplasm and nucleus. PKAcat phosphorylates CREB in the nucleus which results in the induction of CRE-mediated gene transcription. There are two ways for PKA to localize in the nucleus. The first is through diffusion of PKAcat after liberation from PKAreg as a result of cAMP elevation (Harootunian et al., 1993). The second is through nuclear-localized AKAP95 microdomains containing both PDE4 and PKA holoenzyme where nuclear PKAcat at the AKAP95 microdomain is activated under high levels of cAMP (Clister et al., 2019).

In Chapter 2, we find that nuclear accumulation of PKAcat is the key step in promoting cAMP-dependent transcription. This is consistent with previous work that found that nuclear import of PKAcat was the rate-limiting step in the cAMP-dependent transcriptional pathway (Hagiwara et al., 1993). Our findings suggest that without endocytosis, much less PKAcat is accumulated in the nucleus over tens of minutes. We emphasized that somehow endocytosis is promoting nuclear PKAcat accumulation although through unknown mechanisms. Here, I speculate the possible mechanisms for nuclear accumulations of PKAcat in more detail.

In Chapter 2 we found that there was a divide in the cAMP signaling cascade components and how greatly they were affected by the inhibition of endocytosis. On one side of the divide are two components, the first ones we studied that are representative of global cAMP and cytoplasmic PKAcat. Neither global cAMP nor cytoplasmic PKAcat were greatly affected by endocytic blockade. However, on the other side of this divide are the more specific localized responses of nuclear PKAcat, CREB phosphorylation and *PCK1* transcription, all of which were affected greatly

by endocytic blockade. Interestingly, these components of the cAMP signaling cascade reside in the nucleus. How could such a selective signal be produced?

We first hypothesize a simple idea based on fundamental diffusion principles of how the cAMP-dependent transcriptional response is selectively generated by endocytosis. We propose that the combination of global cAMP (i.e. primarily produced at the plasma membrane) and local cAMP (e.g. endosome source) are important in deciding whether nuclear accumulation of PKAcat occurs during the plateau phase of cAMP signaling.

Global cAMP defines the ability of PKAcat to diffuse (speed and distance) in the cell. When the diffusion rate of a protein is fast, it does not concentrate greatly anywhere in the cell as it quickly distributes equally and evenly (**Figure 5.1a**; Berg, 1993). However, when the diffusion rate of a protein is slow, it is most concentrated next to its source and decreases in a concentration gradient as it moves away from its source (**Figure 5.1a**). The distance of this gradient is determined by the diffusion rate, and consequently the slower the rate the longer the distance (**Figure 5.1b**).
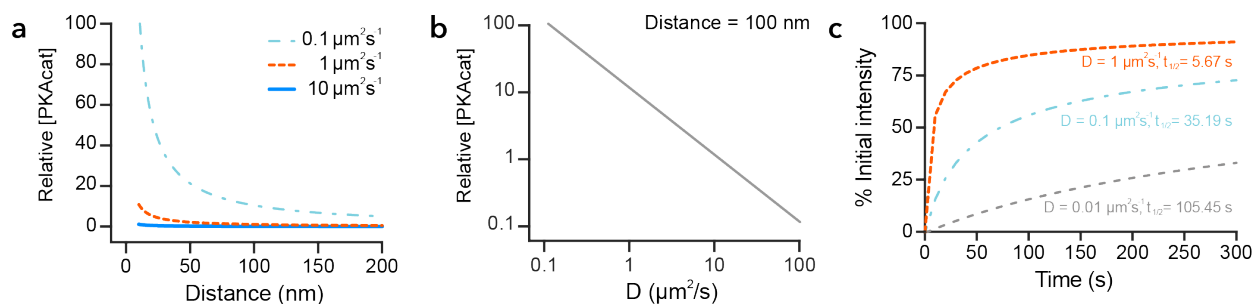
Figure 5.1 Distance and concentration determined by diffusion rates
a & b. Dependence of distance traveled and relative concentrations on diffusion rate. **a**. We used the equation determining the concentration of a molecule due to a pulse with a time of t, $C(r,t) = (i/4\pi Dr)\ erfc\ (r/((4Dt)^{0.5}))$ where D is diffusion, r is distance (See Appendix C; Berg 1993). **b**. We used the equation determining the concentration of a molecule when a pulse is long enough that the concentration approaches a steady-state value, $C(r,t) = (i/4\pi Dr)$ where D is diffusion, r is distance (See Appendix C; Berg 1993) **c**. Bleaching recovery from a 30 μm^2 rectangular FRAP spot. We used the recovery equation adapted for a rectangular bleaching spot $I_{(t)} = I_{(\infty)}\ (1- (w^2(w^2 + 4\ \pi D_c t)^{-1})^{-0.5})$ where w^2 is the area of the rectangular bleaching spot (30 μm^2 for our experiments) and D_c is diffusion coefficient (See Appendix C; Blumenthal et al., 2015).

If there is any free PKAcat, it would readily be captured by a PKAreg as PKAreg exists in excess of

PKAcat in the cell (Walker-Gray et al., 2017). When there are high levels of global cAMP, all or most

of the PKAreg subunits are bound with cAMP, and consequently PKAcat instantly binds PKAreg

and readily unbinds (Cheng et al., 2001; Zawadzki & Taylor, 2004). Therefore, PKAcat spends very

little time on PKAreg and behaves similarly to a freely diffusing protein (Swaminathan et al., 1997).

We speculate that when there are low levels of global cAMP, the behavior of PKAcat is somewhere

in between. There is a mixture of PKAreg subunits that are bound with cAMP so PKAcat can be

released and a population of free PKAcat exists. This free PKAcat can freely bind PKAreg, and will

unbind with a slower timeframe than when there are globally high cAMP levels. This results in

effective diffusion because PKAcat moves in the cell at a slowed diffusion rate due to the on and

off interactions with multiple PKAreg subunits.

Local cAMP determines the amount of PKAcat that is released. Endosomes exist throughout the

cytoplasm, and such local sources of cAMP production can release PKAcat in the cytoplasm to

diffuse in the cell. When global cAMP is at a low level, PKAcat can diffuse further from its original

location, together with local cAMP production by endosomes, an increased the pool of slowly

diffusing PKAcat that can enter the nucleus.

Our data supports this hypothesis as we see both a slowed mobility of PKAcat from our FRAP

experiment (**Figure 2.6**). We estimate this slowed mobility to be 10-100 fold slower than estimated

free diffusion in the cytoplasm ($\sim$30 μm^2/s, Swaminathan et al., 1997). At this slowed diffusion rate,

PKAcat concentrated at the perinuclear region can traverse the distance necessary to enter the

nucleus (**Figure 5.1c**; Blumenthal et al., 2015) .

We additionally propose another method in which nuclear accumulation of PKAcat is promoted by endocytosis. Nuclear accumulation of PKAcat can be regulated by nuclear import or nuclear export. No known nuclear localization sequence has been found in PKAcat, but A kinase interacting protein 1 (AKIP1) and Asn2 (the non-deamidated form of PKAcat) have been suggested to play a role in targeting PKAcat to the nucleus (Pepperkok et al., 2000; Sastri et al., 2005). Additionally, protein kinase inhibitor (PKI), a known regulator of PKAcat, inhibits PKAcat through binding and nuclear export (Wen et al., 1995). Endocytosis may modulate these events to promote PKAcat nuclear import or nuclear retention.

Lastly, it is possible that cytoplasmic PKAcat is affected when endocytosis is blocked, however we cannot detect these differences with our current imaging assays. It is possible that these differences are unseen due to a lack of spatial resolution or low signal to noise. One way to test whether there is a population of endosomes near the perinuclear region important in contributing to nuclear accumulation of PKAcat is to use inverse FRAP. Here we would photobleach an area of the cytoplasm that did not contain perinuclear PKAcat and observe the perinuclear region for a pattern of stable / unstable PKAcat. If a pattern emerged, this would indicate the presence locally released PKAcat by endosomes.

There remains much to be explored in understanding the mechanism in PKAcat nuclear accumulation. Our findings determined that nuclear accumulation of PKAcat is an important key step in promoting endocytic control of cAMP-dependent transcription. It is possible that there are multiple mechanisms of nuclear PKAcat activity at work, and dependent on the cell type and organization, one or a combination of these mechanisms could be working together. Work with the TSHR has found an importance for PKA localized at the Golgi (Godbole et al., 2017). Additionally,

TSHR is a GPCR that has sustained high levels of cAMP. Golgi-localized PKAcat could be working in concert with nuclear localized PKAcat (sensitive to high levels of cAMP) to promote an endocytosis-sensitive cAMP-dependent transcriptional response.

5.3 Integrative cellular signaling

Multiple G protein-coupled receptors are often involved in a single physiological process, as a robust and important way to regulate such a physiological response. We have yet to understand how functional relationships between receptors are affected by endocytosis and whether endosomes provide a privileged location where receptors can have increased or decreased modulation of their signal. We have much to understand in how cells interpret and integrate multiple signaling responses generated by different inputs and receptors. Our goal was to determine how functional relationships between two opposing receptors are regulated as receptors signal and traffic from the plasma membrane to the endosome where they may continue to signal. We used the β2AR and the M2R as an example of receptors with such a functional antagonistic relationship.

Very little has been published with regards to how endosomal signaling affects the functional relationship between two GPCRs. One study describes a synergistic effect when the PTHR and β2AR are coactivated (Jean-Alphonse et al., 2016). β2AR helps increase cAMP production through Gα$_i$ activation at the plasma membrane and the subsequent release of Gβγ. Gβγ then localizes to the endosome to activate AC2, described to be important for PTHR endosomal signaling, and to promote a stronger cAMP response from the endosome. Other studies investigating opposing functional relationships have yet to be described and explored.

Our findings describe that M2R may be active at the endosome to inhibit β2AR-stimulated cAMP-dependent transcription, but activity at the endosome is not required for M2R inhibition. M2R is capable of inhibiting the β2AR cAMP signaling cascade from the plasma membrane. These results

are consistent with PTHR and β2AR study, such that a receptor does not need to be at the endosome to modulate the endosomal GPCR's response.

We amend our previous hypothesis from Chapter 2 and Chapter 5.2, and propose that M2R inhibits global cAMP strongly from the plasma membrane to prevent the strong induction of cAMP-dependent transcription by β2AR at the endosome. If M2R reduces the global cAMP level down to near basal levels, then PKAcat would not diffuse far with a substantial concentration. To test this, we would use the cAMP fluorescence biosensors generated in Chapter 2 to observe cAMP levels during the plateau phase when β2AR and M2R were costimulated. We predict that the cAMP levels at the plateau phase when both receptors are stimulated would be significantly lower than when only β2AR was stimulated. Additionally, we could perform the photobleaching experiment in cells stimulated with both β2AR and M2R agonists. If this hypothesis is true, we would predict that there would very little recovery (similar to basal).

What has been difficult in studying the relationship between M2R and β2AR is that signaling cascades get far more complicated the further downstream the cascade you go. There become more inputs to promote that downstream signal. For instance, CREB is not only phosphorylated by PKAcat, multiple other kinases can phosphorylate CREB from different (non-cAMP) signaling pathways (Du & Montminy, 1998; Naqvi et al., 2014; Shi et al., 2012). Stimulation of M2R alone can increase CREB phosphorylation, which can make interpretation of experiments coactivating β2AR and M2R difficult. There is a great need for more sensitive tools and methods will be necessary to investigate the functional relationships between receptors at the endosome.

5.4 Open questions in the field of endosomal signaling

The goal of this dissertation was to clarify how endosomal signaling promotes a selective signal and how or whether that selective signal could be regulated by another receptor. As always with science, you might answer one question but find yourself asking 10 new ones. We found that PKAcat nuclear entry was a key step in promoting the endosomal signaling, however the mechanism in how endocytosis promotes remains unanswered. We additionally conclude that M2R can inhibit the β2AR endosomal signal, but M2R internalization is not required for this inhibition. More work needs to be done to determine mechanism of regulation by M2R at the plasma membrane on the β2AR endosomal signal. These possibilities are discussed previously in Chapters 5.2 and 5.3, here we discuss open questions that remain unanswered in the field.

Though GPCR endosomal signaling is now widely accepted due to the great body of work in the past few years, we still have many unanswered questions. What components generate the endosomal signal? How is the endosomal signal regulated? What are the prerequisites for a GPCR to signal from the endosome?

Some effectors in the G_s and G_i signaling pathways have been identified. There is some evidence that suggests the importance of different adenylyl cyclases and their role in endosomal signaling. Multiple adenylyl cyclases have been found at intracellular membranes, including the endosome. Work with the TSHR found AC3 and AC5/6 at the plasma membrane and at intracellular vesicles (Calebiro et al., 2009). AC5 has also been observed at intracellular vesicles thought to be endosomes containing D1 dopamine receptor (Kotowski et al., 2011). Soluble adenylyl cyclase (sAC) has been found to be important for endosomal signaling by corticotropin-releasing hormone receptor 1 (CRHR1), because the inhibition of both sAC and endocytosis when CRHR1 was

activated did not produce an additive effect (Inda et al., 2016). AC2 has also been implicated in endosomal signaling of PTHR and PTHR and β2AR primarily through cAMP signaling experiments (Jean-Alphonse et al., 2016). Work in our lab has also identified AC9 present at and trafficking to the endosome with signaling consequences when AC9 trafficking is inhibited (Lazar, 2019). Many of these studies combine localization results with indirect signaling results to suggest which adenylyl cyclases may be playing a role in their signaling pathway.

There have been some ideas proposed in how the endosomal signal is shut off, but endosomal signal termination remains unclear. It is possible that receptors undergo their normal shutoff mechanism through phosphorylation of the receptor and the binding of arrestin to inhibit G protein interaction. Or that through the continuation of their normal trafficking itineraries (recycling, degradation) will eventually results in signal termination.

Although our data do not indicate whether M2R is active at the endosome or not, I curiously began to question how or why a receptor might not signal from the endosome. A possibility is related to one of the termination mechanisms described above, arrestin (or any other protein) binding can precludes G protein binding and therefore, G protein activation. M2R for instance, binds arrestin

strongly at the endosome (**Figure 5.2**). Paradoxically, other GPCRs known to signal from the endosome, such as V2R, also bind arresting strongly at the endosome (Pavlos & Friedman, 2016). V2R however has its

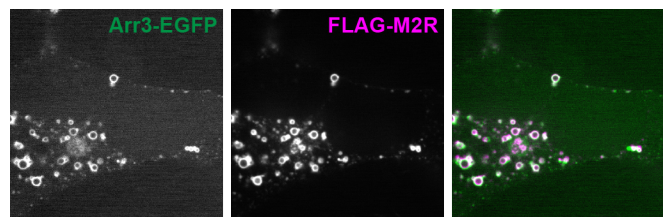

Figure 5.2 M2R colocalizes with arrestin-3 at endosomes Cells stably expressing FLAG-M2R and transfected with Arr3-EGFP were imaged by spinning disk confocal after 30 minutes of 10 μM Carbachol.

phosphorylation sites on its C-terminal tail and can interact with arrestin in the "tail" conformation without engaging the transmembrane core (Cahill et al., 2017). Phosphorylation sites for M2R

important for desensitization reside in intracellular loop 3, and although its unknown if M2R can engage with arrestin in the "tail" conformation, binding arrestin may prevent G protein from engaging with the receptor to result in G protein activation.

Methods and tool development will be critical and important in studying and understanding endosomal signaling in different receptors and cellular contexts. Conformational biosensors have already proven to be extraordinarily useful, but it may be difficult to generate and find a useful and specific nanobody, despite the efforts that have been done to do so (Mcmahon et al., 2017). Non-nanobody conformational biosensors have also been generated and adapted from structural studies for use in visualizing active GPCRs (Wan et al., 2018). Additionally, the development of biosensors to study signaling live with high spatial and temporal resolution will greatly add depth to our endosomal signaling knowledge.

5.5 References

Berg, H. C. (1993). *Random walks in biology*. Retrieved from

https://press.princeton.edu/titles/112.html

Blumenthal, D., Goldstien, L., Edidin, M., & Gheber, L. A. (2015). Universal Approach to FRAP

Analysis of Arbitrary Bleaching Patterns. *Scientific Reports*, *5*(1), 11655.

https://doi.org/10.1038/srep11655

Cahill, T. J., Thomsen, A. R. B., Tarrasch, J. T., Plouffe, B., Nguyen, A. H., Yang, F., … Lefkowitz,

R. J. (2017). Distinct conformations of GPCR–β-arrestin complexes mediate desensitization,

signaling, and endocytosis. *Proceedings of the National Academy of Sciences*, *114*(10),

2562–2567. https://doi.org/10.1073/pnas.1701529114

Calebiro, D., Nikolaev, V. O., Gagliani, M. C., De Filippis, T., Dees, C., Tacchetti, C., … Lohse, M.

J. (2009). Persistent cAMP-signals triggered by internalized G-protein-coupled receptors.

PLoS Biology, *7*(8). https://doi.org/10.1371/journal.pbio.1000172

Cheng, X., Phelps, C., & Taylor, S. S. (2001). Differential binding of cAMP-dependent protein

kinase regulatory subunit isoforms Ialpha and IIbeta to the catalytic subunit. *The Journal of

Biological Chemistry*, *276*(6), 4102–4108. https://doi.org/10.1074/jbc.M006447200

Clister, T., Greenwald, E. C., Baillie, G. S., Zhang, J., & Zhang Correspondence, J. AKAP95

Organizes a Nuclear Microdomain to Control Local cAMP for Regulating Nuclear PKA _

Elsevier Enhanced Reader.pdf. , 26 Cell Chemical Biology § (2019).

Du, K., & Montminy, M. (1998). CREB is a regulatory target for the protein kinase Akt/PKB. *The

Journal of Biological Chemistry*, *273*(49), 32377–32379.

https://doi.org/10.1074/jbc.273.49.32377

Godbole, A., Lyga, S., Lohse, M. J., & Calebiro, D. (2017). Internalized TSH receptors en route to

the TGN induce local Gs-protein signaling and gene transcription. *Nature Communications*,

8(1), 23–42. https://doi.org/10.1038/s41467-017-00357-2

Hagiwara, M., Brindle, P., Harootunian, A., Armstrong, R., Rivier, J., Vale, W., … Montminy2, M. R. *Coupling of Hormonal Stimulation and Transcription via the Cyclic AMP-Responsive Factor CREB is Rate Limited by Nuclear Entry of Protein Kinase A.* , 13 § (1993).

Harootunian, A. T., Adams, S. R., Wen, W., Meinkoth, J. L., Taylor, S. S., & Tsien, R. Y. (1993). Movement of the free catalytic subunit of cAMP-dependent protein kinase into and out of the nucleus can be explained by diffusion. *Molecular Biology of the Cell*, *4*(10), 993–1002. https://doi.org/10.1091/mbc.4.10.993

Inda, C., Claro, P. A. dos S., Bonfiglio, J. J., Senin, S. A., Maccarrone, G., Turck, C. W., & Silberstein, S. (2016). Different cAMP sources are critically involved in G protein-coupled receptor CRHR1 signaling. *Journal of Cell Biology*, *214*(2), 181–195. https://doi.org/10.1083/jcb.201512075

Jean-Alphonse, F. G., Wehbi, V. L., Chen, J., Noda, M., Taboas, J. M., Xiao, K., & Vilardaga, J.-P. (2016). β2-adrenergic receptor control of endosomal PTH receptor signaling via Gβγ. *Nature Chemical Biology*, *13*(3), 259–261. https://doi.org/10.1038/nchembio.2267

Kotowski, S. J., Hopf, F. W., Seif, T., Bonci, A., & von Zastrow, M. (2011). Endocytosis Promotes Rapid Dopaminergic Signaling. *Neuron*, *71*(2), 278–290. https://doi.org/10.1016/j.neuron.2011.05.036

Lazar, A. M. (2019). *Elucidating the regulation of adenylyl cyclase type 9 by dynamic membrane trafficking*.

Mcmahon, C., Baier, A. S., Zheng, S., Pascolutti, R., Ong, J. X., Erlandson, S. C., … Kruse, A. C. (2017). Platform for rapid nanobody discovery in vitro. *BioRxiv*. https://doi.org/10.1101/151043

Naqvi, S., Martin, K. J., & Arthur, J. S. C. (2014). CREB phosphorylation at Ser [133] regulates

transcription via distinct mechanisms downstream of cAMP and MAPK signalling. *Biochemical Journal*, *458*(3), 469–479. https://doi.org/10.1042/BJ20131115

Pavlos, N. J., & Friedman, P. A. (2016). GPCR Signaling and Trafficking: The Long and Short of It. *Trends in Endocrinology & Metabolism*. https://doi.org/10.1016/j.tem.2016.10.007

Pepperkok, R., Hotz-Wagenblatt, A., König, N., Girod, A., Bossemeyer, D., & Kinzel, V. (2000). Intracellular distribution of mammalian protein kinase A catalytic subunit altered by conserved Asn2 deamidation. *Journal of Cell Biology*, *148*(4), 715–726. https://doi.org/10.1083/jcb.148.4.715

Sastri, M., Barraclough, D. M., Carmichael, P. T., & Taylor, S. S. (2005). A-kinase-interacting protein localizes protein kinase A in the nucleus. *Proceedings of the National Academy of Sciences*, *102*(2), 349–354. https://doi.org/10.1073/pnas.0408608102

Shi, G.-X., Cai, W., & Andres, D. A. (2012). Rit-mediated stress resistance involves a p38-mitogen- and stress-activated protein kinase 1 (MSK1)-dependent cAMP response element-binding protein (CREB) activation cascade. *The Journal of Biological Chemistry*, *287*(47), 39859–39868. https://doi.org/10.1074/jbc.M112.384248

Swaminathan, R., Hoang, C. P., & Verkman, A. S. (1997). Photobleaching recovery and anisotropy decay of green fluorescent protein GFP-S65T in solution and cells: cytoplasmic viscosity probed by green fluorescent protein translational and rotational diffusion. *Biophysical Journal*, *72*(4), 1900–1907. https://doi.org/10.1016/S0006-3495(97)78835-0

Walker-Gray, R., Stengel, F., & Gold, M. G. (2017). Mechanisms for restraining cAMP-dependent protein kinase revealed by subunit quantitation and cross-linking approaches. *Proceedings of the National Academy of Sciences of the United States of America*, *114*(39), 10414–10419. https://doi.org/10.1073/pnas.1701782114

Wan, Q., Okashah, N., Inoue, A., Nehmé, R., Carpenter, B., Tate, C. G., & Lambert, N. A. (2018).

Mini G protein probes for active G protein-coupled receptors (GPCRs) in live cells. *The Journal of Biological Chemistry*, *293*(19), 7466–7473. https://doi.org/10.1074/jbc.RA118.001975

Wen, W., Meinkotht, J. L., Tsien, R. Y., & Taylor, S. S. (1995). Identification of a signal for rapid export of proteins from the nucleus. *Cell*, *82*(3), 463–473. https://doi.org/10.1016/0092-8674(95)90435-2

Zawadzki, K. M., & Taylor, S. S. (2004). cAMP-dependent protein kinase regulatory subunit type IIbeta: active site mutations define an isoform-specific network for allosteric signaling by cAMP. *The Journal of Biological Chemistry*, *279*(8), 7029–7036. https://doi.org/10.1074/jbc.M310804200

Appendices: Protocols for detecting
cAMP and modeling diffusion

A. cAMP Dual Luciferase assay
Materials

pSF CMV GloSensor20F IRES Rluc stable cell line, previously generated in Chapter 2 from pGloSensor20F, Promega and pSF CMV EMCV Rluc, Boca Scientific

Coelenterazine, Gold Biotechnology CZ2.5: Stock is 1 or 2 mM in ethanol.

D-Luciferin, Na Salt, Gold Biotechnology LUCNA-1g: Stock is 100 mM in 10 mM HEPES

Braden's Stop buffer (1x)
    25 mM HEPES, pH 7.4
    1 mM EDTA
    0.4 mM DTT
    0.2% TritonX-100
    2% Glycerol

Imaging media
    DMEM without phenol red (Gibco, 31053)
    30 mM HEPES

24 well plate

Protocol
Day 0: Seed cells.
    1. Plate cells in 10 cm dish at 60-70% confluency.

Day 1: Transfect cells
Transfect cells with dual luciferase 2 µg GloSensor plasmid (pSF CMV Glo20F IRES Rluc), or use stables.

Day 2: Assay day
    1. Lift transfected cells and spin down in cell culture centrifuge at ¾ speed for 10 minutes.
    2. Resuspend cells in 4 mL of imaging media.
    3. Add luciferin, 64 µL 100 mM luciferin to 4 mL cells in imaging media.
    4. Aliquot 200 µL cells/well into the central 16 wells of a 24 well plate.
    5. Place cells in incubator for 1 hour.
    6. Prepare for assay 20 minutes before luciferin incubation is up:
        a. Turn on computer, camera and heated chamber.
        b. Make up 2x drugs, and place in incubator to warm.
    7. When ready, take cells and drug mix out of the incubator to the cAMP luminometer. Add 200 µL drugs to each well and place inside heated chamber and start imaging.
        a. 121 frames (20 minutes), 10 second exposure (10000 ms), continuous intervals.
    8. While the plate is imaging prepare buffer for coelenterazine.
        a. Prepare Stop buffer (either make fresh or thaw 5x Stop buffer, -80°C.)
        b. After thawed, add coelenterazine for a final concentration of 10 µM coelenterazine in stop buffer.
    9. When plate has finished, add 100 µL 5x Stop buffer with coelenterazine (final concentration 2 µM coelenterazine/well) to each well.

10. Immediately image renilla luminescence.
     a.   5 frames, 10 second exposure, Continuous intervals

Analysis
1.   Generate 4 ROIs for background measurement.
2.   Generate 16 ROIs for each well.
3.   Background subtract each well/frame of the firefly luciferase luminescence.
4.   Background subtract each well for the renilla luciferase luminescence.
5.   Divide firefly luciferase luminescence by renilla luciferase luminescence for each well.
6.   Plot luminescence ratio of firefly/renilla vs time.

B. cAMP Homogenous Time Resolved Fluorescence Assay
B.1 Method
The original kits were gifted by Nicolas Pierre (CisBio) and instructed for 384 well plates. I adapted the protocol for use in white 96 half area well plates.

cAMP Gs Dynamic Kit, CisBio (#62AM4PEB)

New kit reagent preparation:
Warm reagents to room temperature for 30 minutes before reconstitution.

    Anti cAMP Eu^{3+} Cryptate (K) 5x stock
    Add 1.1 ml water to vial, aliquot 100 μL into microcentrifuge tubes.

    cAMP-d2 (d2) 5x stock
    Add 1.1 ml water to vial, aliquot 100 μL into microcentrifuge tubes.

    cAMP standard (280 nM)
    Add 0.45 ml water to vial, aliquot 112.5 μL into microcentrifuge tubes.

Keep stocks frozen for 6 months, or one week at 4°C.

Protocol
Day 0:
    Seed cells into 6 well plate.

Day 1:
    1. Prepare reagents, warm conjugate & lysis buffer to room temperature and thaw cAMP standard on ice.
    2. Prepare cells:
        a. Wash cells once with PBS with EDTA, and lift cells (3 wells of a 6 well).
        b. Resuspend cells in 10 mL.
        c. Spin down cells and resuspend in 2 mL media.
    3. While cells are spinning down, prepare standards.

Table B1.1 Preparation of Standards

Standard	Preparation	cAMP working solution (nM)	[cAMP] (nM)
Std 7	Reconstituted reagent in water	2848	712
Std 6	50 μL Std 7 + 150 μL media	712	178
Std 5	50 μL Std 6 + 150 μL media	178	44.5
Std 4	50 μL Std 5 + 150 μL media	44.5	11.125
Std 3	50 μL Std 4 + 150 μL media	11.125	2.78
Std 2	50 μL Std 3 + 150 μL media	2.78	0.70
Std 1	50 μL Std 2 + 150 μL media	0.70	0.17
Std 0	200 μL media	0	0

4. Prepare plate for cell treatment
Table B1.2 Example plate layout

	1	2	3	4
A	Std 7	Std 7	neg	neg
B	Std 6	Std 6	cell neg	cell neg
C	Std 5	Std 5	unstim cells	unstim cells
D	Std 4	Std 4	sample 1	sample 1
E	Std 3	Std 3	sample 2	sample 2
F	Std 2	Std 2	sample 3	sample 3
H	Std 1	Std 1	sample 4	sample 4
I	Std 0	Std 0	sample 5	sample 5

Each well will have 100 µl total at the end of the experiment:
- 25 µL media or agonist treatment
- 25 µL standard or cells
- 25 µL cAMP-d2 in lysis buffer, or just lysis buffer
- 25 µL Eu^{3+} cryptate in lysis buffer

Table B1.3 Components added per well

Standards	Negative control	Cell neg control	Cell samples
25 µL Media	25 µL Media	25 µL Media	25 µL Treatment
25 µL Standard	25 µL Media	25 µL Cells	25 µL Cells
25 µL cAMP-d2	25 µL Lysis buffer	25 µL Lysis buffer	25 µL cAMP-d2
25 µL Eu^{3+}-cryptate	25 µL Eu^{3+}-cryptate	25 µL Eu^{3+}-cryptate	25 µL Eu^{3+}-cryptate

There are TWO incubations. For the first incubation (drug treatment), add the reagents in BLUE:
   a. Add 25 µL media to wells that will have standards/controls, OR 25 µl agonist treatment to wells with samples.
   b. Add 25 µL of standard or cells to respective wells.

   5. Incubate plate for 30 minutes (room temperature or 37°C).
   6. Make working stock solutions of Eu^{3+}-cryptate and cAMP-d2 by diluting 1:4 (100 µL + 400 µL conjugate and lysis buffer).
   7. Prepare for the second incubation (antibody and cAMP conjugate), add the reagents in RED:
   a. Add 25 µL conjugate & lysis buffer to negative control and cell negative control and add 25 µL cAMP-d2 (in conjugate & lysis buffer) to the rest of the samples (standards and cell samples).
   b. Add 25 µL Eu^{3+}-cryptate (in conjugate & lysis buffer) to all samples.
   8. Incubate for 1 hour at room temperature. (I put it in a drawer.)
   9. Read plate after one hour on the Tecan M200 Infinite Pro using Tecan i-Control.

159

B.2 Analysis

Data analysis: https://www.cisbio.com/usa/drug-discovery/htrf-ratio-and-data-reduction

Example data:
317/620 nm

Temperature: 22.9 °C

<>	1	2	3	4
A	14435	14335	15026	14099
B	14199	14750	13287	12755
C	14429	14610	15372	14386
D	12800	13111	14299	14704
E	12547	12638	15010	14669
F	12597	12580	15446	15953
G	12518	12935	14845	14250
H	12712	12705	15783	15332

317/665 nm

Temperature: 23.2 °C

<>	1	2	3	4
A	1139	1112	1089	878
B	1193	1396	5434	5087
C	1964	2379	1036	1075
D	3503	3671	2532	2873
E	6374	6453	2229	2254
F	7829	8333	1138	1120
G	9876	9790	1922	1354
H	1100	1074	1862	1612

In Microsoft Excel:

1. Determine ratio of 665 to 620 signal.

$$\text{ratio} = \frac{665_{nm} \times 10^4}{620_{nm}}$$

2. Background correct the ratio.

$$\Delta\,\text{ratio} = \text{ratio}_{std} - \text{ratio}_{neg} \qquad \text{or} \qquad \Delta\,\text{ratio} = \text{ratio}_{sample} - \text{ratio}_{cellneg}$$

3. For interassay comparison, calculate ΔF and ΔF_{max}.

$$\Delta F = \frac{\text{ratio}_{sample} - \text{ratio}_{cellneg}}{\text{ratio}_{cell\,neg}}$$

Use $\frac{\Delta F}{\Delta F_{max}}$ to compare assay to assay.

In GraphPad Prism:

4. For actual concentrations, open a tutorial in Prism "RIA or ELISA: Interpolate unknowns from sigmoidal curve"
5. Put in background corrected ratios for the standard curve and the unknowns.
6. Calculate log concentration of cAMP.
7. Interpolate unknowns for standard curve by using 4PL, sigmoidal method.

C. Modeling diffusion
Matlab R2018b code

For Figure 5.1a

```matlab
function out = diffusion(D)
    N = 100 % number of ACs on endosome (in molecules)
    i = 30 * N % rate of production assumes kcat 30 sec-1 per Dessauer and
    Gilman 1997 (~agrees with Levitzki 1974 turkey RBC and Takai et al 1974 E
    coli)
    t = 20 % 20 second pulse
    r = linspace(0.01, 0.25, 200); % radius of observer from 10 nm to 250 nm.

    out = (i./(4*pi*D*r)).*erfc(r/((4*D*t)^0.5)) % Berg eq 2.9
    outint10 = @(r) (i./(4*pi*10*r)).*erfc(r/((4*10*t)^0.5))
    q = integral(outint10, 0.00001, 0.1); % sets the reference to 10 um, and
    so divided y by ~220. integrated number is at 100 nm.

    plot(r*1000,out/q)
end
```

For Figure 5.1b

```matlab
function out = diffusion2(r)
    N = 100  % number of ACs on endosome (in molecules)
    i = 30 * N  % rate of production assumes kcat 30 sec-1 per Dessauer and
    Gilman 1997 (~agrees with Levitzki 1974 turkey RBC and Takai et al 1974 E
    coli)
    D = linspace(0.1, 100, 200) % Diffusion constant 0.1 to 100 um^2/s
    r = 0.1 % distance from source, 100 nm

    out = (i./(4*pi*D*r)); % Berg eq 2.11
    outint10 = @(r) (i./(4*pi*10*r));
    q = integral(outint10, 0.00001, 0.1); % sets the reference to 10 um, and
    so divided y by ~220. integrated number is at 100 nm.
    y = out/q

    loglog(D,y)
    xlim([0.1, 100])
    ylim([0.1,100])
end
```

For Figure 5.1c

```matlab
function out = rectangular(Dc)
    t= [0:10:300] %time 0 to 300s intervals of 10s
    Ii=1 % plateau, intensity at time infinity, assume full recovery
    A=30 % um2s-1, Area of bleaching region
    % Dc is in um2s-1 diffusion constant

    It=Ii*(1-sqrt(A*(A+4*pi*Dc*t).^-1)) % Blumenthal et al. 2015, supplemental
    equation 4

    plot(t,It)
end
```
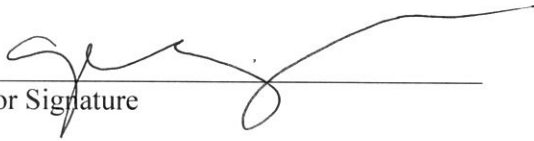
162

Publishing Agreement

It is the policy of the University to encourage the distribution of all theses, dissertations, and manuscripts. Copies of all UCSF theses, dissertations, and manuscripts will be routed to the library via the Graduate Division. The library will make all theses, dissertations, and manuscripts accessible to the public and will preserve these to the best of their abilities, in perpetuity.

Please sign the following statement:

I hereby grant permission to the Graduate Division of the University of California, San Francisco to release copies of my thesis, dissertation, or manuscript to the Campus Library to provide access and preservation, in whole or in part, in perpetuity.

Author Signature

08/19/2019

Date